

Supplementary Information for

Phase Stability, Electronic, Mechanical, Lattice Distortion, and Thermal Properties of Complex Refractory-Based High Entropy Alloys TiVCrZrNbMoHfTaW with Varying Elemental Ratios

Sahib Hasan^{1,2}, Puja Adhikari^{1,*}, Saro San¹, and Wai-Yim Ching¹

1. Department of Physics and Astronomy, University of Missouri-Kansas City, Kansas City, MO 64110, USA
2. Department of Sciences, College of Basic Education, Al Muthanna University, Samawah 66001, Iraq

*Correspondence: chingw@umkc.edu

This PDF file includes:

Materials and Methods
Supplementary Text
Figs. S1 to S17
Tables S1 to S3
Python code
References (1 to 26)

Materials and Methods

Mechanical properties calculations

Ab initio calculation method within the density functional theory (DFT) is a very powerful method for mechanical properties calculations. In this section, we followed the method of Hongzhi Yao *et al.* work¹ to calculate the mechanical properties. A scheme has been applied to calculate the elastic constants of the high entropy solid solutions. Starting with the simple Hook's famous law^{2,3} that relates the stress components σ_i with the strain components ε_j by the relation:

$$\sigma_i = \sum_{j=1}^6 C_{ij} \varepsilon_j \quad (S1)$$

C_{ij} is the elastic constants. From knowing the elastic constants, we calculate the other mechanical properties: compliance tensor S_{ij} , Young's modulus (E), Bulk modulus (K), Shear modulus (G), and Poisson's ratio (η). Here, the Voigt – Reuss –Hill (VRH)^{4,5} approximation has been used to derive the above mechanical parameters. According to this approximation, the upper and lower bounds for the structural parameters, such as bulk and shear modulus are respectively given by:

$$K_V = \frac{(C_{11} + C_{22} + C_{33})}{9} + \frac{2(C_{12} + C_{13} + C_{23})}{9} \quad (S2)$$

$$K_R = \frac{1}{(S_{11} + S_{22} + S_{33}) + 2(S_{12} + S_{13} + S_{23})} \quad (S3)$$

$$G_V = \frac{(C_{11} + C_{22} + C_{33} - C_{12} - C_{13} - C_{23})}{15} + \frac{(C_{44} + C_{55} + C_{66})}{5} \quad (S4)$$

$$G_R = \frac{15}{4(S_{11} + S_{22} + S_{33}) - 4(S_{12} + S_{13} + S_{23}) + 3(S_{44} + S_{55} + S_{66})} \quad (S5)$$

So, the average values of the mechanical parameters are given by:

$$K = \frac{(K_V + K_R)}{2} \quad (S6)$$

$$G = \frac{(G_V + G_R)}{2} \quad (S7)$$

$$E = \frac{9KG}{(3K+G)} \quad (S8)$$

$$\eta = \frac{(3K - 2G)}{2(3K + G)} \quad (S9)$$

The machinability index (μ_M) can be expressed as follows ⁶:

$$\mu_M = \frac{K}{C_{44}} \quad (S10)$$

The formula of Tian *et al.* ⁷ was used to calculate the macro Vicker's hardness parameter H_V :

$$H_V = 0.92 \left(\frac{G}{K} \right)^{1.137} G^{0.708} \quad (S11)$$

Another formula⁷ can be used to estimate Vicker's hardness:

$$H_V = 1.887((G/K)^2 G)^{0.585} \quad (S12)$$

Debye temperature and thermal conductivity calculations

Debye temperature (θ_D) and the average sound velocity (v_m) can be calculated as follows ⁸⁻¹¹:

$$\theta_D = \frac{h}{k_B} \left[\frac{3n}{4\pi} \left(\frac{N_A \cdot \rho}{M} \right) \right]^{\frac{1}{3}} v_m \quad (S13)$$

$$v_m = \left[\frac{1}{3} \left(\frac{2}{v_s^3} + \frac{1}{v_l^3} \right) \right]^{-\frac{1}{3}} \quad (S14)$$

Here, ρ is the theoretical density of the solid solution model, h , k_B , and N_A are Planck's constant, Boltzmann constant, and Avogadro's number, respectively. M is the molecular weight and n is the number of atoms in the supercell. v_s and v_l are the transverse (shear) and longitudinal sound velocities respectively. The compressional (longitudinal) waves and shear waves are estimated by using the values of bulk modulus (K) and shear modulus (G) according to Voigt-Reuss-Hill approach based on the following formulas ¹²:

$$v_s = \sqrt{\frac{G}{\rho}} \quad (S15)$$

$$v_l = \sqrt{\frac{3K + 4G}{3\rho}} \quad (S16)$$

Clarke's formula for the minimum thermal conductivity (κ_{min}) is given as follows^{13,14}:

$$\kappa_{min} = 0.87k_B \left(\frac{N_A \cdot n \cdot \rho}{M} \right)^{\frac{2}{3}} \sqrt{\frac{E}{\rho}} \quad (S17)$$

Cahill's formula for the minimum thermal conductivity is given by^{15,16}:

$$\kappa_{min} = \frac{k_B}{2.48} \left(\frac{n}{V} \right)^{\frac{2}{3}} (v_l + 2v_s) \quad (S18)$$

Slack's formula^{17,18} for thermal conductivity (κ) or for lattice thermal conductivity (κ_L) (in case of the electronic part of thermal conductivity (κ_e) is negligible) is given by:

$$\kappa = A \frac{M_{ave} \Theta_D^3 \Omega}{\left(\gamma_\alpha^2 \cdot n^{\frac{2}{3}} \cdot T \right)} \quad (S19)$$

$$M_{ave} = \frac{M}{n \cdot N_A} \quad (S20)$$

Where V is the volume of the supercell, A is constant that can be approximated to be $3.1 \cdot 10^{-18}$ when κ in $\text{W} \cdot \text{m}^{-1} \cdot \text{K}^{-1}$. γ_α is the acoustic Grüneisen parameter, Ω is the volume per atom, and T is the temperature in Kelvin unit.

The acoustic Grüneisen constant (γ_α) was calculated by using the following formula¹⁹:

$$\gamma_\alpha = \frac{3}{2} \left(\frac{3v_l^2 - 4v_s^2}{v_l^2 + 2v_s^2} \right) \quad (S21)$$

Julian^{17,20,21} derived the following formula for the constant A in the Slack's formula (formula (S29)) for κ :

$$A = \frac{2.436 \times 10^{-6}}{1 - \frac{0.514}{\gamma_\alpha} + \frac{0.228}{\gamma_\alpha^2}} \quad (S22)$$

The mixed model²² can give an empirical formula for lattice thermal conductivity (κ_L) as follows:

$$\kappa_L = \frac{(6\pi^2)^{\frac{2}{3}} M_{ave} \nu_s^3}{4\pi^2 \cdot \frac{2}{V^{\frac{2}{3}} \gamma^2 T}} \quad (S23)$$

An empirical formula was used for calculating an estimation of melting temperature (T_{melt}) of the six RHEAs solid solutions with a standard error about ± 300 K by using the elastic constants²³⁻²⁵:

$$T_{melt} = \left[553K + \left(\frac{5.91K}{GPa} \right) C_{11} \right] \mp 300K \quad (S24)$$

Thermal expansion coefficient (α) can be roughly estimated from the following formula using the value of shear modulus²⁶:

$$\alpha = \frac{1.6 \times 10^{-3}}{G} \quad (S25)$$

Supplementary Text

From our calculations for BO and BL data, we succinctly describe the following observations:

1. Cr–Zr bond lengths (BLs) are distributed between (2.6–3.7Å) with BO(0.02–0.15) for all models.
2. Cr–Ta bonds have BLs between(2.5–3.7Å) with BO(0.05–0.25) in the models from m1to m4, while they have shorter BLs between (2.5–3.2Å) with less BO(0.05–0.2) in m5 and m6.
3. Cr–W bonds have BLs between(2.4–3.7Å) with BO(0.05–0.26) in the models from m1to m4, while they have shorter BLs between (2.5–3.3Å) with less BO(0.05–0.23) in m5 and m6.
4. Cr–Nb BLs are distributed between (2.5–3.8Å) with BO(0.01–0.18) for m1 and m3 models. In m4 and m5, Cr–Nb BLs are distributed between (2.5–3.6Å) with BO(0.01–0.17), whereas they have shorter BLs between (2.5–3.2Å) with less BO(0.01–0.15) in m6.
5. Cr–Mo BLs are distributed between (2.5–3.4Å) with BO(0.04–0.25) for m1 and m5 models. In m2 and m3, Cr–Mo BLs are distributed between (2.5–3.6Å) with BO(0.05–0.3), whereas they have shorter BLs between (2.5–3.2Å) with less BO(0.04–0.22) in m6.
6. Cr–Hf bonds have BLs between(2.5–3.8Å) with BO(0.02–0.2) in m1, and they have similar BLs with less BO(0.03–0.16) in m2 and m3. In m4, Cr–Hf BLs are distributed between (2.6–3.6Å) with BO(0.03–0.15) whereas they have shorter BLs between (2.6–3.3Å) with less BO(0.02–0.14) in m5.
7. Cr–Cr bonds have BLs between(2.3–3.6Å) with BO(0.05–0.3) in models from m1 to m3, and they have BLs (2.3–4.0Å) with less BO(0.01–0.26) in m4. In m5, Cr–Cr BLs are distributed between (2.3– 3.4Å) with BO(0.05–0.24) whereas they have shorter BLs between (2.4–3.2Å) with less BO(0.05–0.2) in m6.
8. Hf–W BLs are distributed between (2.6– 3.6Å) with BO(0.02–0.17) for the models from m1 to m4, while they have shorter BLs(2.6–3.4Å) with the same BO in m5.
9. Hf–Ta BLs are distributed between (2.7–3.7Å) with BO(0.03–0.17) for the models from m1 to m4, while they have shorter BLs(2.7–3.4Å) with the same BO in m5.

- 10.** Mo–W BLs are distributed between (2.5–3.5Å) with BO(0.05–0.25) for the models from m1 to m5, while they have shorter BLs(2.5–3.2Å) with less BO(0.04–0.22) in m6.
- 11.** Mo–Ta BLs are distributed between (2.5–3.5Å) with BO(0.04–0.25) for the models from m1 to m5, while they have shorter BLs(2.6–3.3Å) with less BO(0.04–0.21) in m6.
- 12.** Mo–Mo bonds have BLs between(2.5–3.5Å) with BO(0.05–0.25) in the models from m1 to m4. In m5, Mo–Mo BLs are distributed between (2.5–3.4Å) with BO(0.05–0.25) whereas they have shorter BLs between (2.5–3.3Å) with less BO(0.03–0.22) in m6.
- 13.** Mo–Hf BLs are distributed between (2.6–3.6Å) with BO(0.03–0.17) for the models from m1 to m4, while they have shorter BLs(2.6–3.4Å) with BO(0.02–0.17) in m5.
- 14.** Nb–Hf bonds have BLs between(2.7–3.6Å) with BO(0.02–0.12) in the models from m1 to m3. In m4, Nb–Hf BLs are distributed between (2.7–3.8Å) with BO(0.02–0.12) whereas they have shorter BLs between (2.7–3.4Å) with less BO(0.01–0.11) in m5.
- 15.** Nb–Mo bonds have BLs between(2.5–3.6Å) with BO(0.02–0.21) in models from m1 to m3, and they have BLs (2.6–3.5Å) with less BO(0.02–0.17) in m4. In m5, Nb–Mo BLs are distributed between (2.6–3.5Å) with BO(0.02–0.19) whereas they have shorter BLs between (2.6–3.3Å) with less BO(0.02–0.16) in m6.
- 16.** Nb–W BLs are distributed between (2.6–3.6Å) with BO(0.03–0.19) for the models from m1 to m5, while they have shorter BLs(2.6–3.3Å) with BO(0.02–0.16) in m6.
- 17.** Nb–Ta bonds have BLs between(2.6–3.6Å) with BO(0.03–0.19) in models from m1 to m3. They have BLs (2.7–3.5Å) with less BO(0.03–0.17) in m4 and m5, whereas they have shorter BLs between (2.6–3.3Å) with less BO(0.02–0.16) in m6.
- 18.** Nb–Nb BLs are distributed between (2.6–3.6Å) with BO(0.02–0.13) for the models from m1 to m5, while they have shorter BLs(2.6–3.2Å) with BO(0.01–0.11) in m6.
- 19.** Ta–Ta bonds have BLs between(2.7–3.7Å) with BO(0.05–0.25) in models from m1 to m4. They have BLs (2.6–3.3Å) with BO(0.05–0.25) in m5, whereas they have shorter BLs between (2.7–3.2Å) with less BO(0.05–0.21) in m6.
- 20.** Ta–W bonds have BLs between(2.6–3.6Å) with BO(0.05–0.27) in models from m1 to m4. They have BLs (2.6–3.4Å) with BO(0.05–0.26) in m5, whereas they have shorter BLs between (2.6–3.2Å) with less BO(0.05–0.22) in m6.

- 21.** Ti–Zr BLs are distributed between (2.6–3.8Å) with BO(0.03–0.15) for the models from m1 to m4, while they have shorter BLs(2.6–3.4Å) with the same values of BO in m5.
- 22.** Ti–W bonds have BLs between(2.5–3.7Å) with BO(0.05–0.25) in models m1, m2, and m4. They have BLs (2.5–3.5Å) with BO(0.04–0.23) in m3 and m5, whereas they have shorter BLs between (2.5–3.3Å) with less BO(0.04–0.2) in m6.
- 23.** Ti–V bonds have BLs between(2.5–3.8Å) with BO(0.03–0.24) in models from m1 to m3, and they have BLs (2.4–3.9Å) with less BO(0.03–0.24) in m4. In m5, Ti–V BLs are distributed between (2.5– 3.6Å) with BO(0.03–0.2) whereas they have shorter BLs between (2.5–3.3Å) with less BO(0.03–0.17) in m6.
- 24.** Ti–Ti bonds have BLs between(2.6–3.7Å) with BO(0.02–0.23) in models m1 and m3, and they have BLs (2.5–3.8Å) with less BO(0.05–0.2) in m2. In m4, Ti–Ti BLs are distributed between (2.5–4.0Å) with BO(0.0–0.22). In m5, Ti–Ti BLs are distributed between (2.6–3.6Å) with BO(0.05–0.18) whereas they have shorter BLs between (2.6–3.3Å) with less BO(0.05–0.15) in m6.
- 25.** Ti–Ta bonds have BLs between(2.6–4.0Å) with BO(0.01–0.23) in models from m1 to m3, and they have BLs (2.6–3.8Å) with BO(0.05–0.24) in m4. In m5, Ti–Ta BLs are distributed between (2.6– 4.0Å) with BO(0.01–0.2) whereas they have shorter BLs between (2.6–3.3Å) with less BO(0.05–0.18) in m6.
- 26.** Ti–Nb bonds have BLs between(2.5–3.7Å) with BO(0.03–0.19) in models m1 and m2, and they have BLs (2.6–3.5Å) with less BO(0.03–0.16) in m3 and m5. In m4, Ti–Nb BLs are distributed between (2.5–4.0Å) with BO(0.01–0.22), whereas they have shorter BLs between (2.6–3.3Å) with less BO(0.03–0.13) in m6.
- 27.** Ti–Mo BLs are distributed between (2.5–3.6Å) with BO(0.04–0.24) for the models from m1 to m5, while they have shorter BLs(2.5–3.3Å) with BO(0.05–0.21) in m6.
- 28.** Ti–Hf BLs are distributed between (2.6–3.8Å) with BO(0.02–0.15) for m1and m2 models, while they have BLs(2.7–4.0Å) with BO(0.01–0.18) in m4.
- 29.** Ti–Cr bonds have BLs between(2.4–3.9Å) with BO(0.04–0.22) in models m1, m3, m4, and m5. They have BLs (2.4–3.8Å) with BO(0.04–0.25) in m2, whereas they have shorter BLs between (2.4–3.3Å) with less BO(0.05–0.18) in m6.

30. V–Zr bonds have BLs between (2.6–3.8Å) with BO(0.03–0.15) in models from m1 to m3. They have shorter BLs (2.6–3.4Å) with BO(0.03–0.17) in m4, and they have BLs between (2.6–3.6Å) with BO(0.02–0.15) in m5.

31. V–W bonds have BLs between (2.5–3.6Å) with BO(0.03–0.26) in models from m1 to m4. They have BLs (2.5–3.4Å) with BO(0.04–0.24) in m5, whereas and they have shorter BLs between (2.5–3.3Å) with less BO(0.03–0.21) in m6.

32. V–V BLs are distributed between (2.4–3.7Å) with BO(0.04–0.25) for models from m1 to m5, while they have shorter BLs (2.5–3.3Å) with less BO(0.04–0.2) in m6.

33. V–Ta bonds have BLs between (2.5–3.8Å) with BO(0.04–0.24) in models m1, m3, and m4, and they have BLs (2.5–3.7Å) with higher BO(0.04–0.28) in m2. In m5, V–Ta BLs are distributed between (2.5–3.5Å) with BO(0.04–0.23), whereas they have shorter BLs between (2.5–3.3Å) with less BO(0.03–0.2) in m6.

34. V–Nb bonds have BLs between (2.5–3.7Å) with BO(0.03–0.2) in models m1, m3, and m4, and they have BLs (2.5–3.8Å) with BO(0.02–0.18) in m2. In m5, V–Nb BLs are distributed between (2.6–3.6Å) with BO(0.02–0.16), whereas they have shorter BLs between (2.6–3.3Å) with less BO(0.03–0.15) in m6.

35. V–Mo bonds have BLs between (2.5–3.6Å) with BO(0.05–0.27) in models from m1 to m3, and they have BLs (2.4–3.6Å) with less BO(0.05–0.24) in m4. In m5, V–Mo BLs are distributed between (2.4–3.4Å) with BO(0.05–0.25), whereas they have shorter BLs between (2.5–3.3Å) with less BO(0.04–0.22) in m6.

36. V–Hf BLs are distributed between (2.6–3.7Å) with BO(0.03–0.17) for models from m1 to m4, while they have shorter BLs (2.6–3.5Å) with less BO(0.02–0.14) in m5.

37. V–Cr bonds have BLs between (2.3–3.7Å) with BO(0.02–0.25) in m1, and they have BLs (2.3–3.8Å) with higher BO(0.03–0.28) in m2. In m3, they have BLs (2.3–3.6Å) with BO(0.05–0.27). In m4 and m5, V–Cr BLs are distributed between (2.4–3.6Å) with BO(0.05–0.24), whereas they have shorter BLs between (2.4–3.3Å) with less BO(0.05–0.21) in m6.

38. W–W bonds have BLs between (2.6–3.5Å) with BO(0.05–0.3) in models m1 and m2, and they have BLs (2.6–3.5Å) with less BO(0.05–0.26) in m3 and m4. In m5, W–W BLs are distributed between (2.6–3.3Å) with BO(0.03–0.25), whereas they have shorter BLs between (2.6–3.2Å) with less BO(0.03–0.22) in m6.

39. Zr–Hf bonds have BLs between (2.8–4.0 Å) with BO(0.0–0.11) in m1, and they have BLs (2.7–4.0 Å) with higher BO(0.0–0.13) in m2. In m3 and m4, Zr–Hf BLs are distributed between (2.7–4.1 Å) with BO(0.0–0.1), whereas they have shorter BLs between (2.8–3.4 Å) with less BO(0.02–0.09) in m5.

40. Zr–Zr bonds have BLs between (2.8–4.0 Å) with BO(0.0–0.11) in models m1 and m2, and they have BLs (2.8–3.5 Å) with BO(0.03–0.11) in m3. In m4, Zr–Zr BLs are distributed between (2.7–4.0 Å) with BO(0.0–0.1), whereas they have shorter BLs between (3.0–3.4 Å) with less BO(0.02–0.04) in m5.

41. Zr–W bonds have BLs between (2.7–3.5 Å) with BO(0.02–0.15) in m1, and they have BLs (2.7–3.6 Å) with BO(0.03–0.17) in m2 and m3. In m4, Zr–W BLs are distributed between (2.6–3.7 Å) with BO(0.03–0.15), whereas they have shorter BLs between (2.7–3.3 Å) with BO(0.02–0.16) in m5.

42. Zr–Ta BLs are distributed between (2.7–3.7 Å) with BO(0.03–0.17) for models from m1 to m4, while they have shorter BLs (2.7–3.5 Å) with less BO(0.02–0.14) in m5.

43. Zr–Nb bonds have BLs between (2.7–3.7 Å) with BO(0.02–0.13) in models from m1 to m3. In m4, Zr–Nb BLs are distributed between (2.7–3.5 Å) with BO(0.02–0.11), whereas they have shorter BLs between (2.7–3.4 Å) with BO(0.02–0.11) in m5.

44. Zr–Mo BLs are distributed between (2.6–3.7 Å) with BO(0.03–0.16) in m1, m2, and m4, while they have shorter BLs (2.6–3.4 Å) with less BO(0.03–0.15) in m3 and m5.

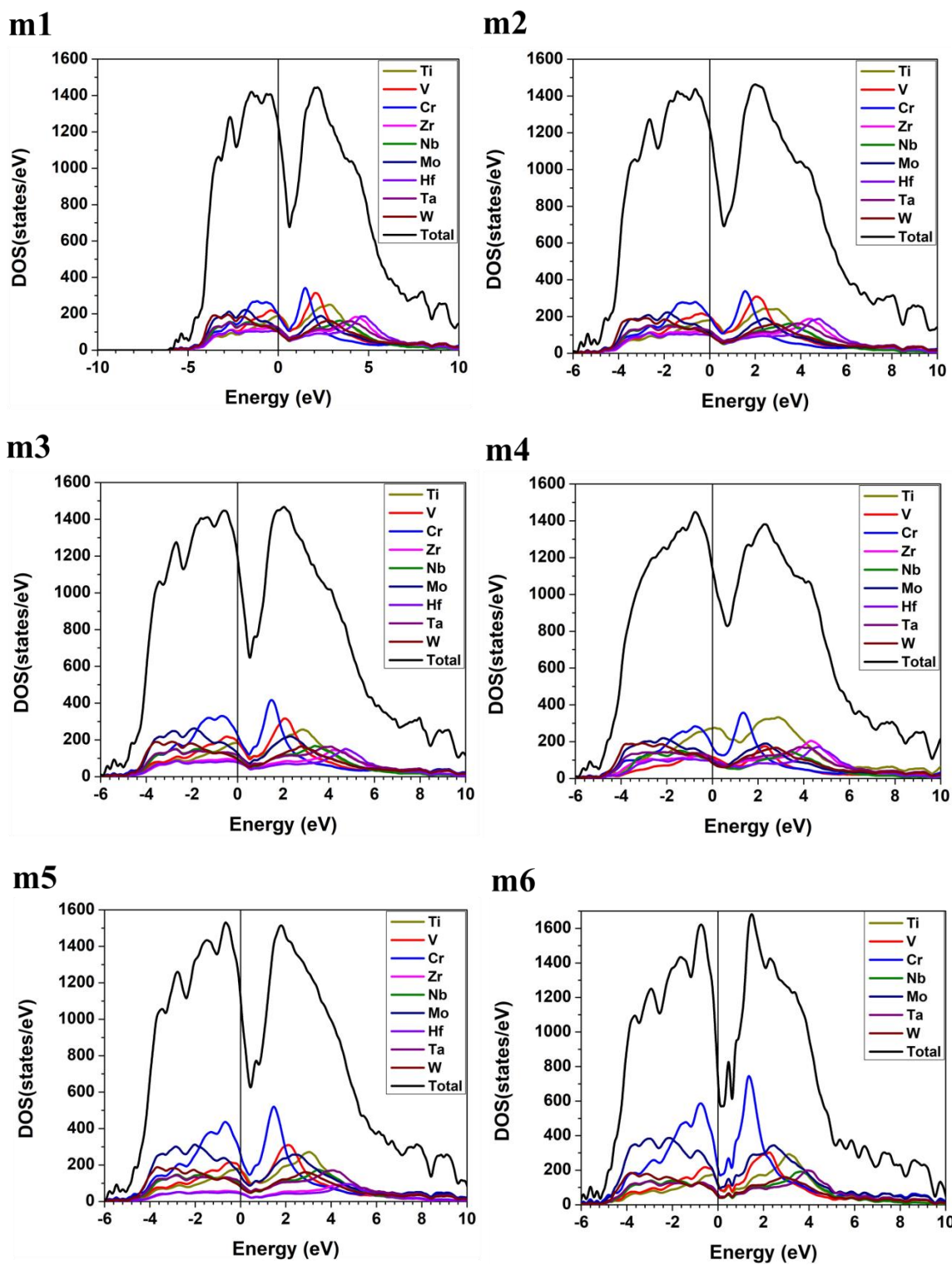
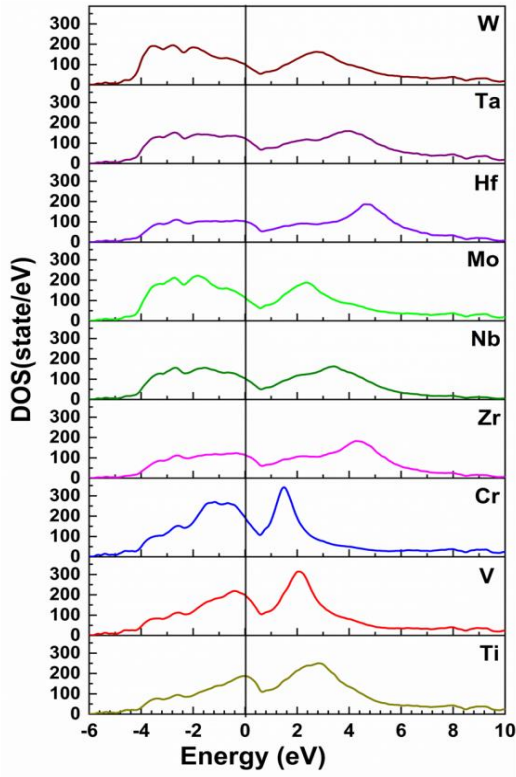
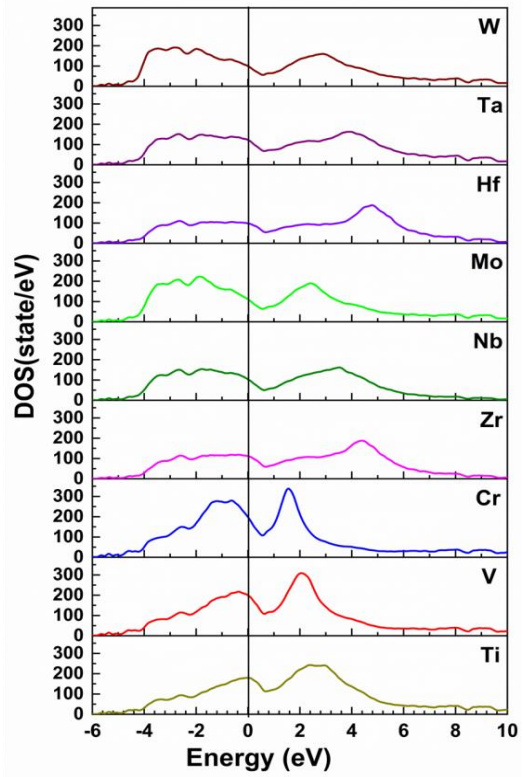


Figure S1. Calculated total density of states (TDOS) and partial density of states (PDOS) of the six RHEAs models at the range from -6 eV to 10 eV.

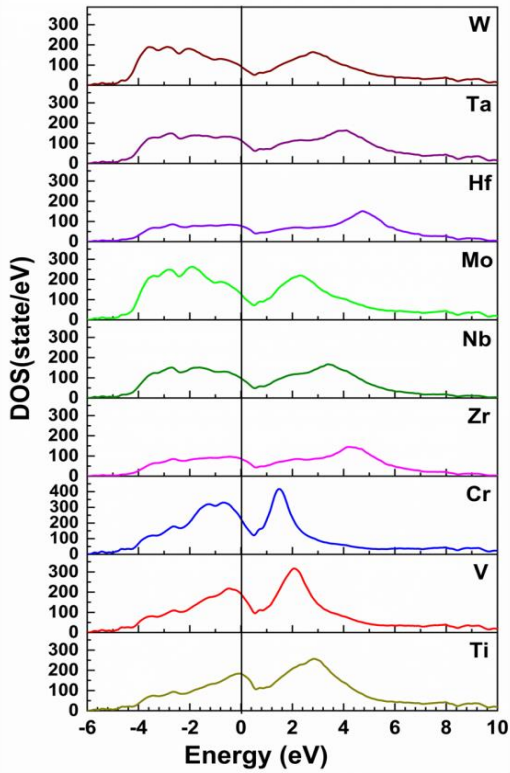
m1



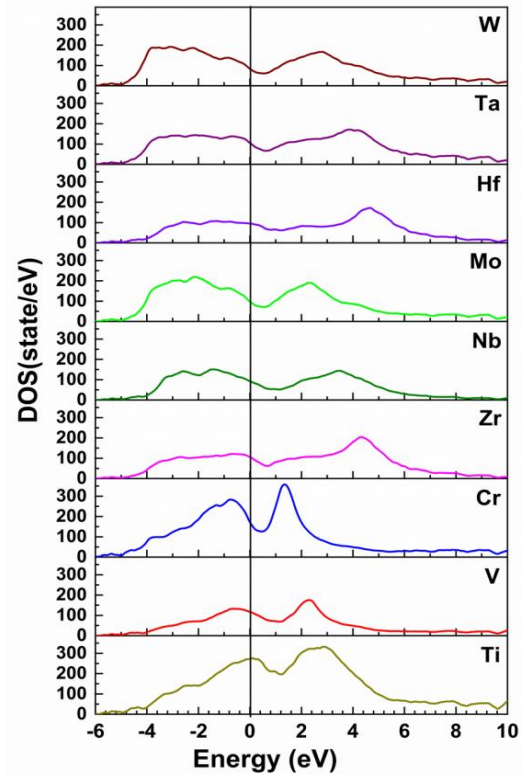
m2



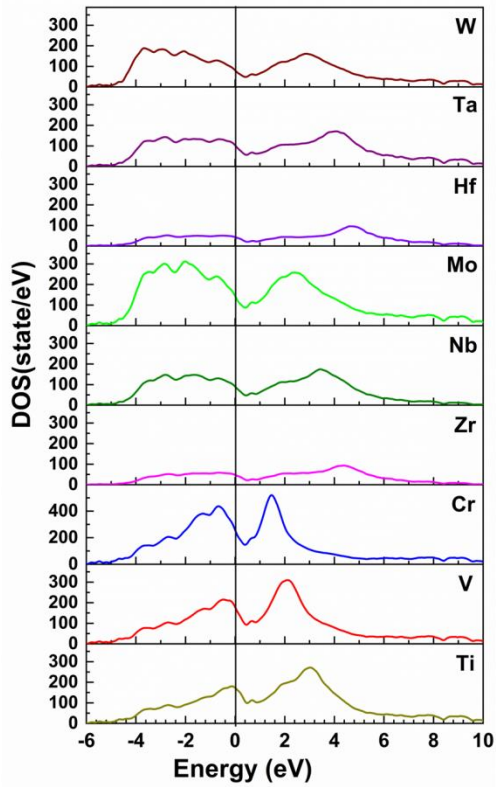
m3



m4



m5



m6

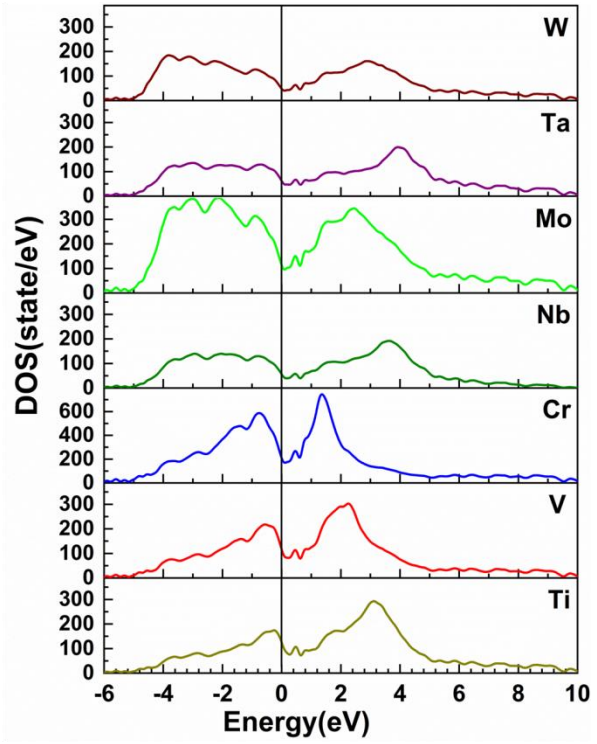


Figure S2. Calculated partial density of states (PDOS) of each element in the six RHEAs models at the range from -6 eV to 10 eV.

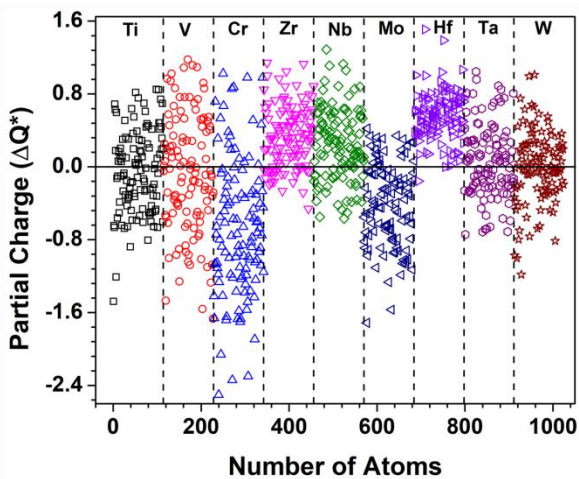
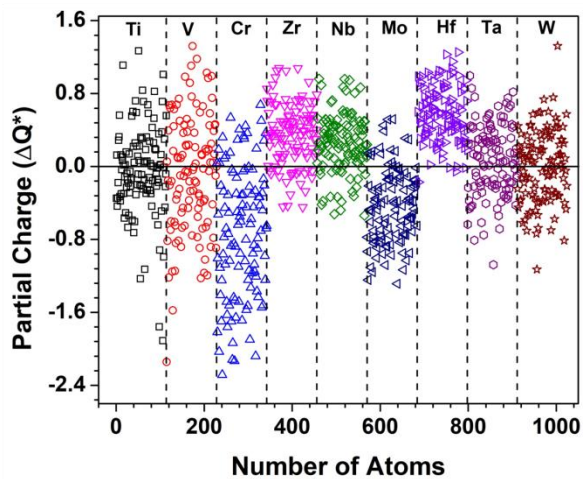
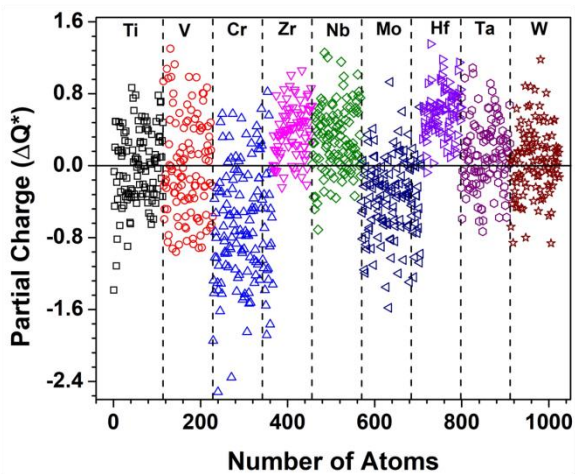
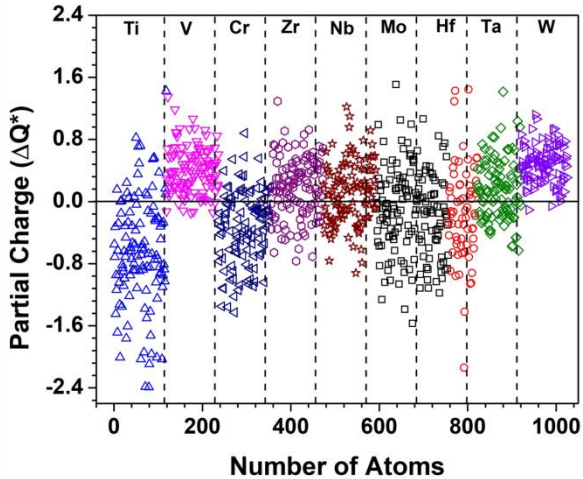
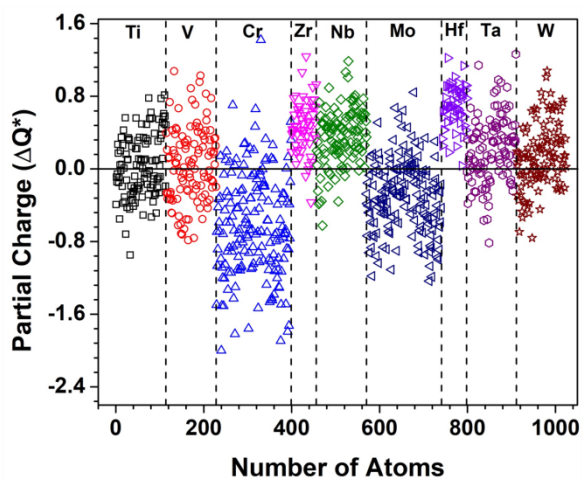
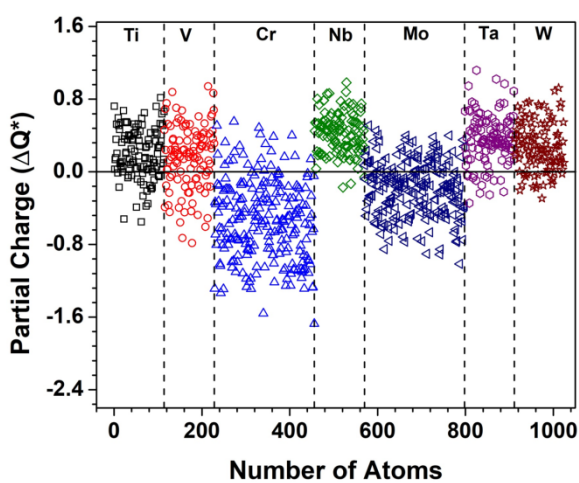
m1**m2****m3****m4****m5****m6**

Figure S3. Distribution of partial charge (PC) in the six RHEAs models.

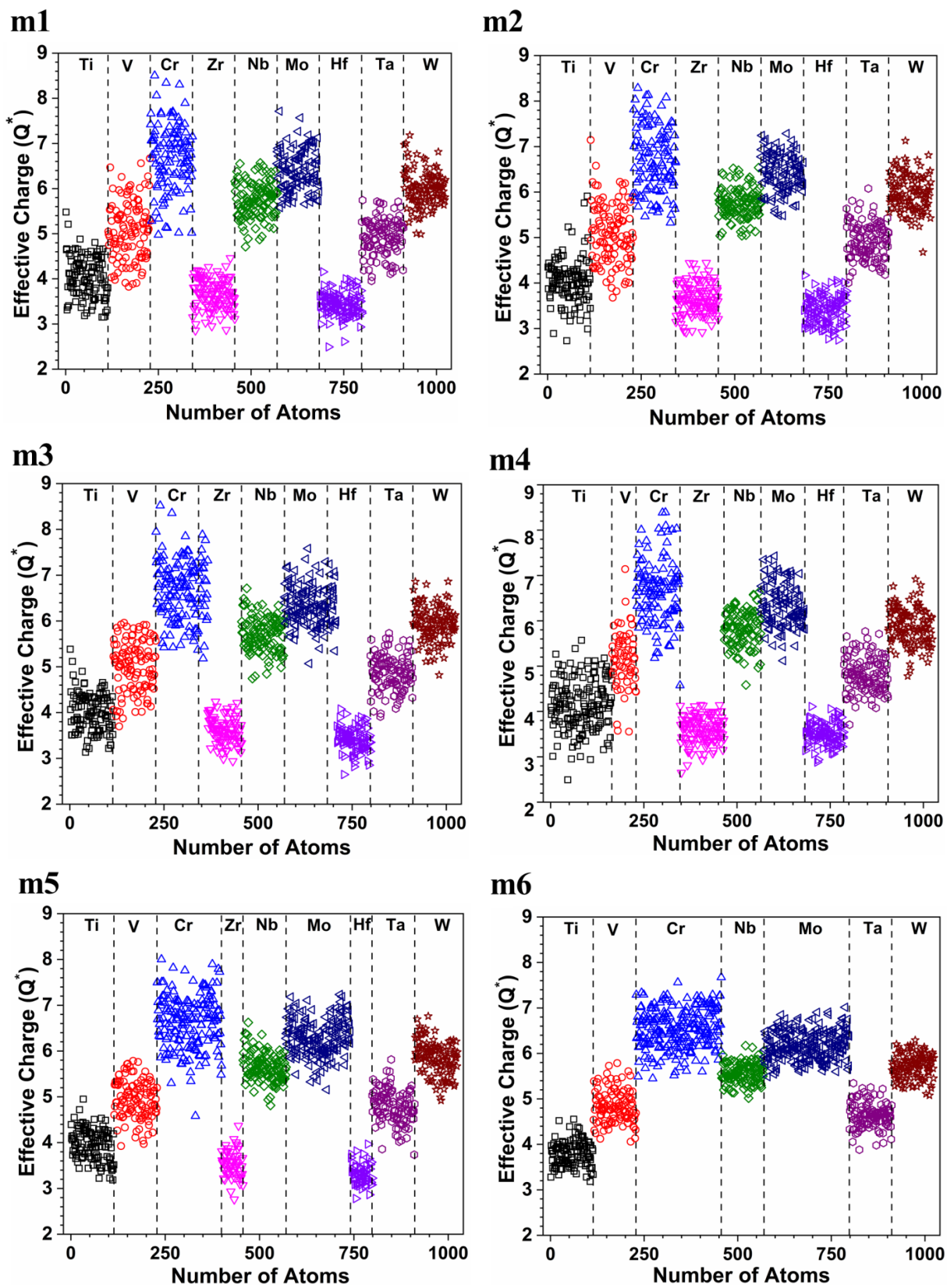
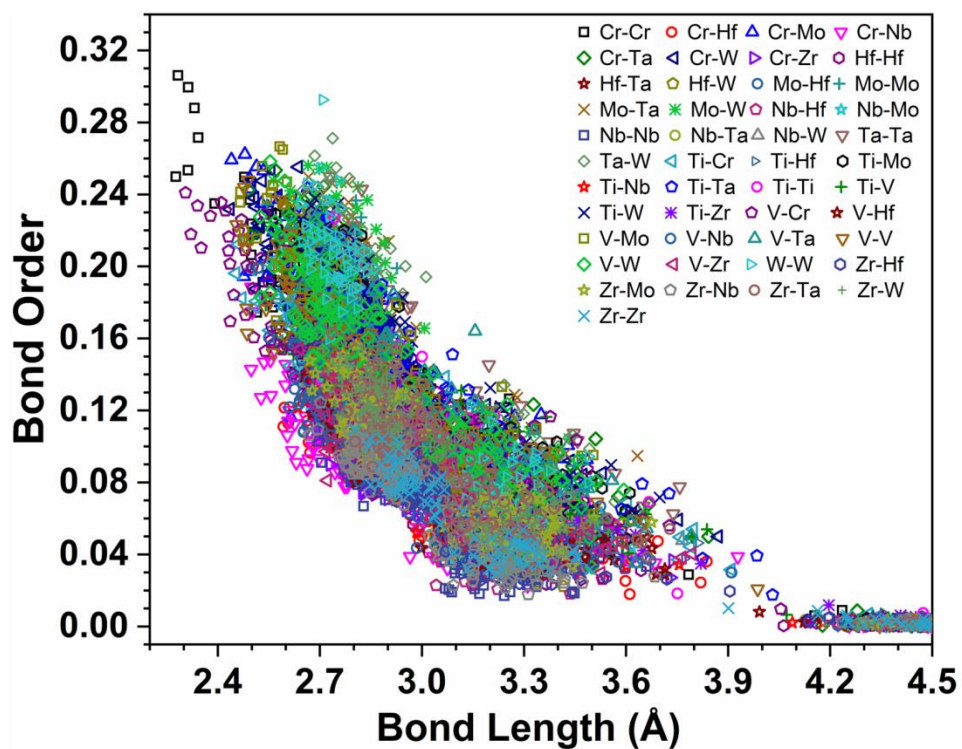
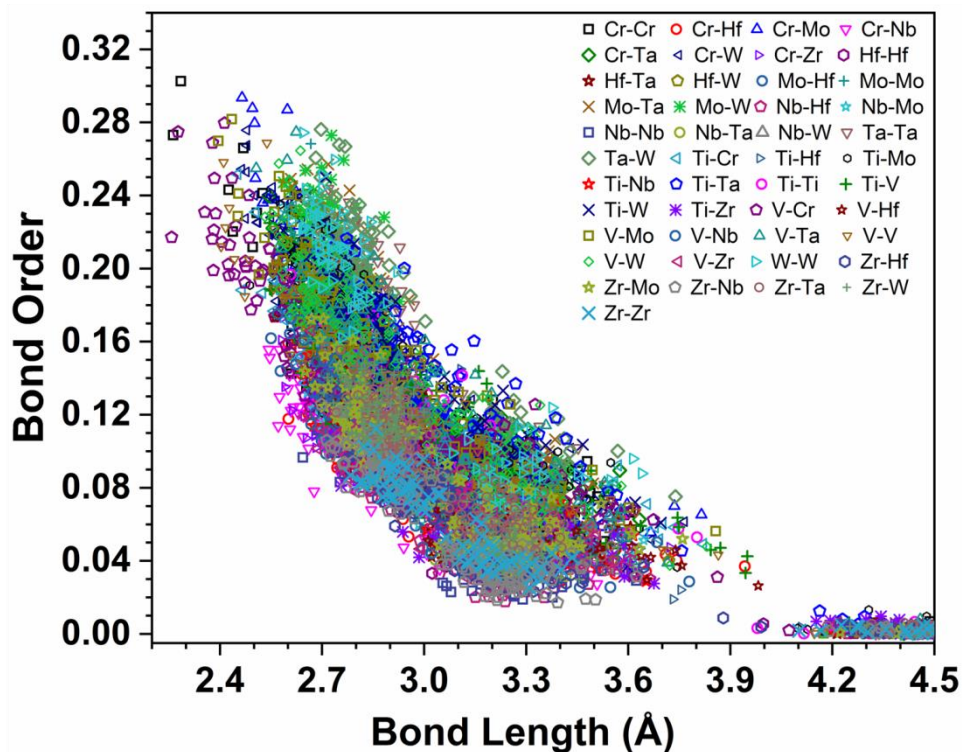


Figure S4. Distribution of effective charge (Q^*) in the six RHEAs models.

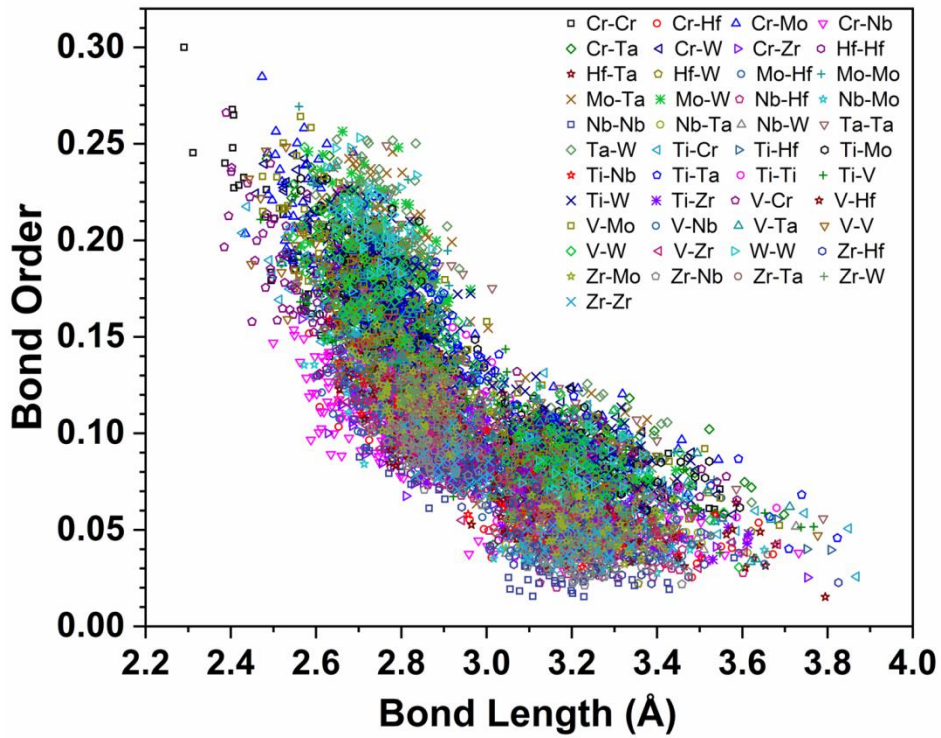
m1



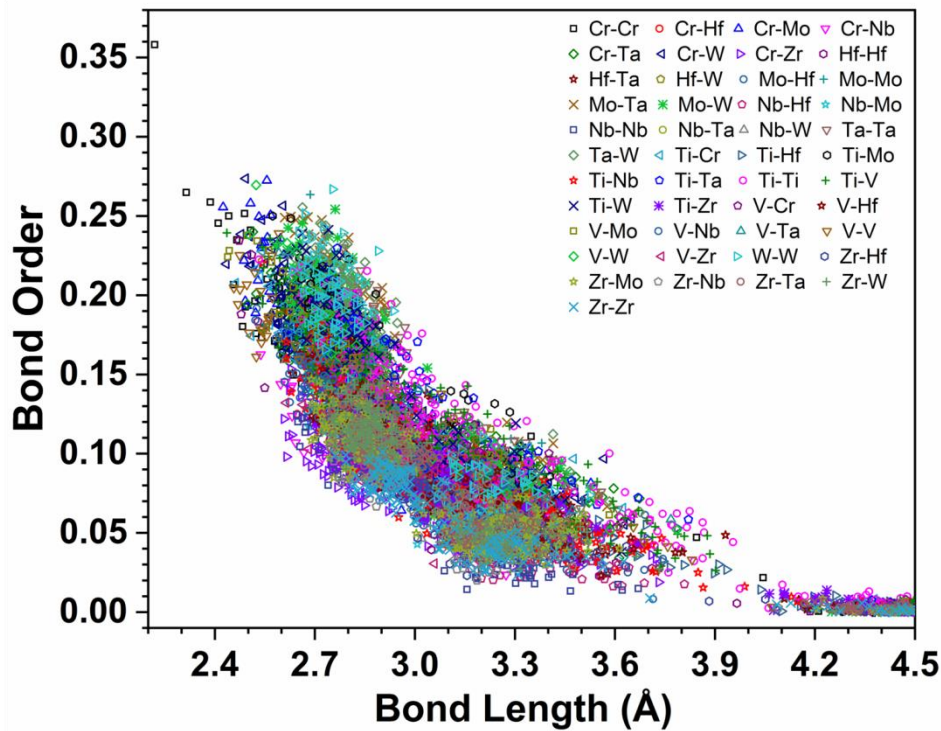
m2



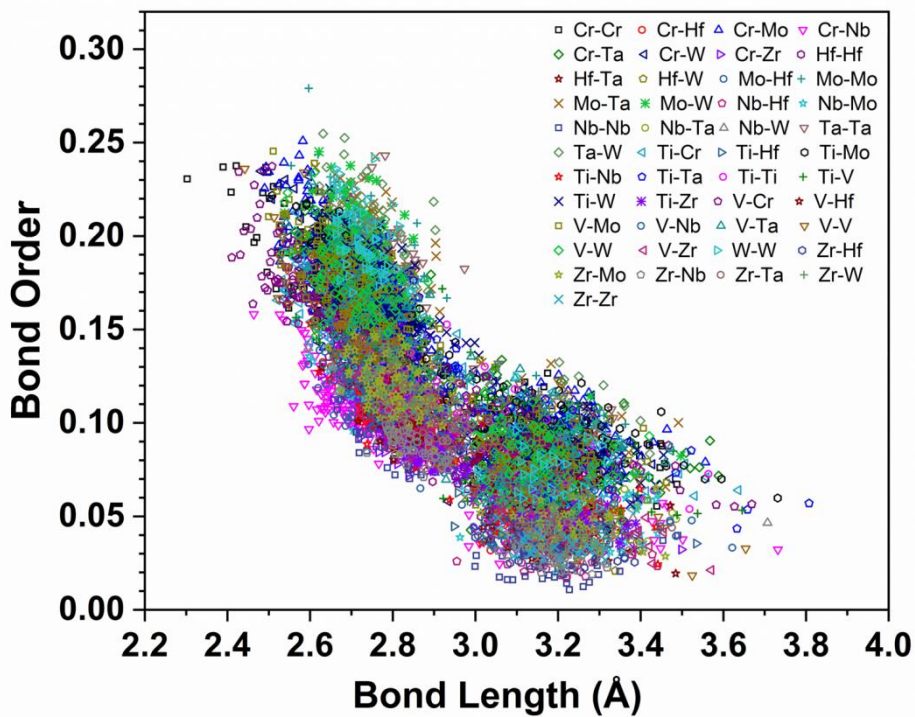
m3



m4



m5



m6

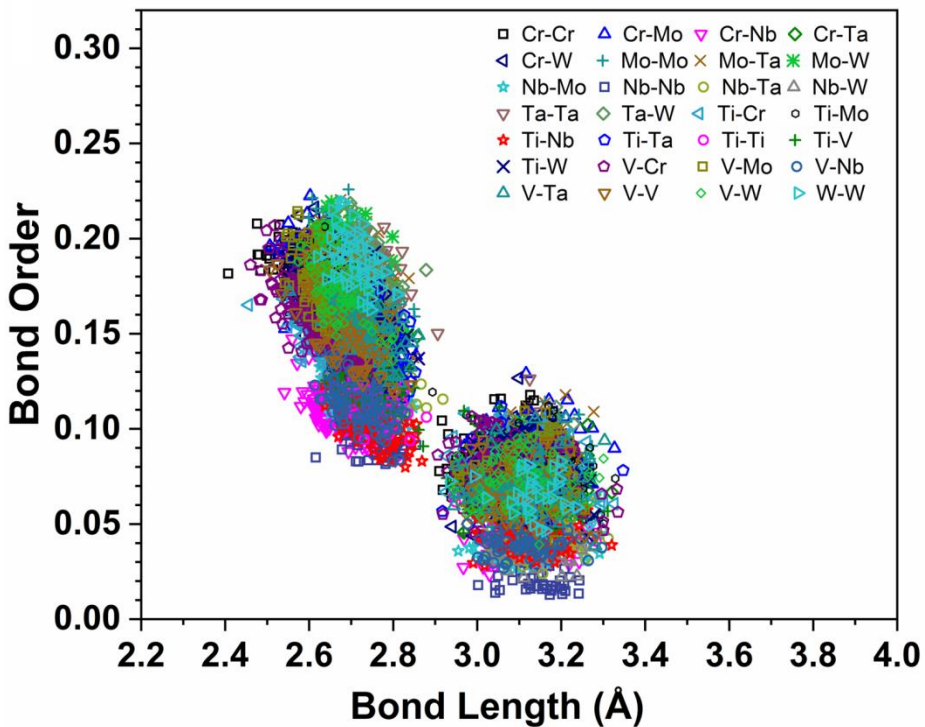
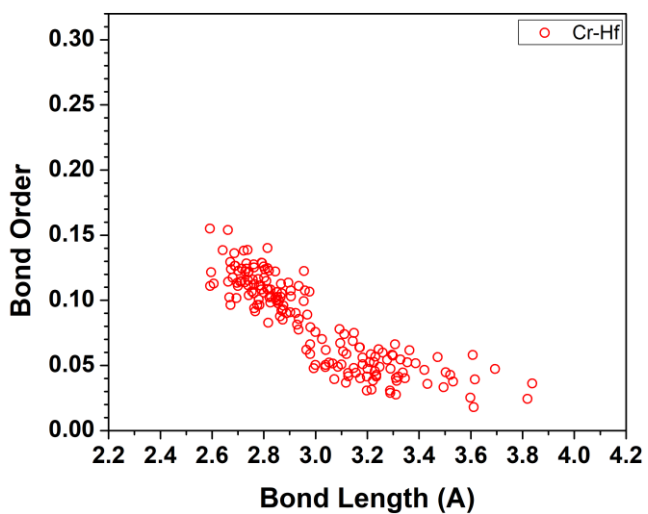
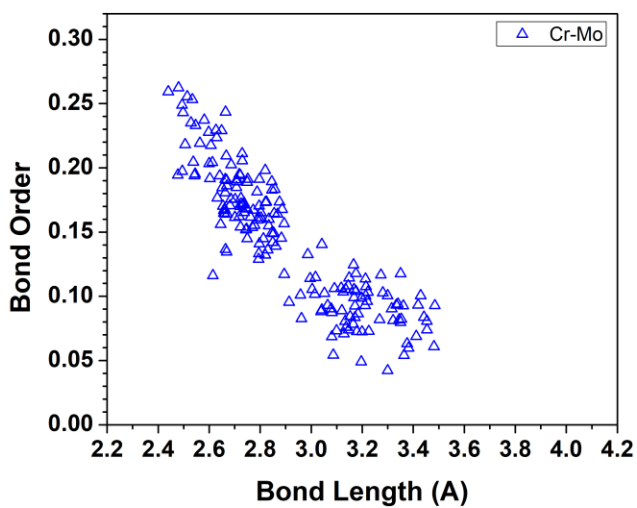
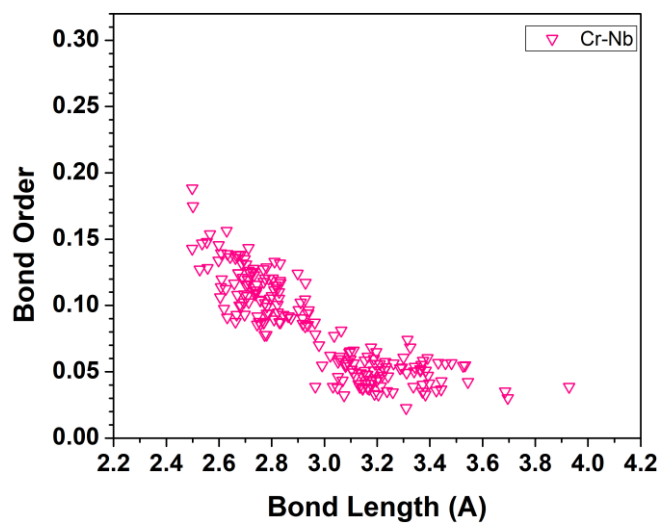
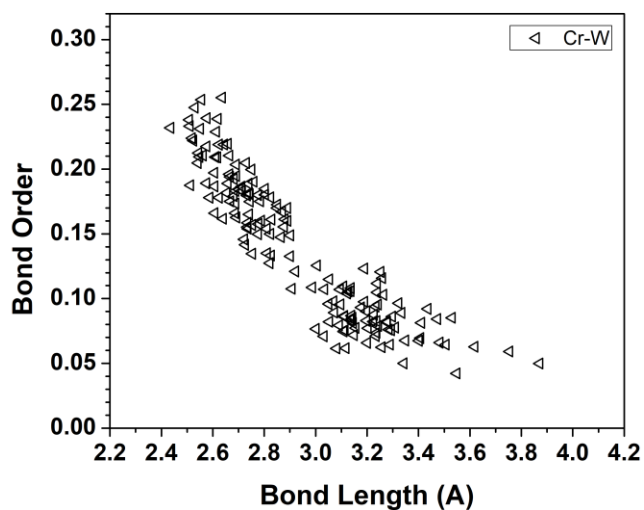
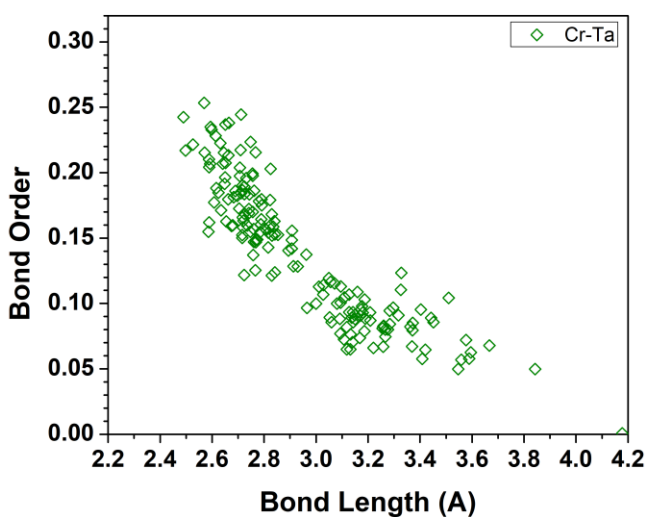
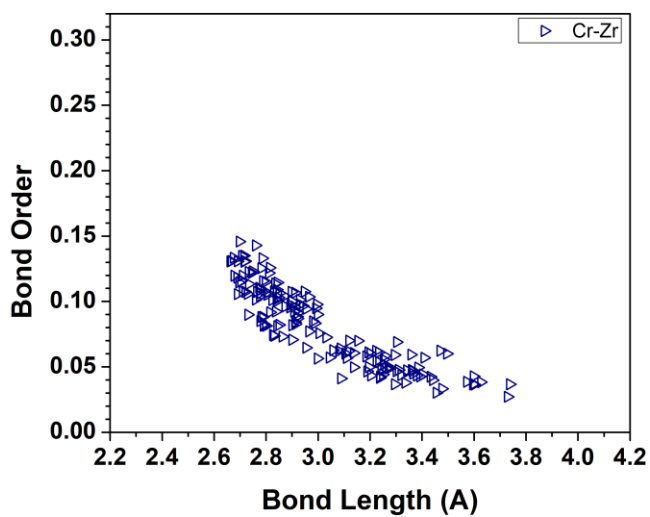
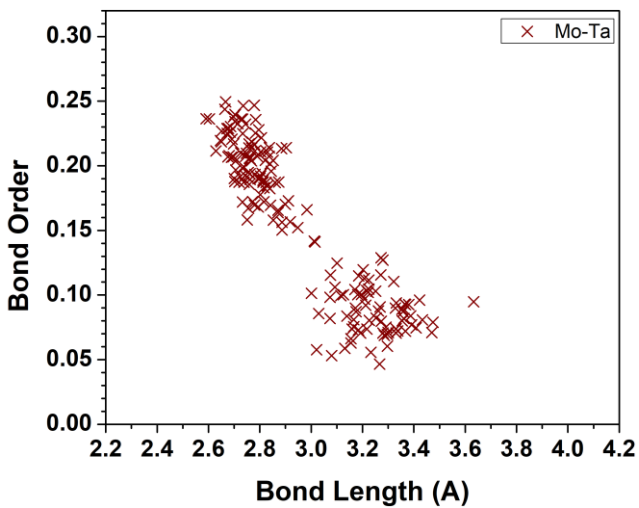
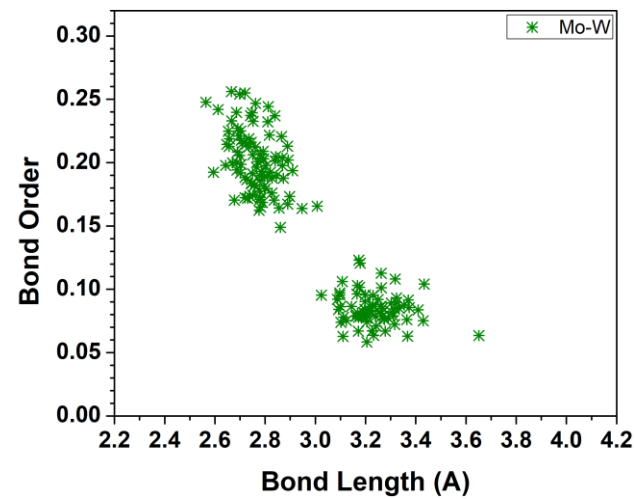
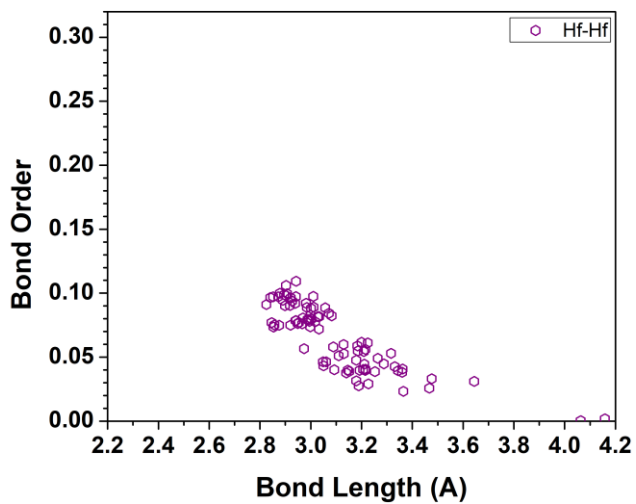
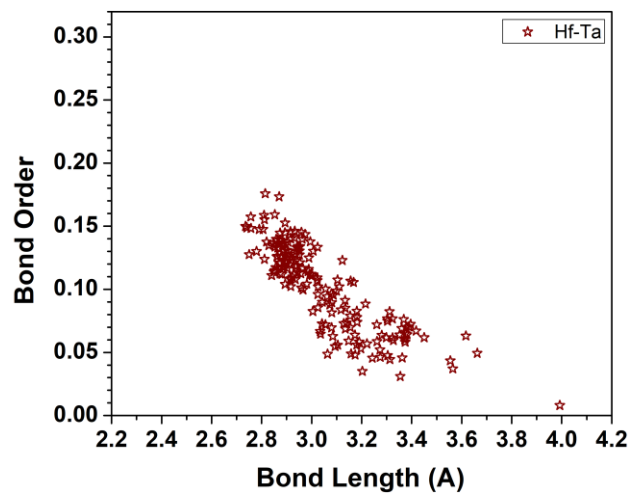
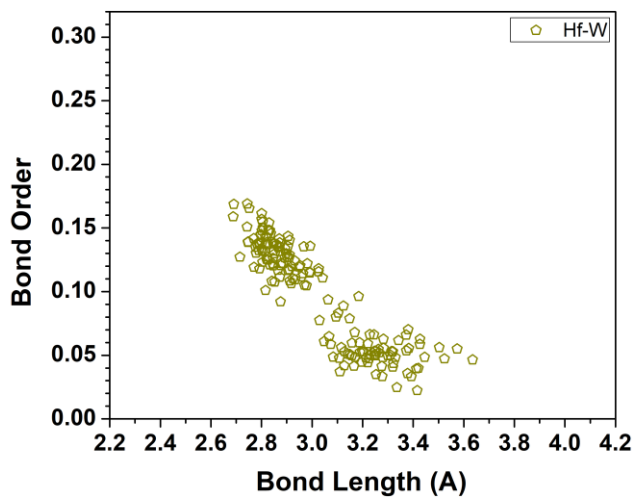
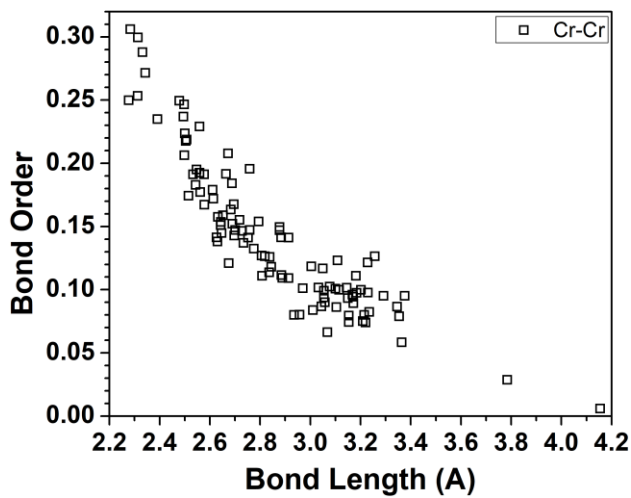
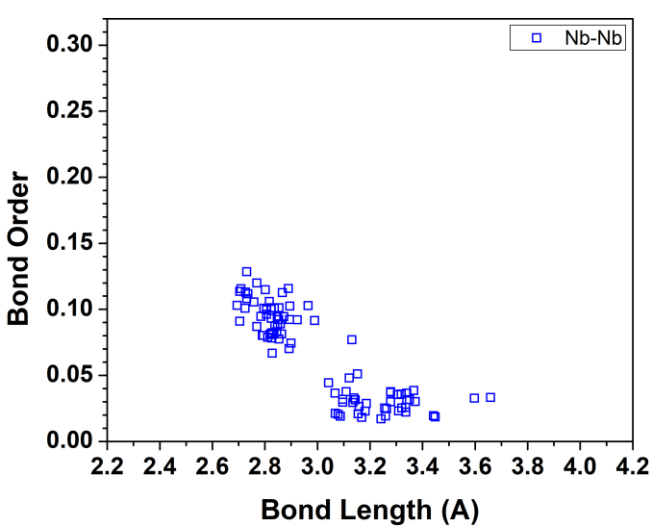
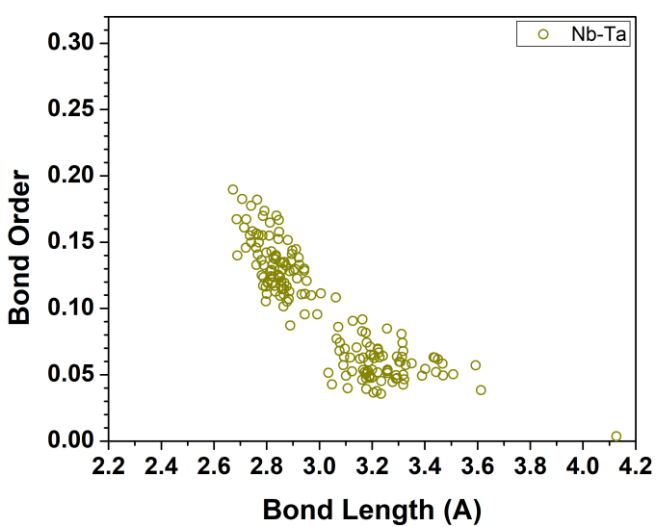
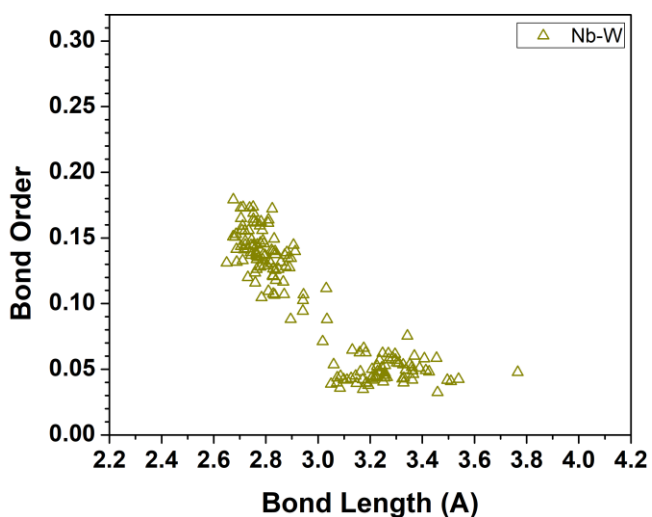
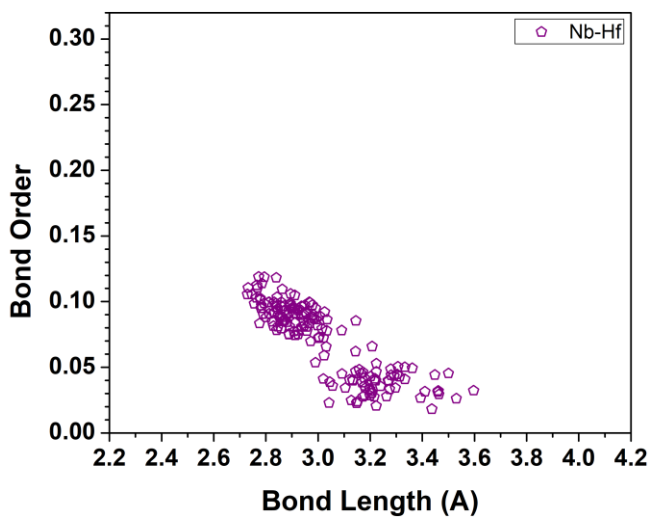
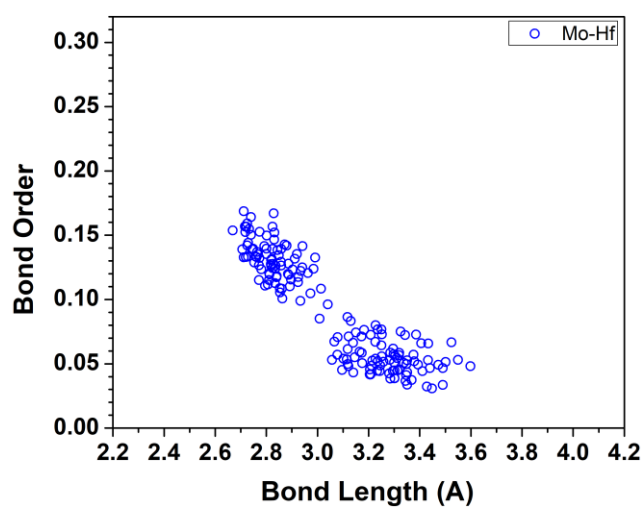
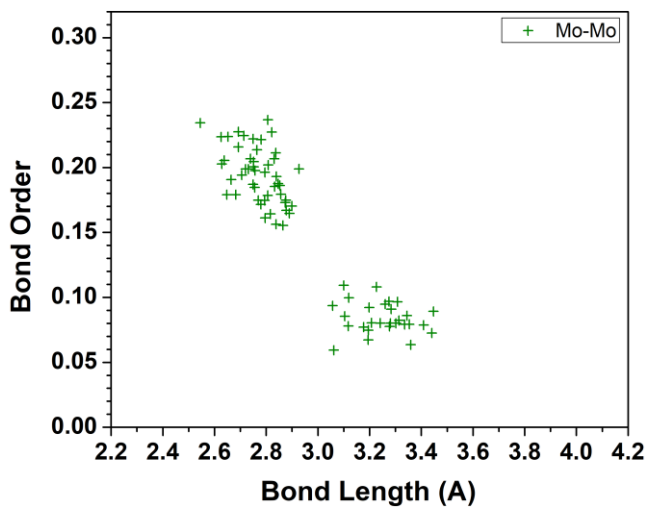


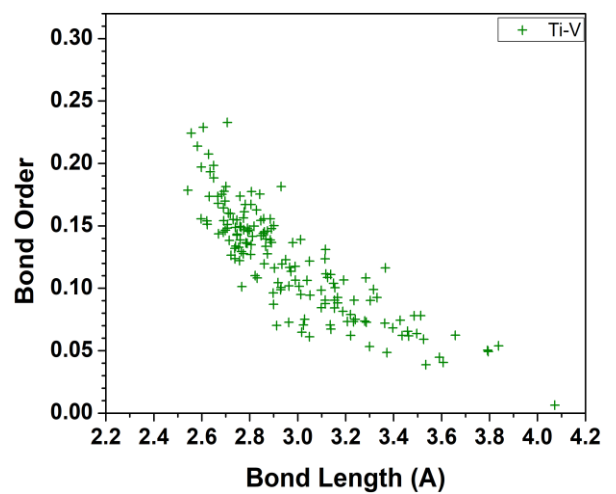
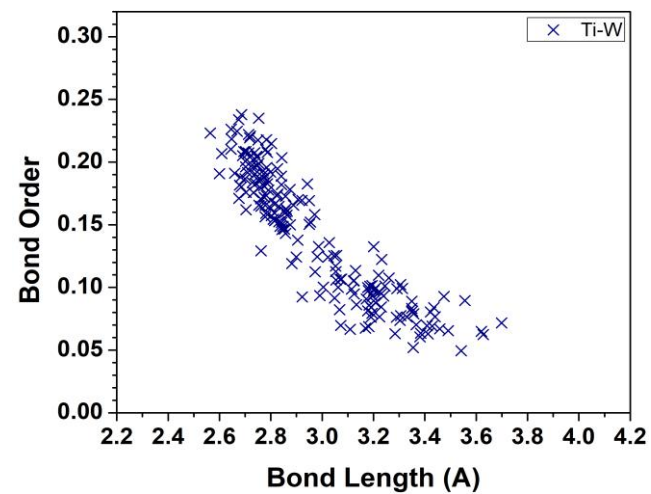
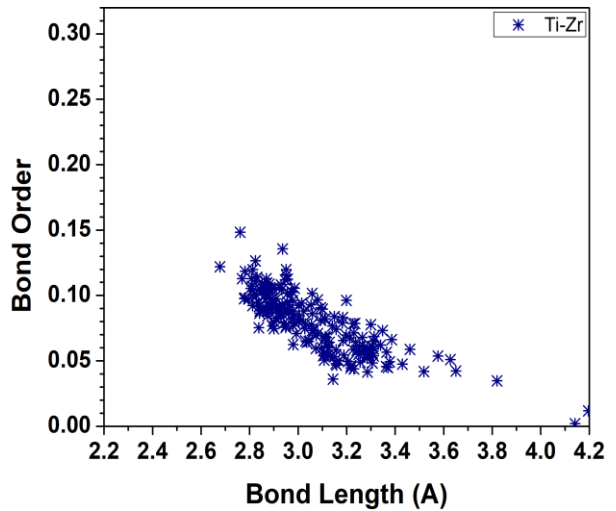
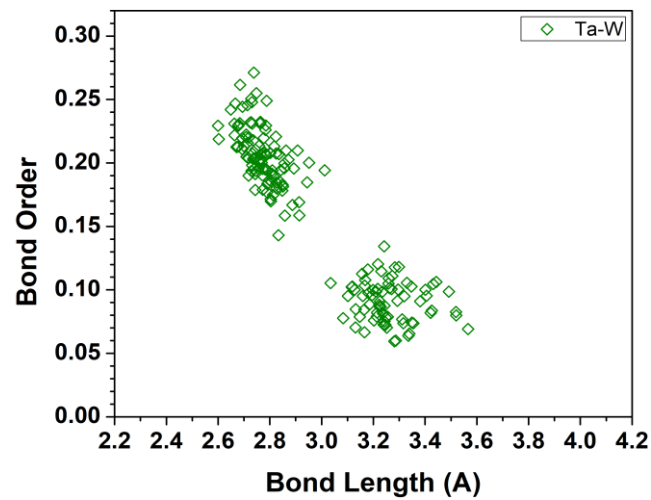
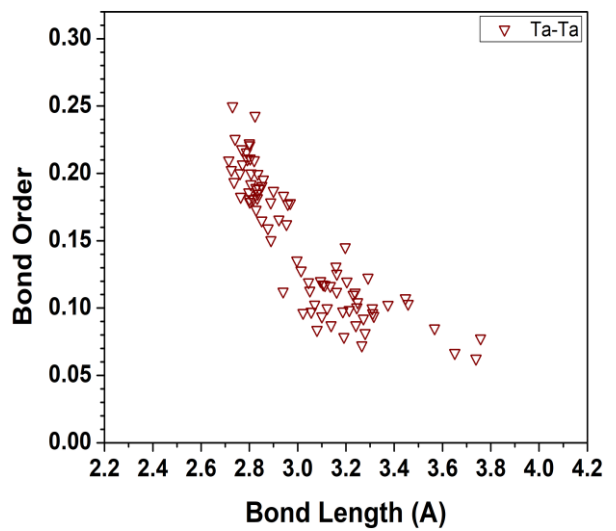
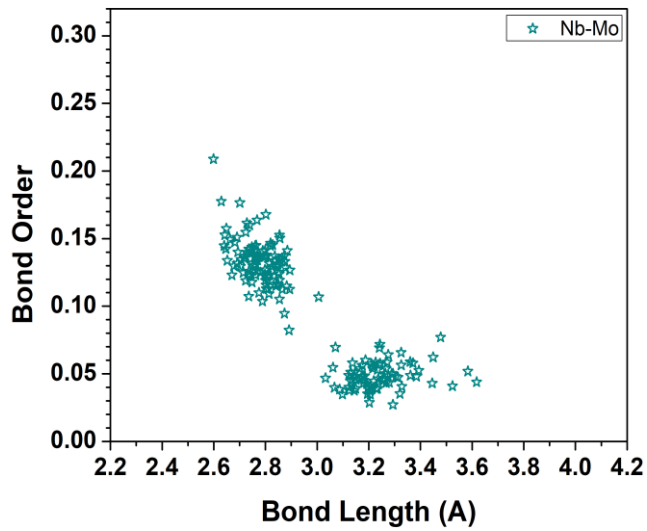
Figure S5. Bond order (BO) versus bond length (BL) distribution in the six RHEAs models.

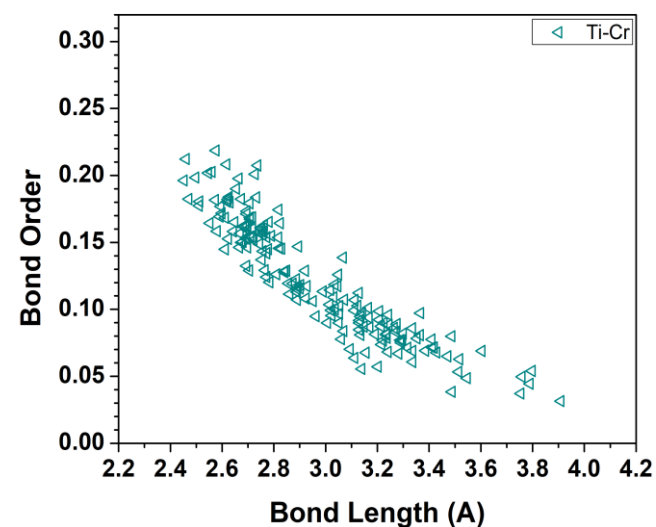
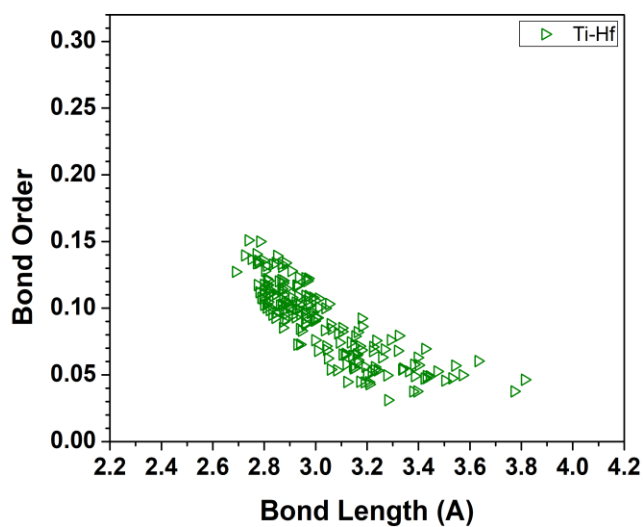
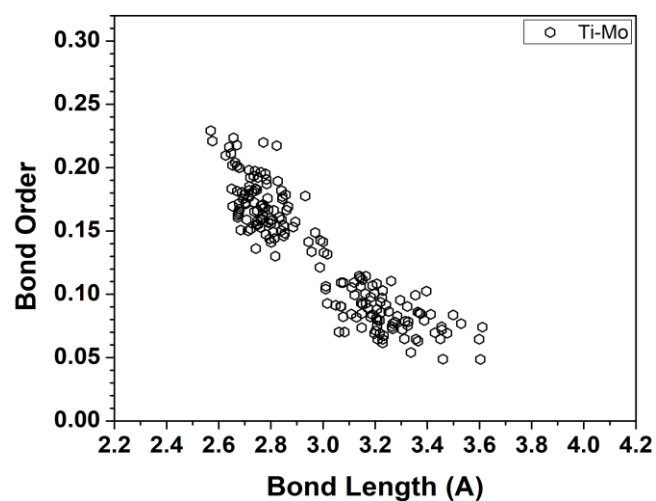
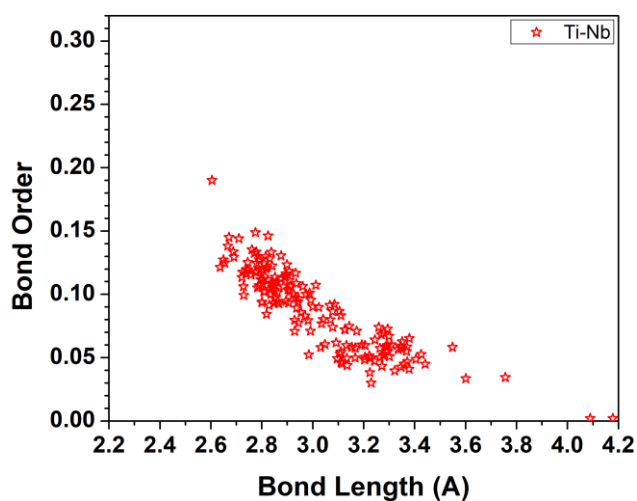
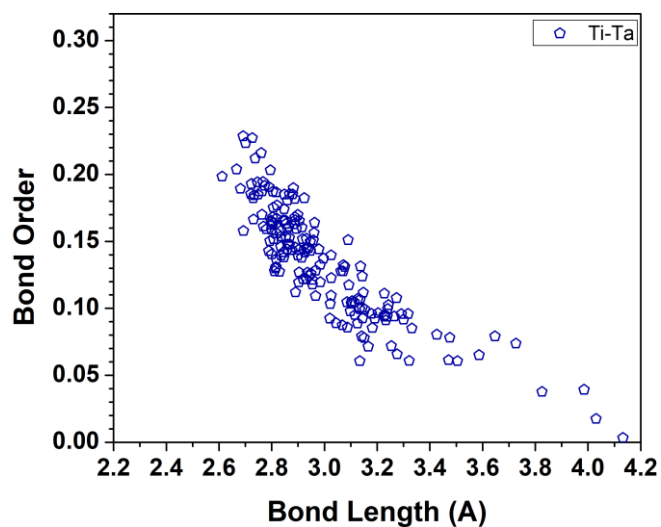
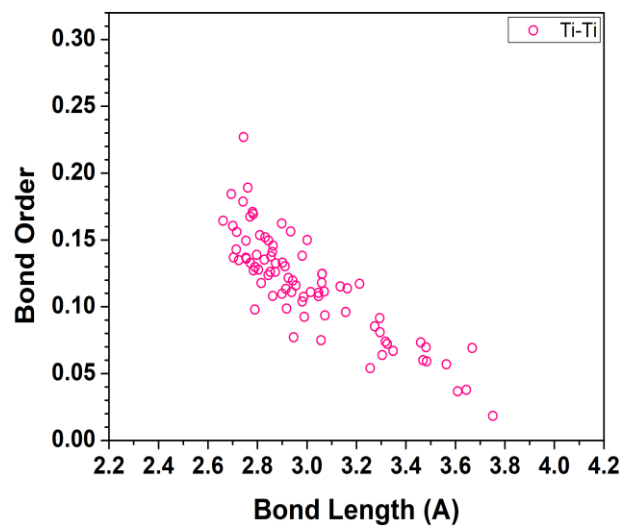
m1

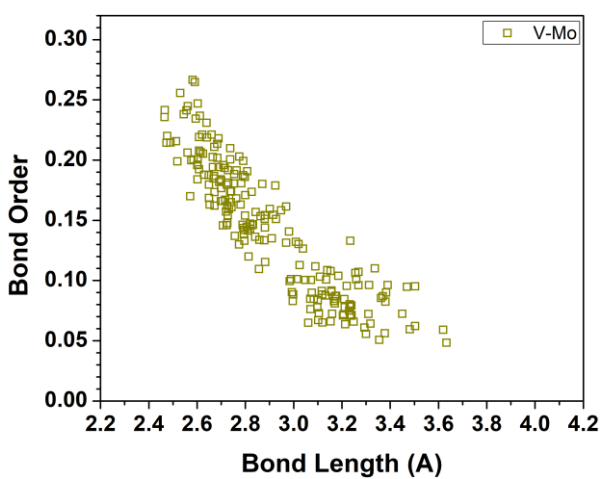
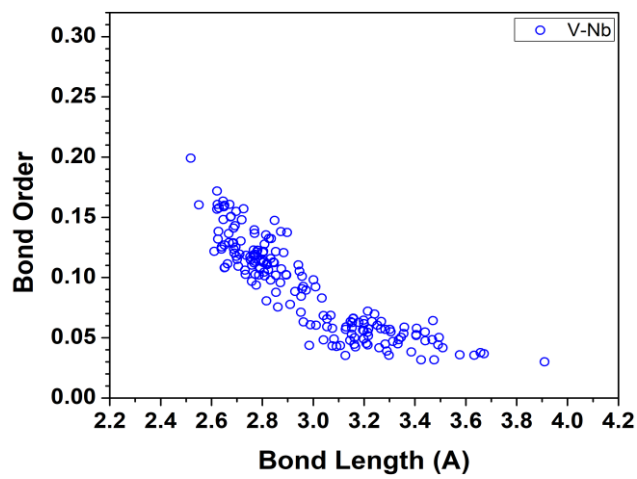
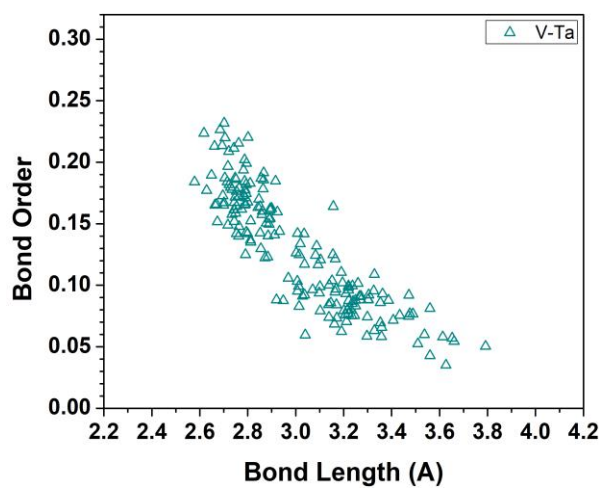
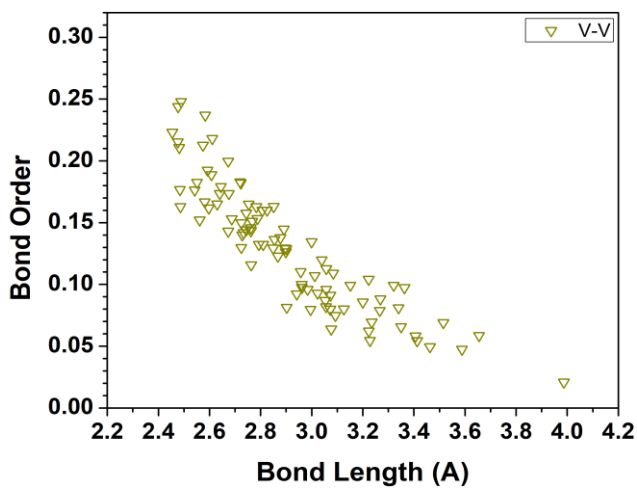
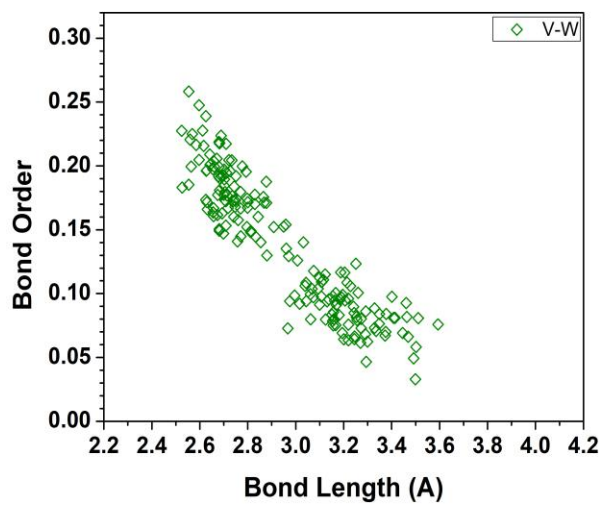
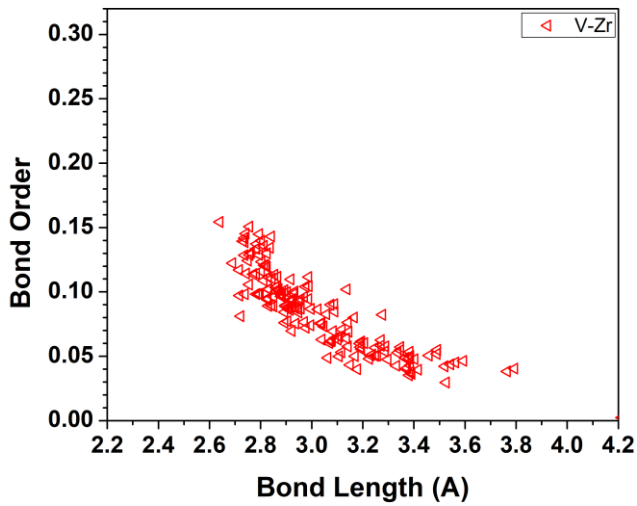


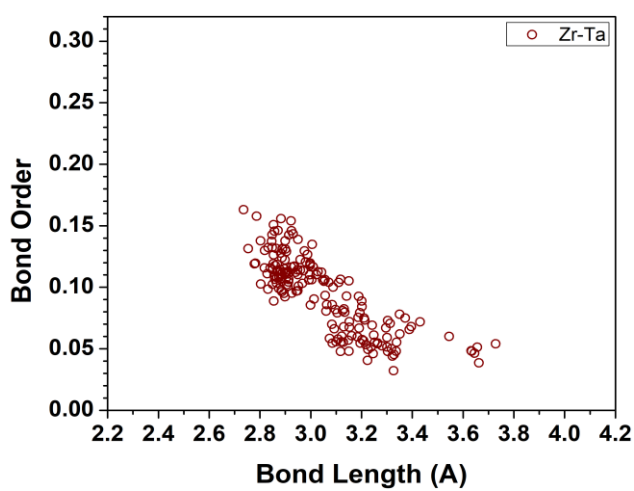
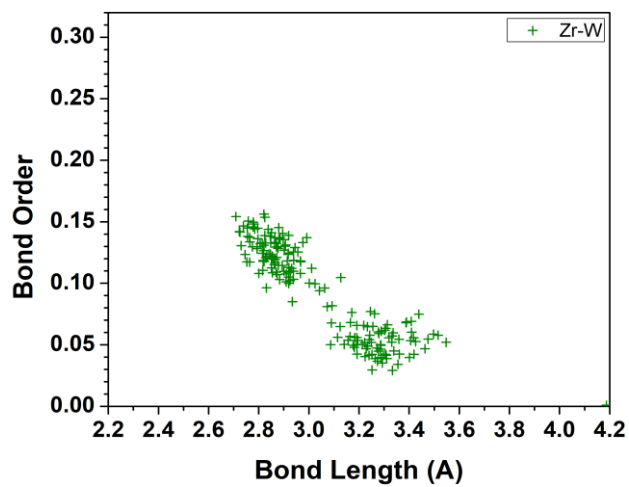
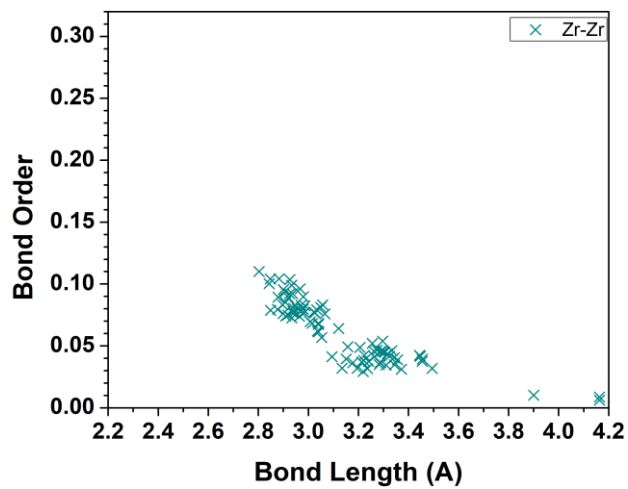
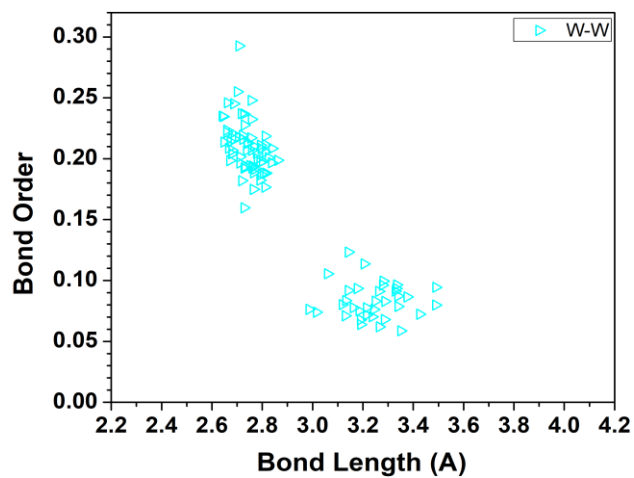
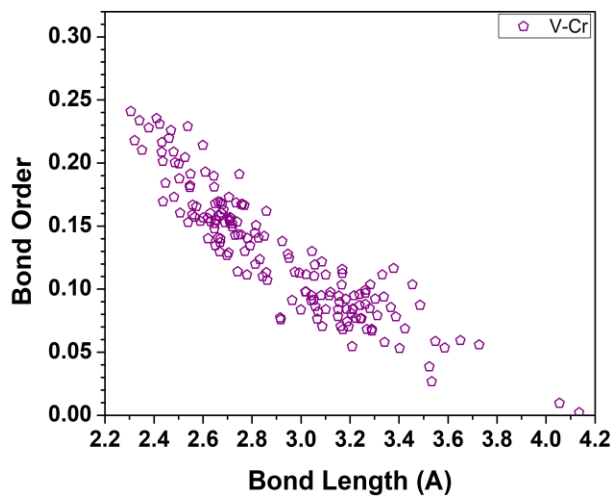
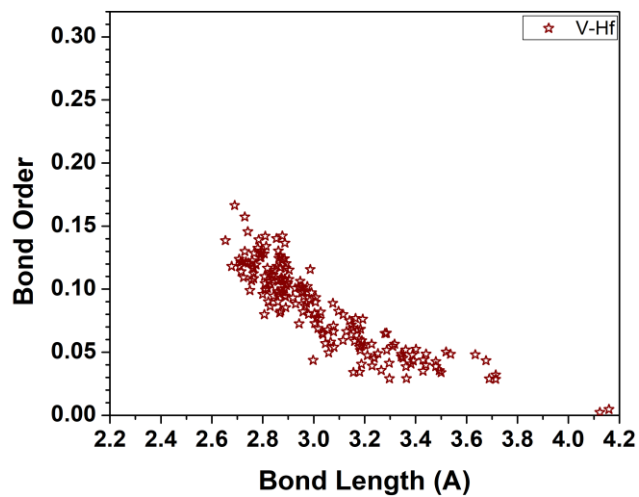


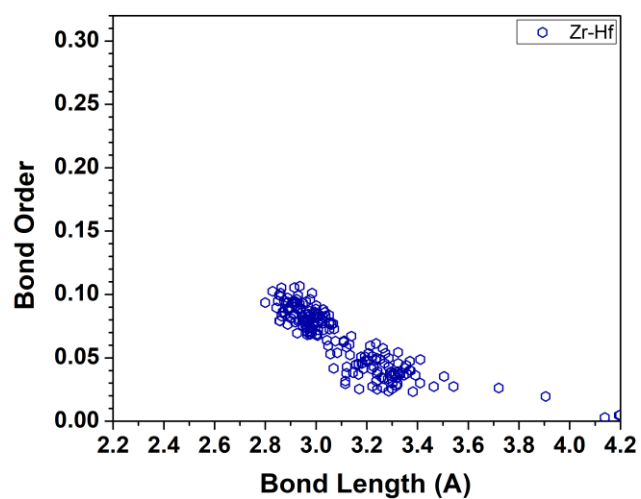
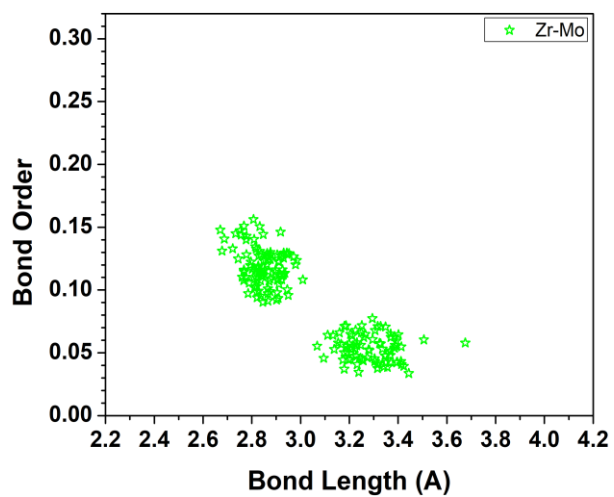
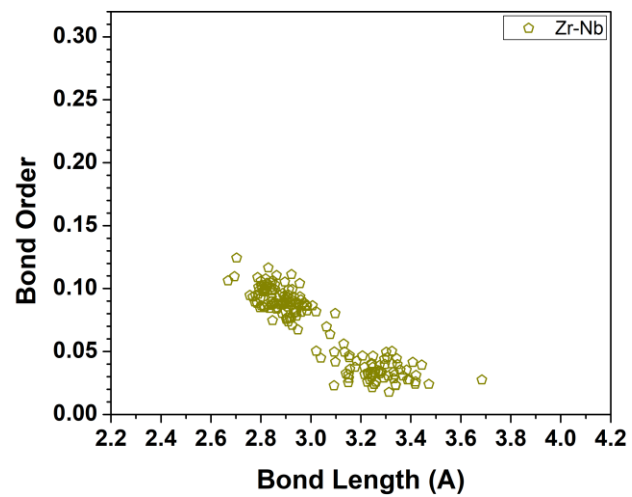




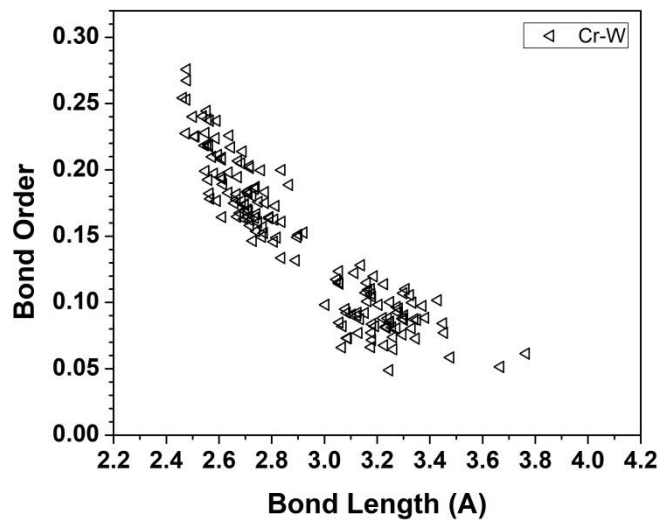
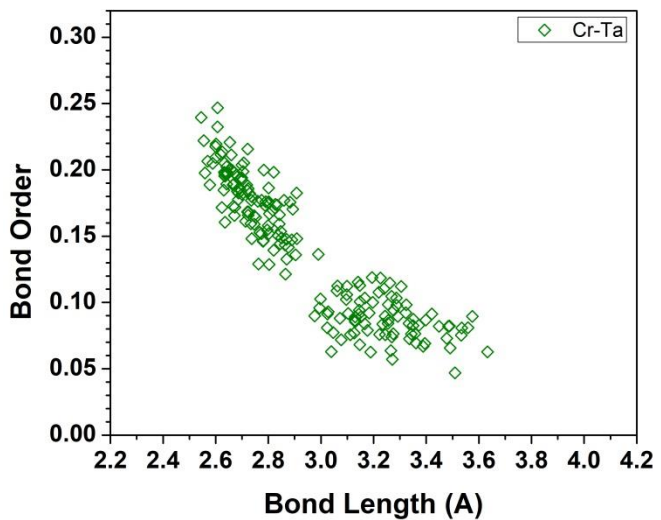
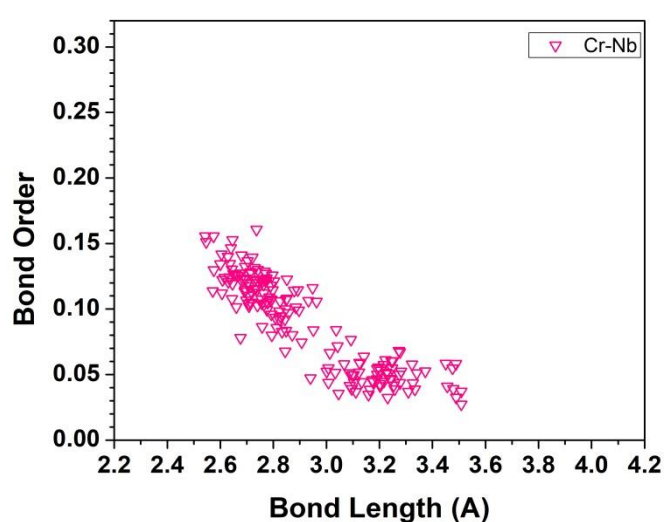
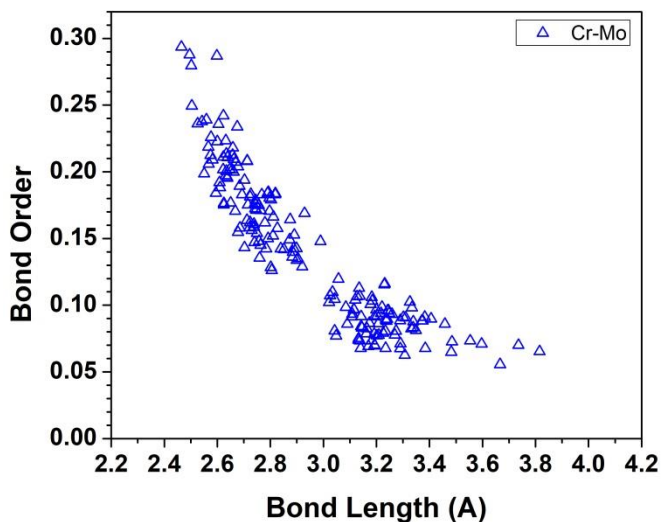
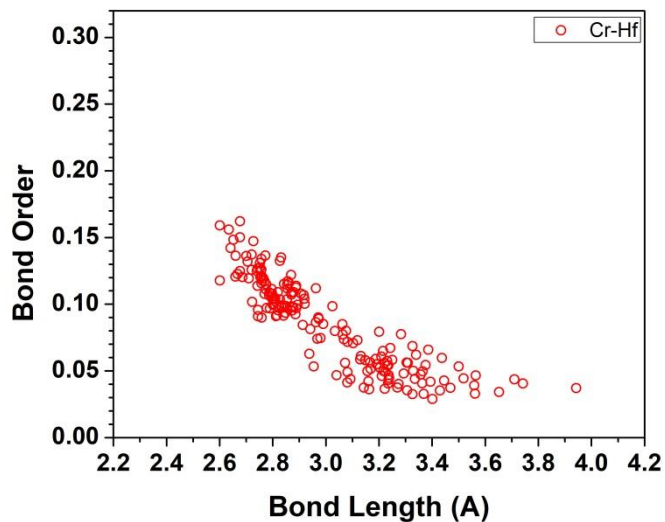
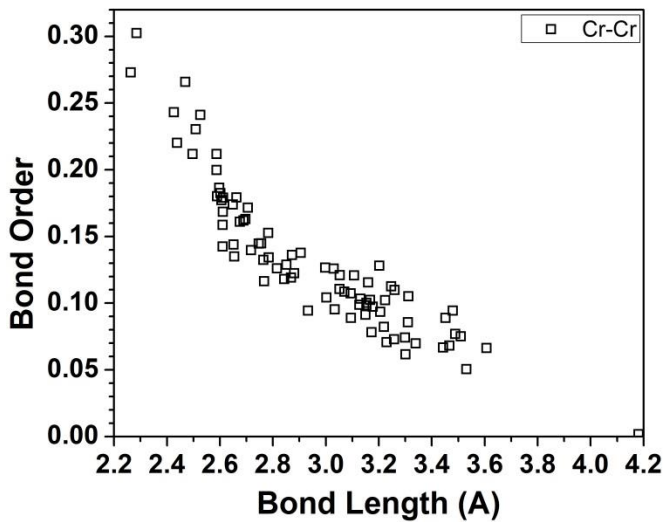


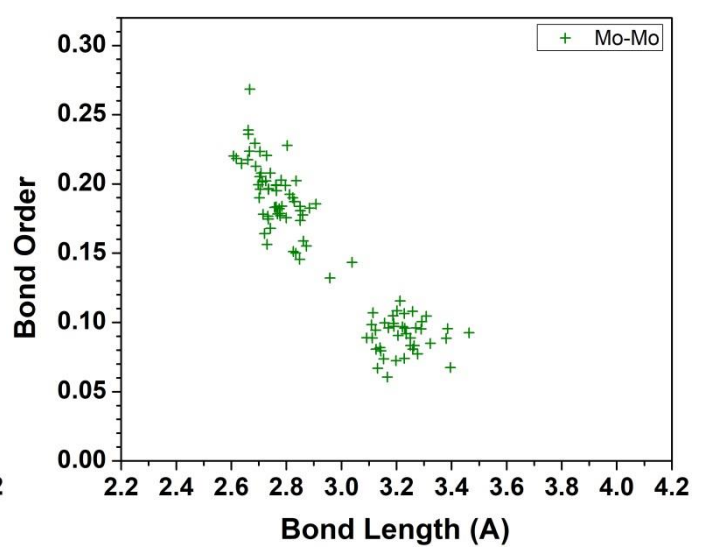
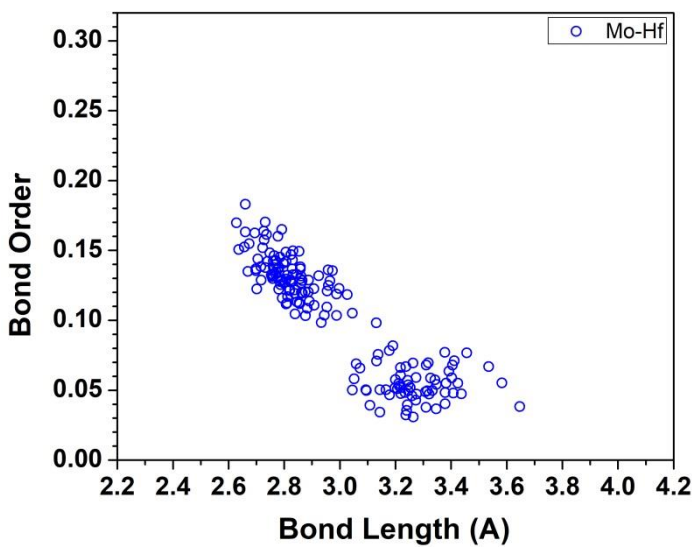
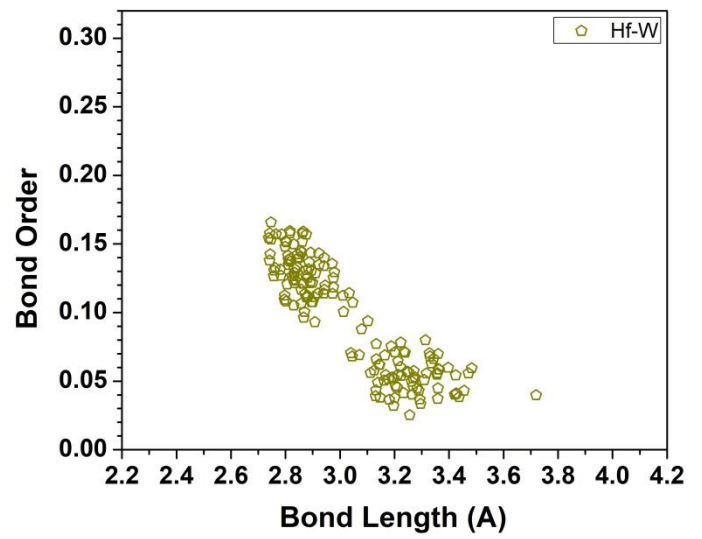
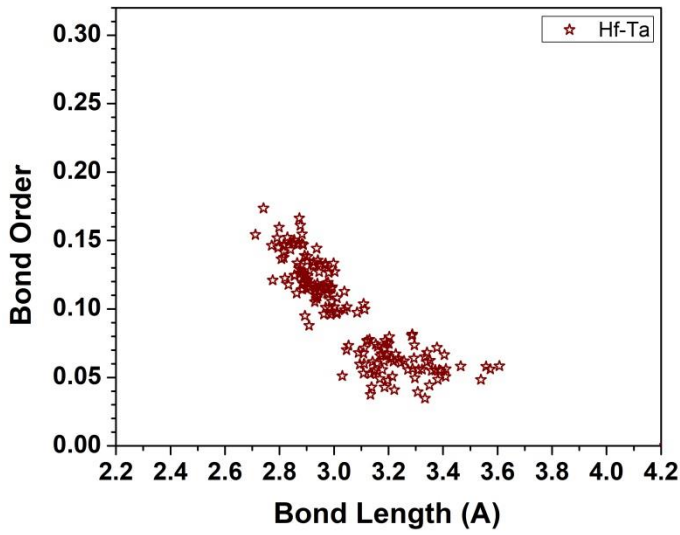
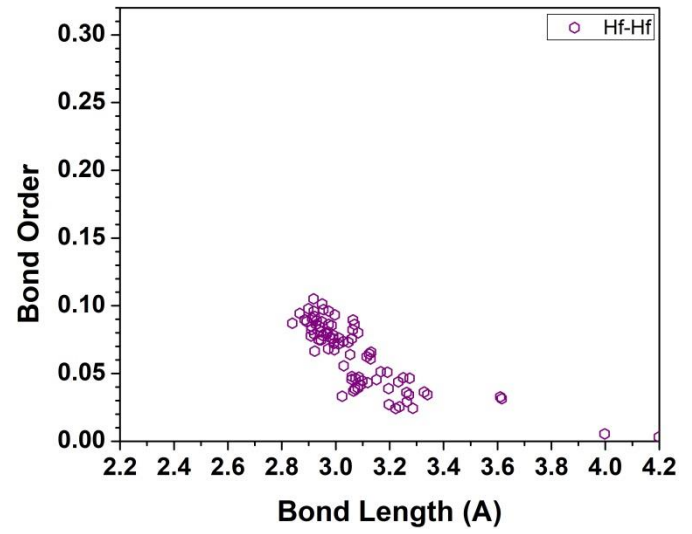
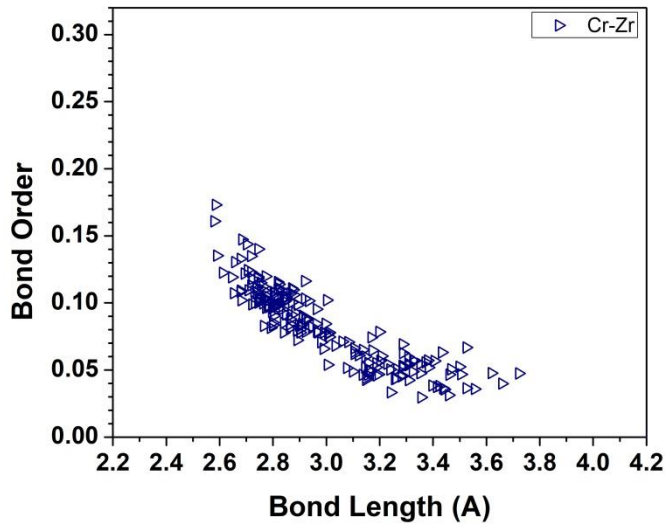


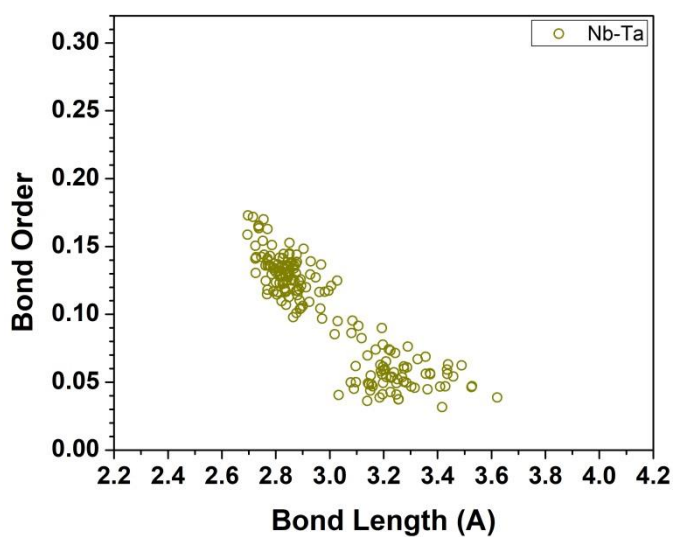
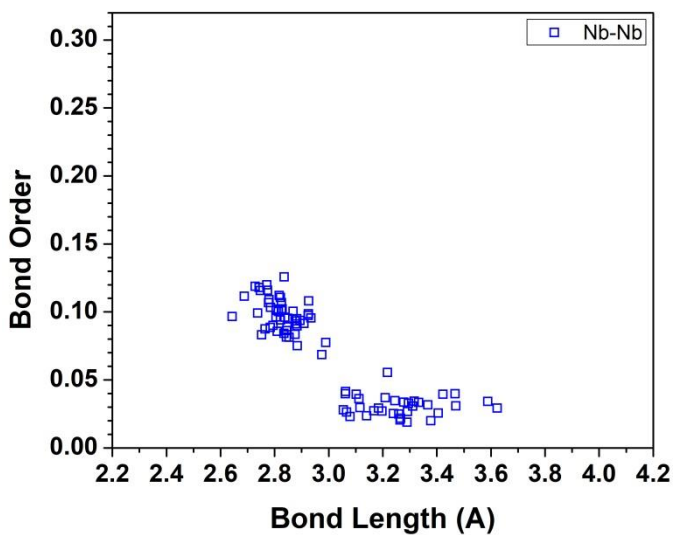
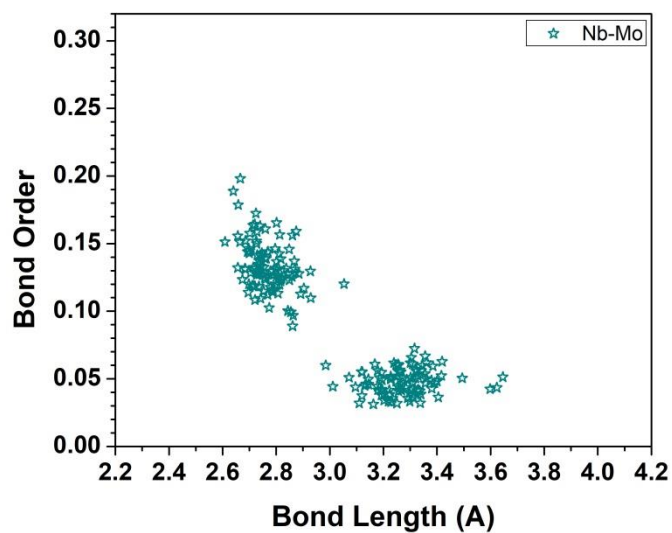
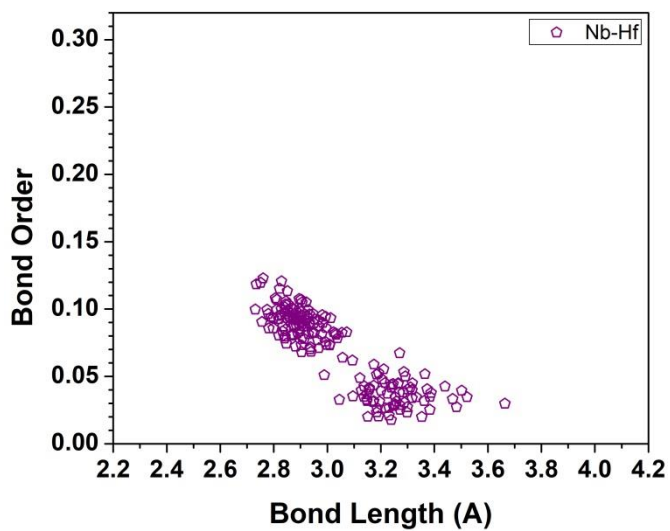
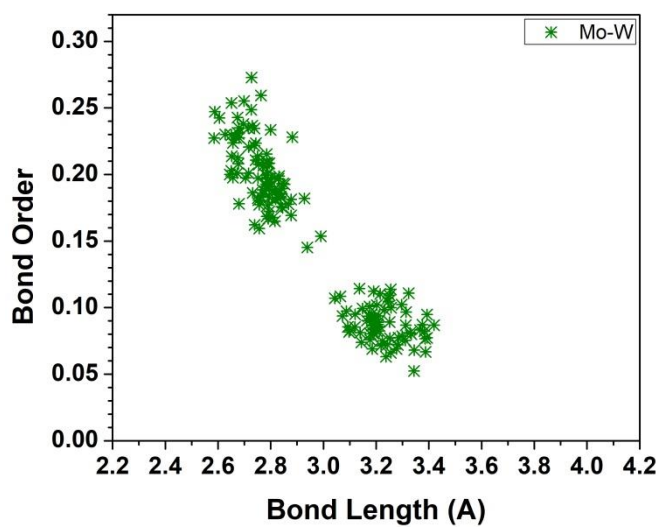
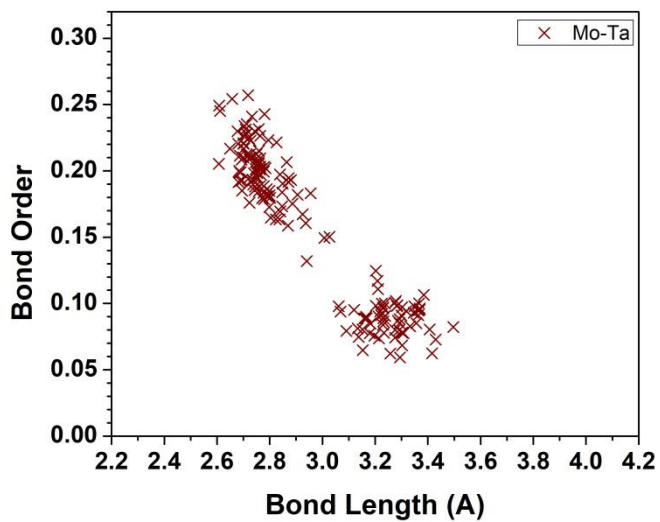


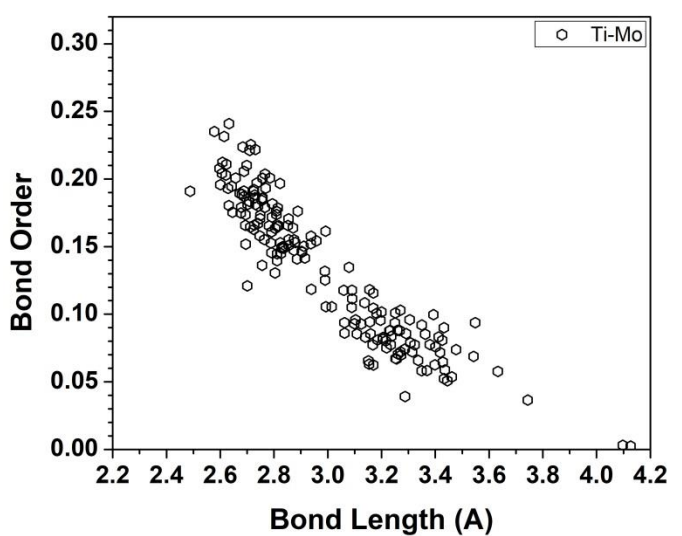
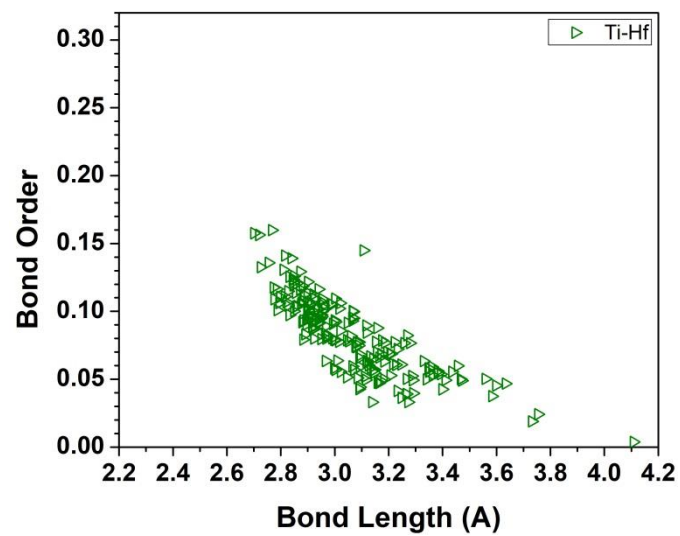
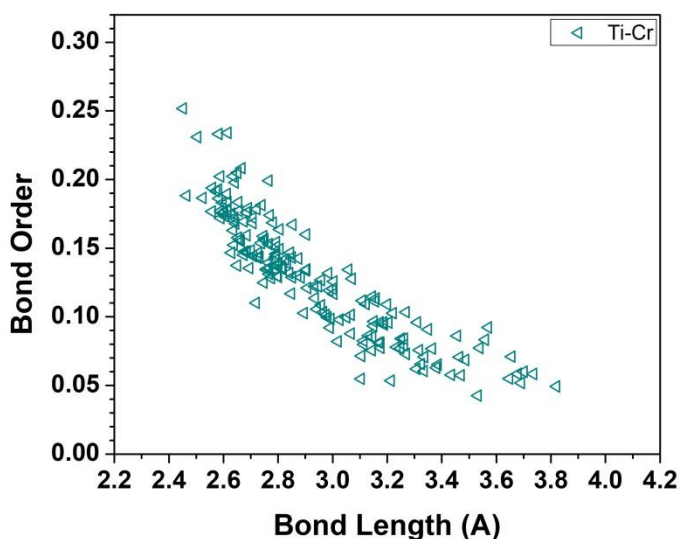
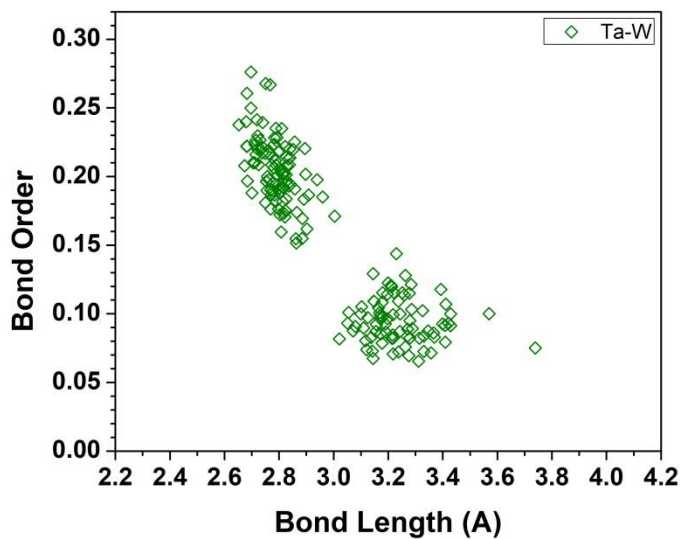
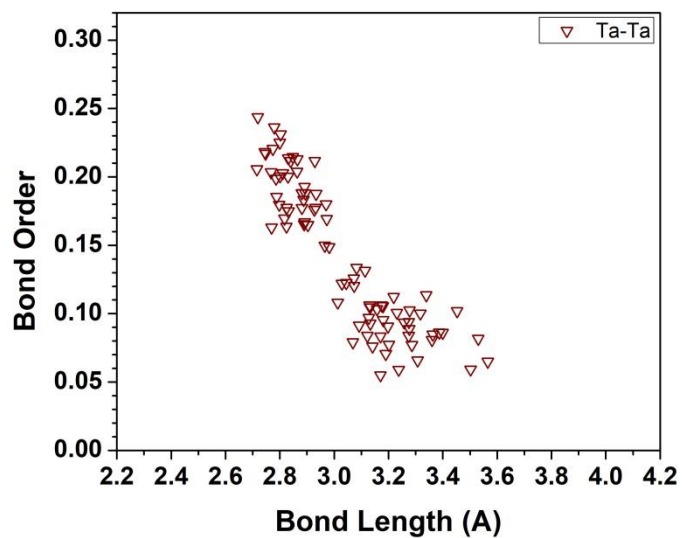
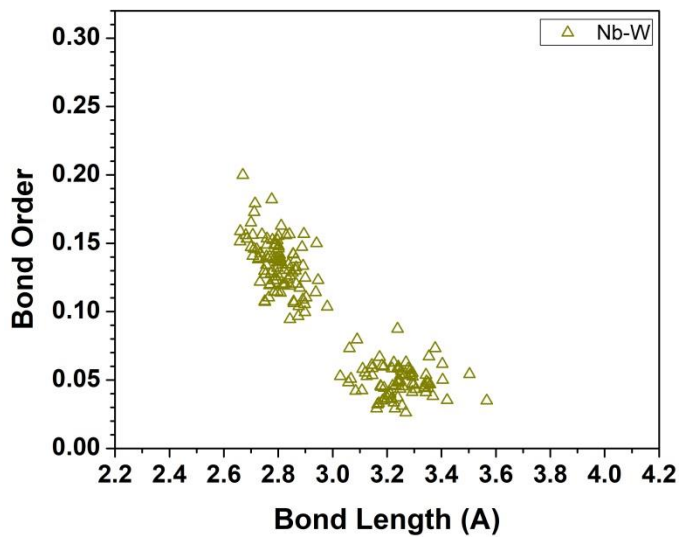


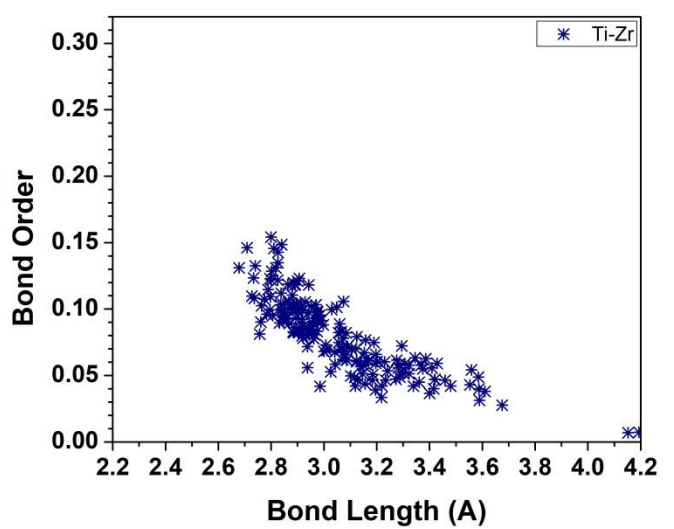
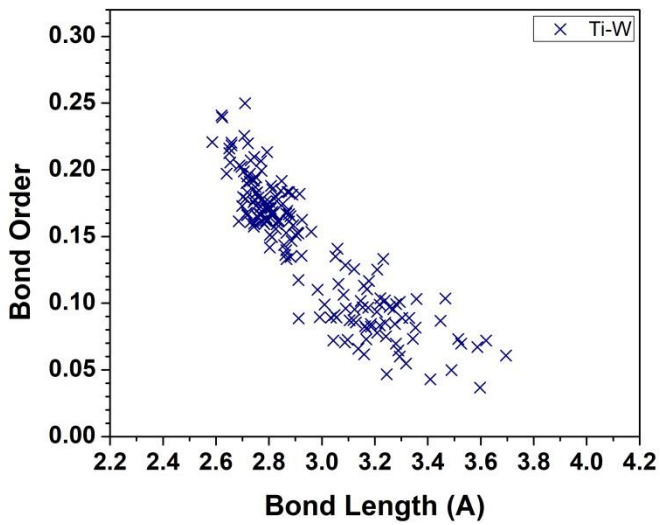
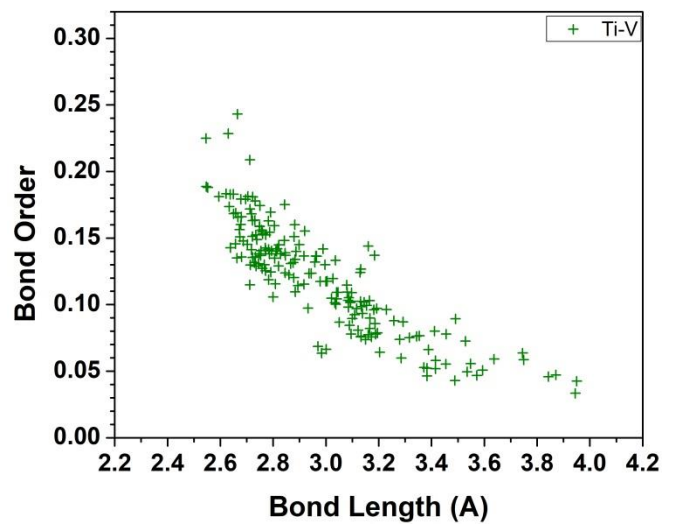
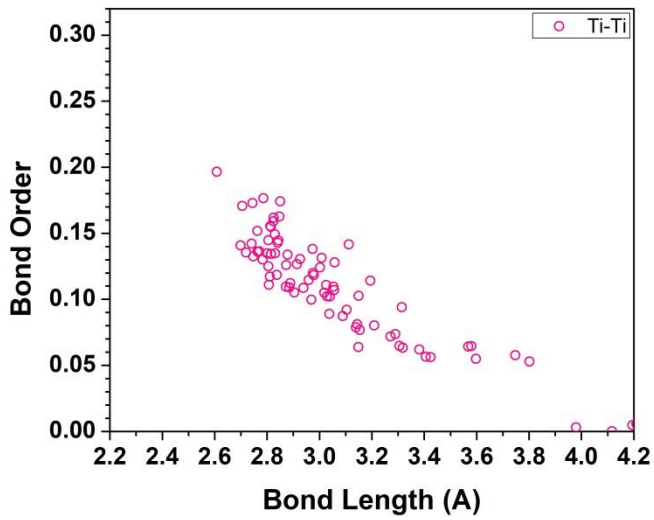
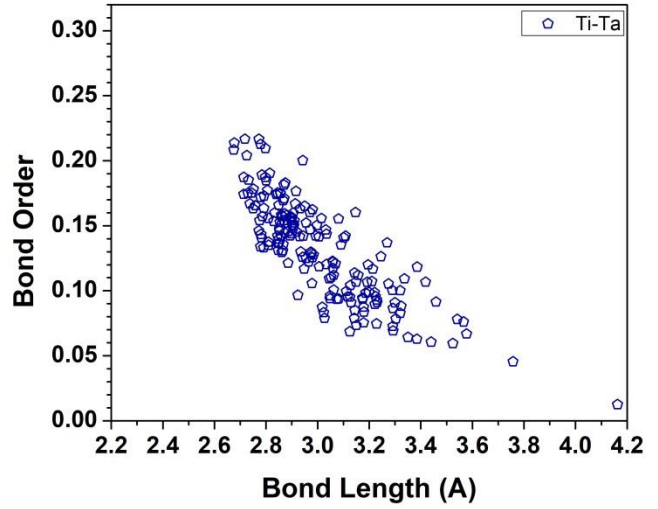
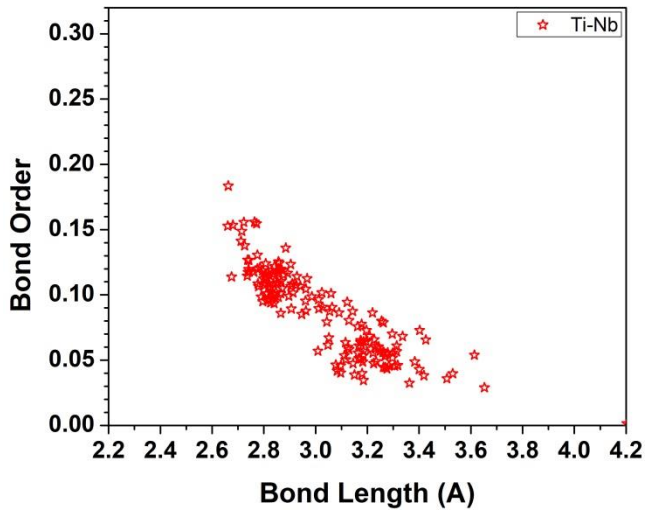
m2

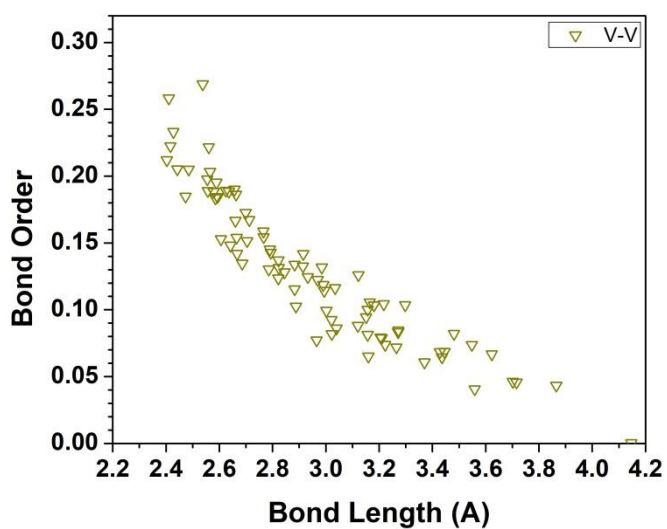
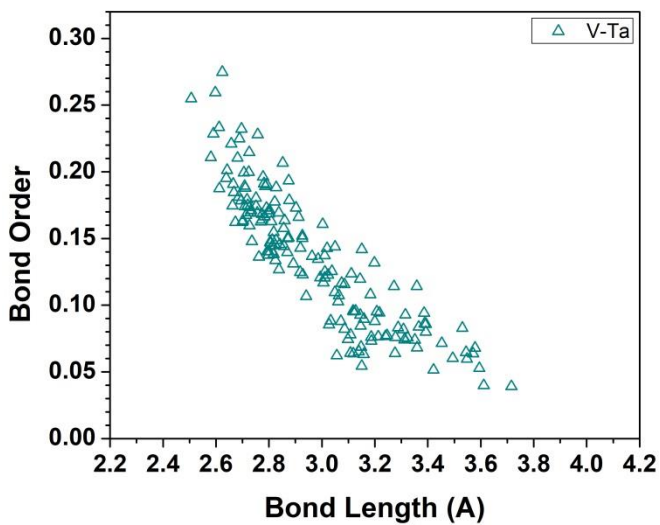
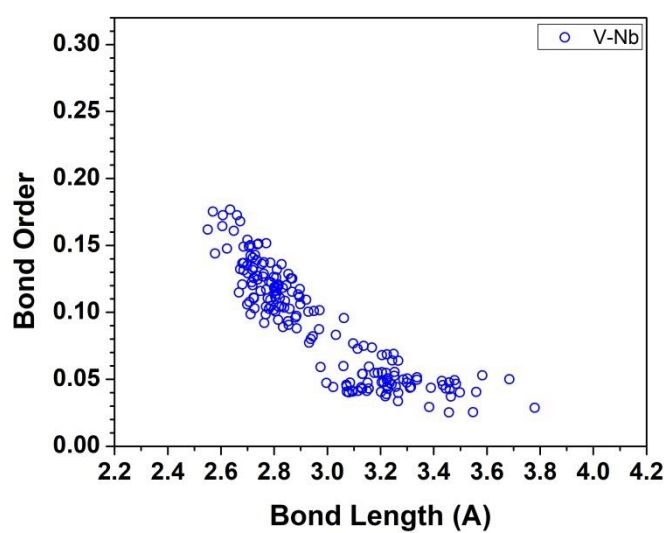
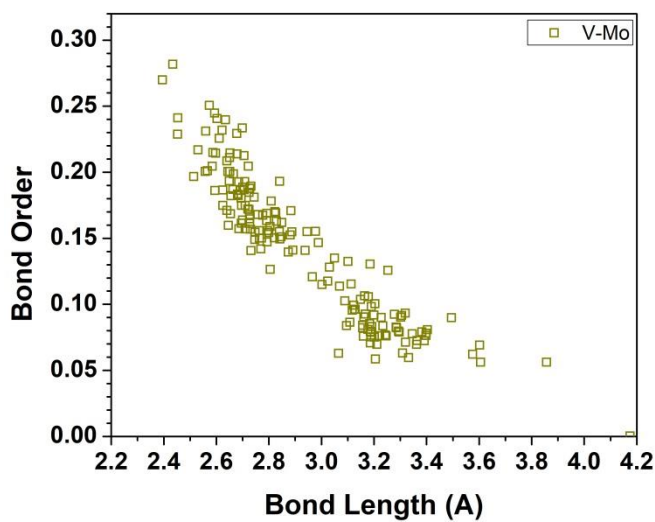
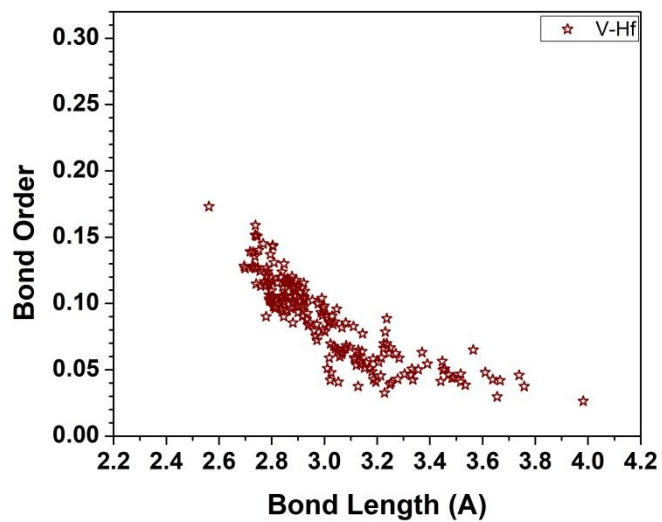
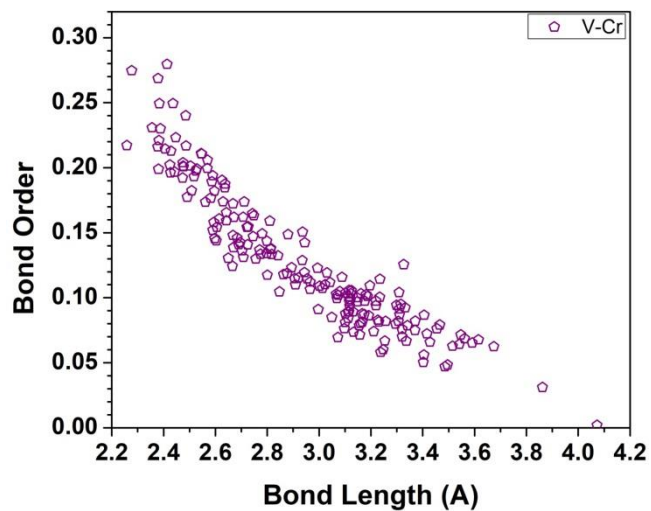


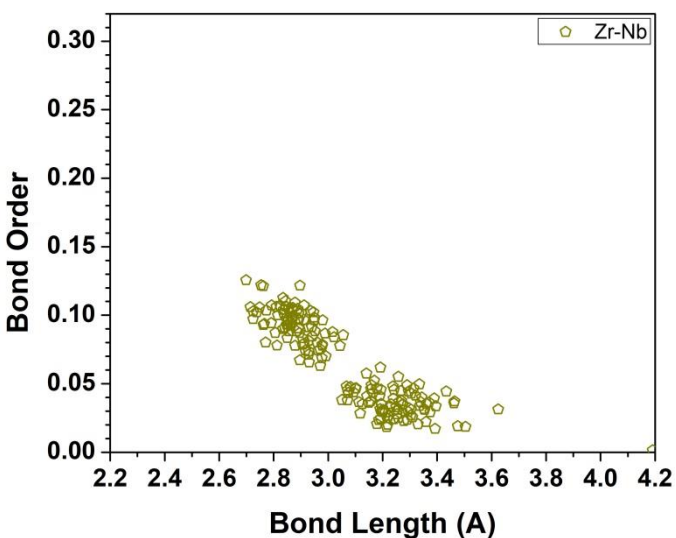
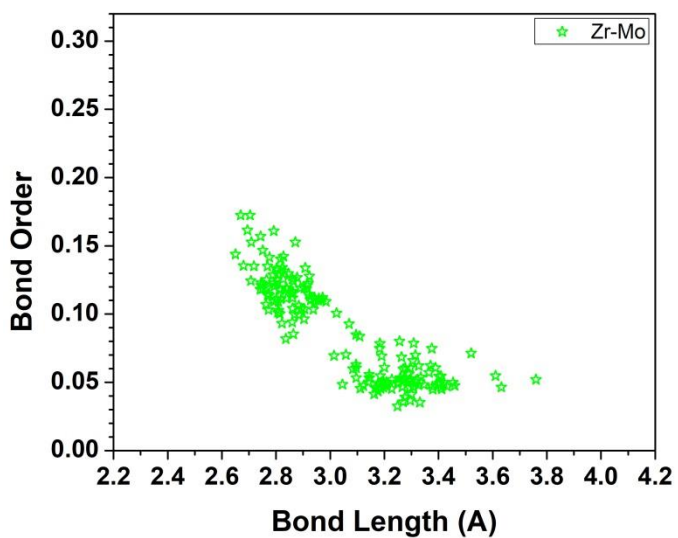
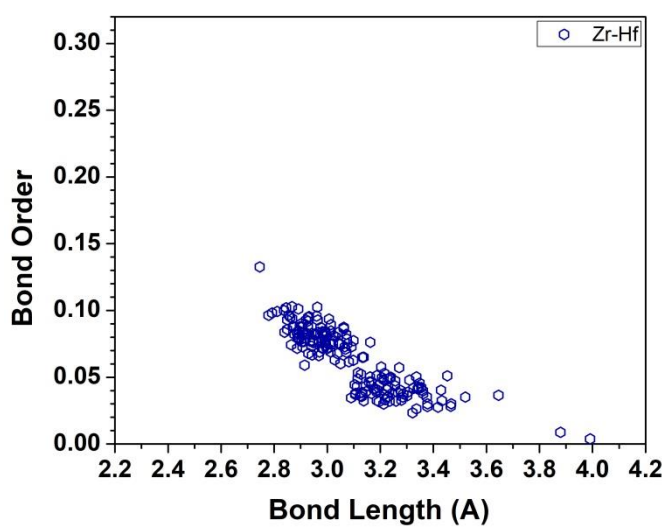
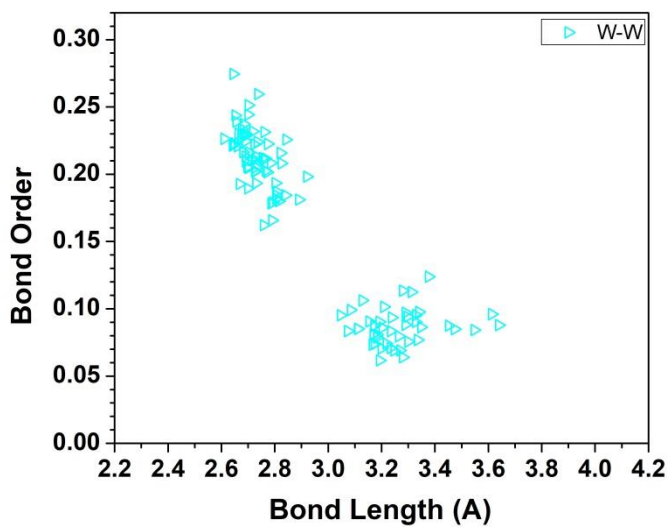
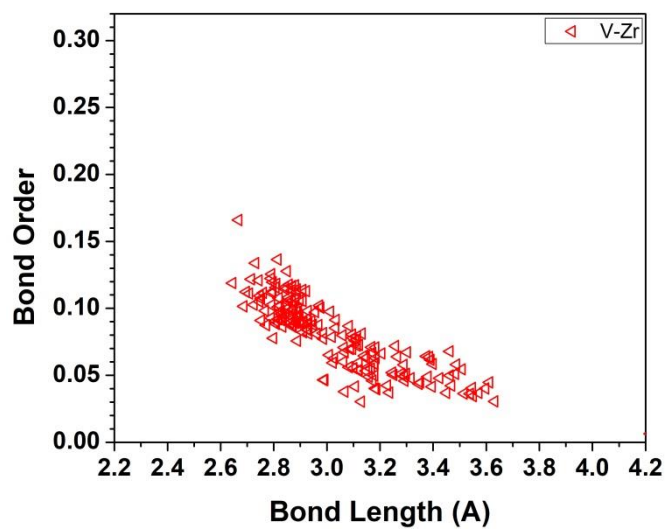
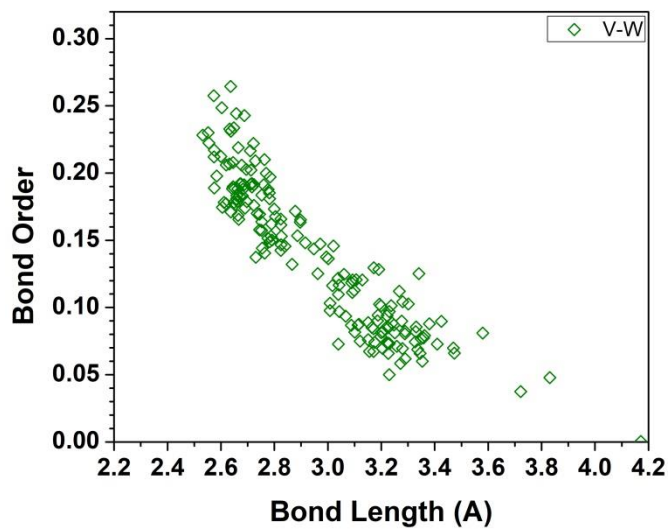


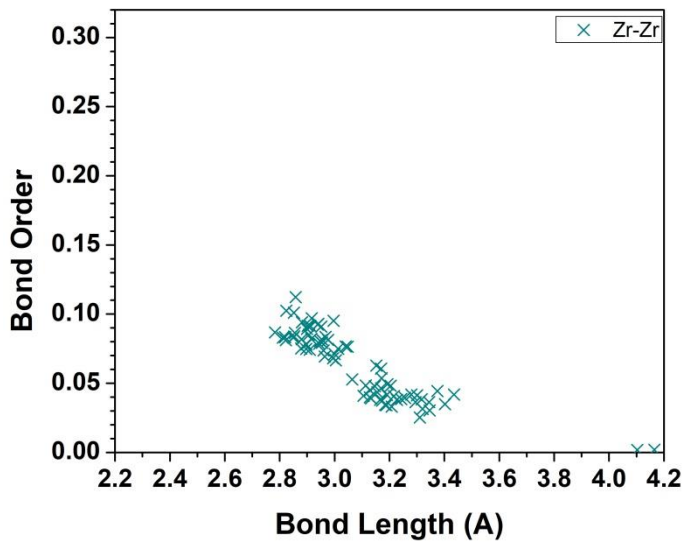
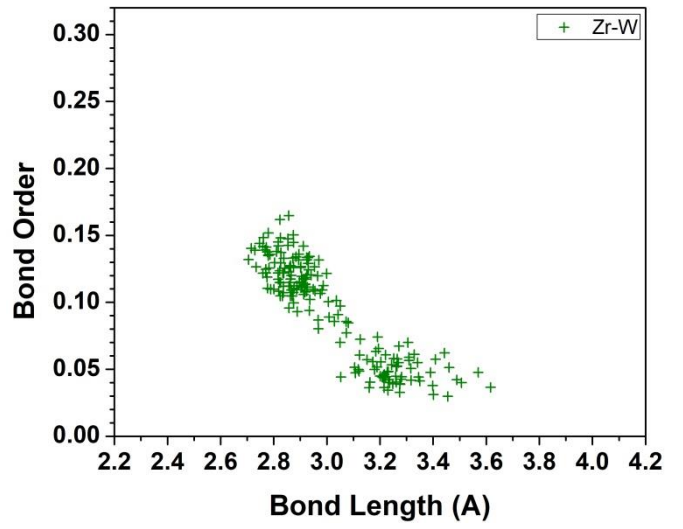
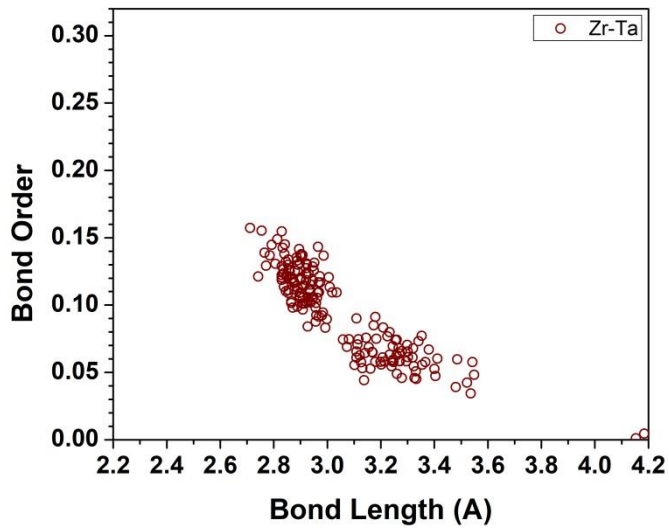




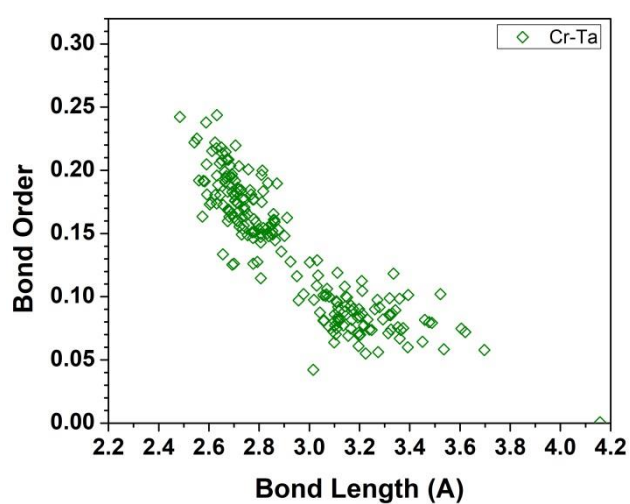
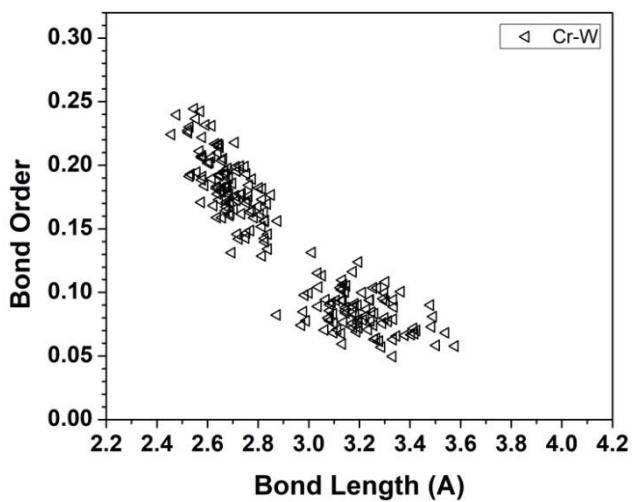
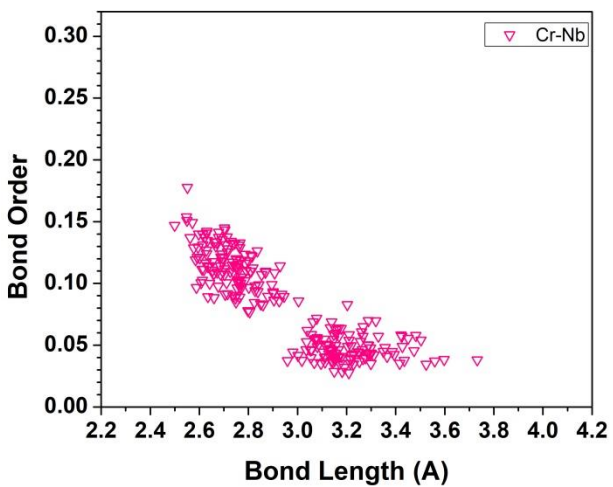
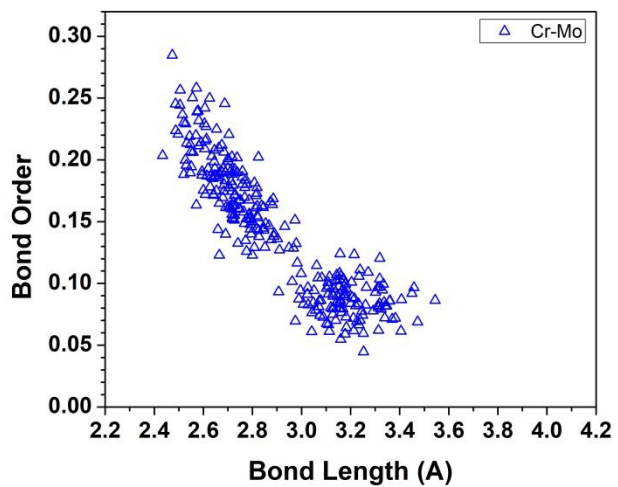
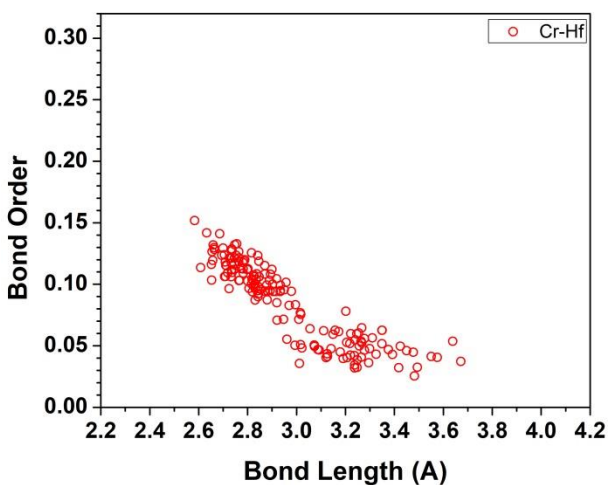
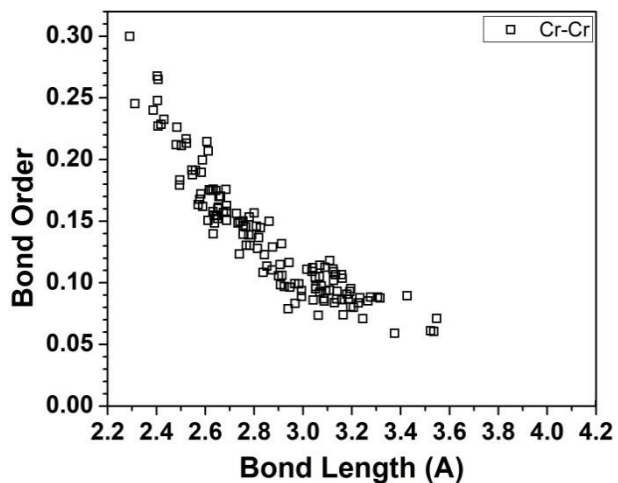


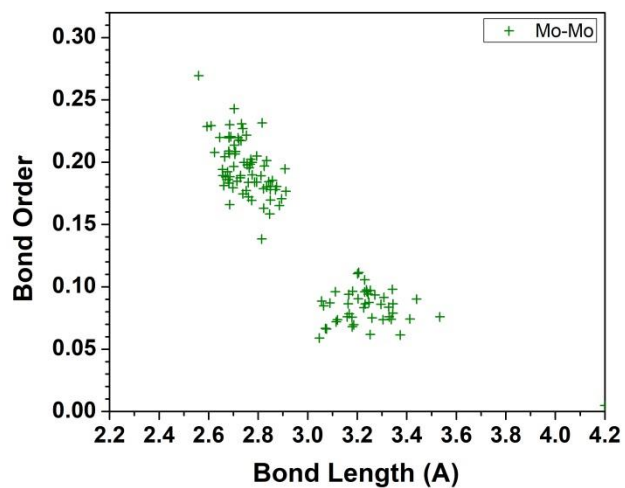
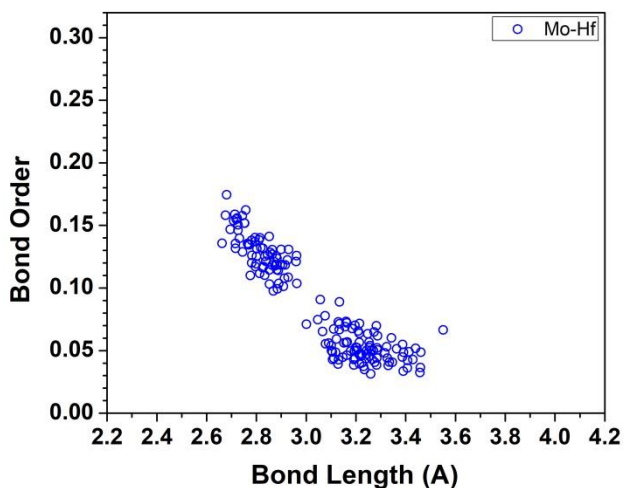
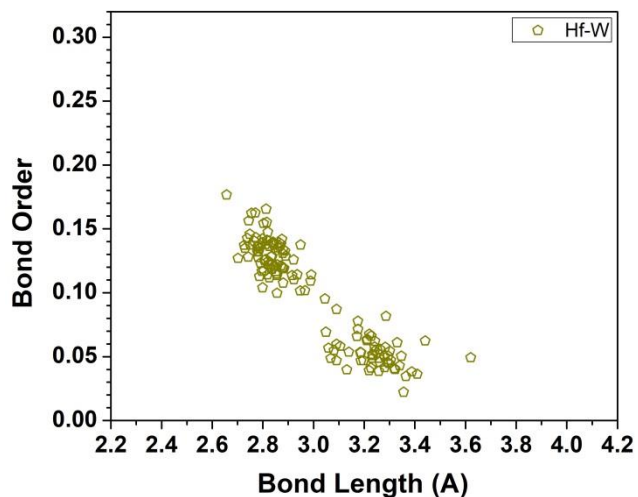
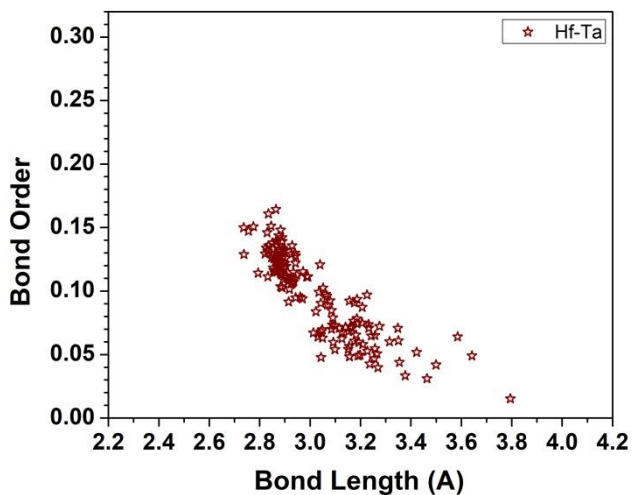
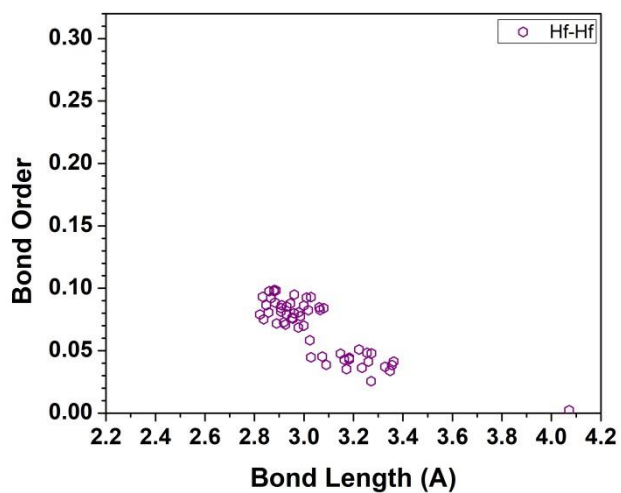
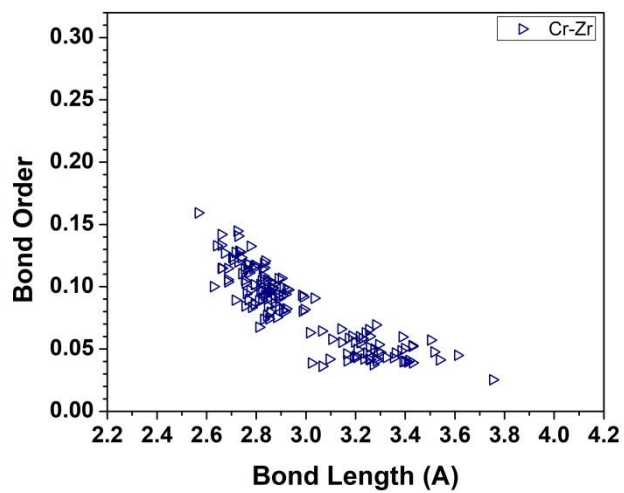


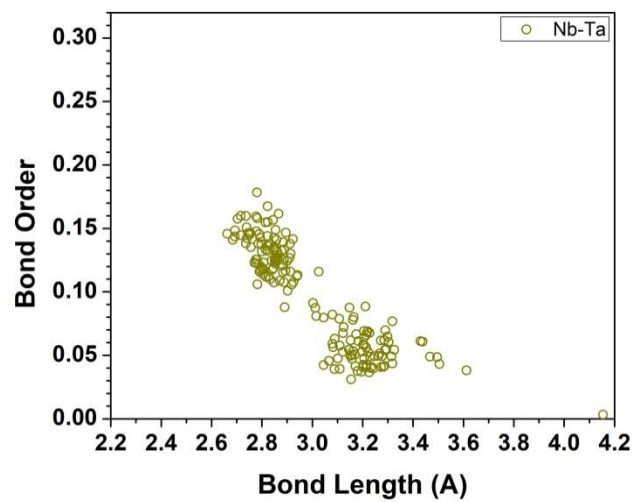
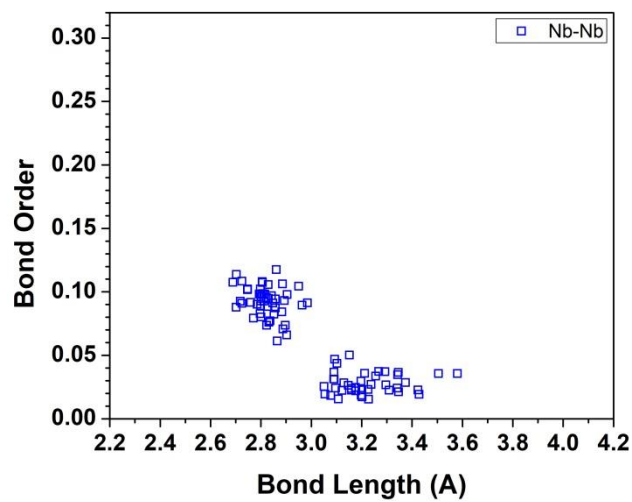
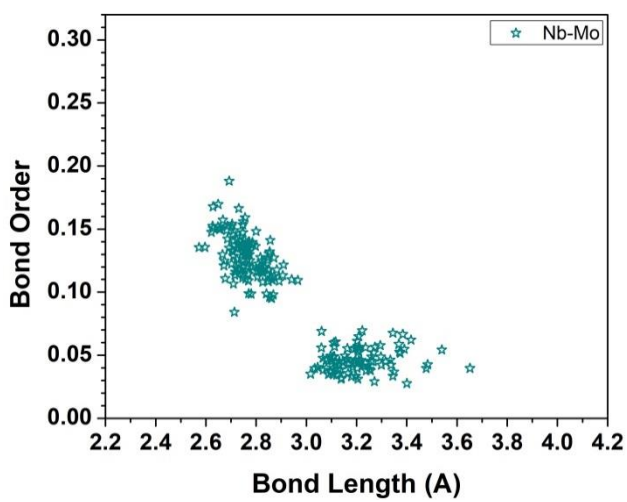
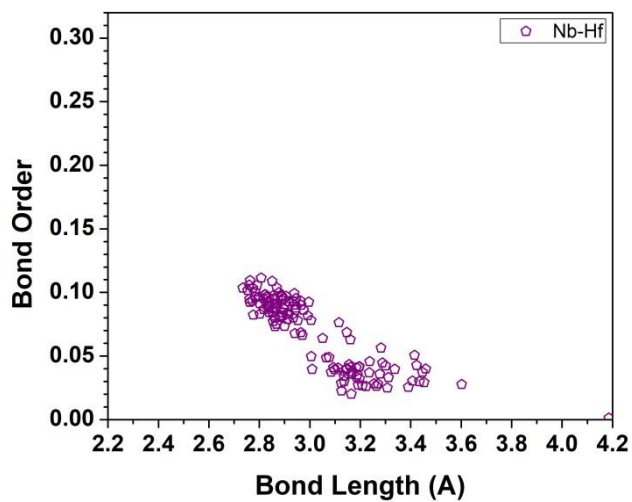
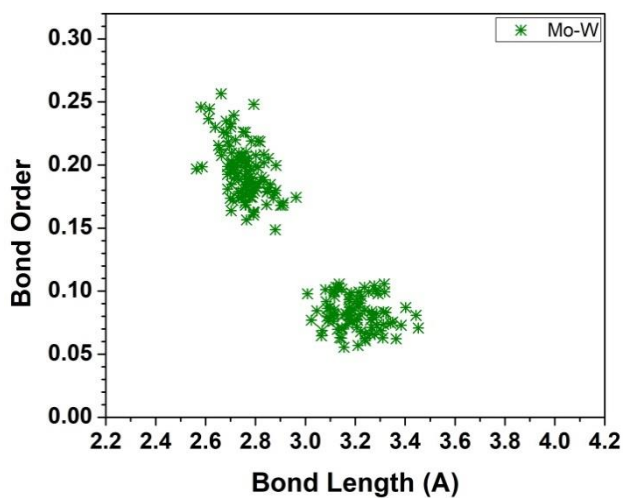
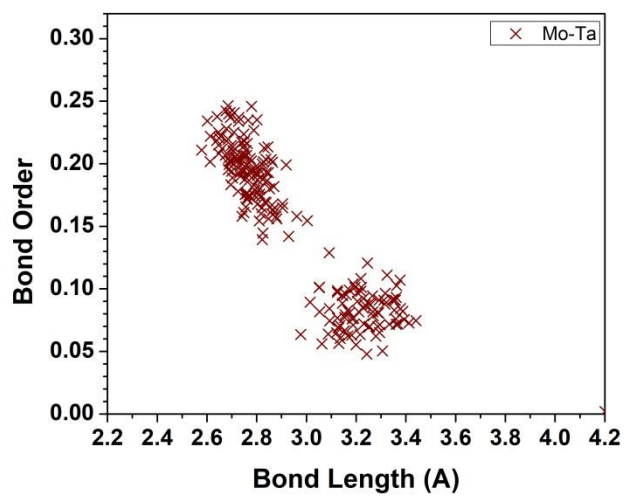


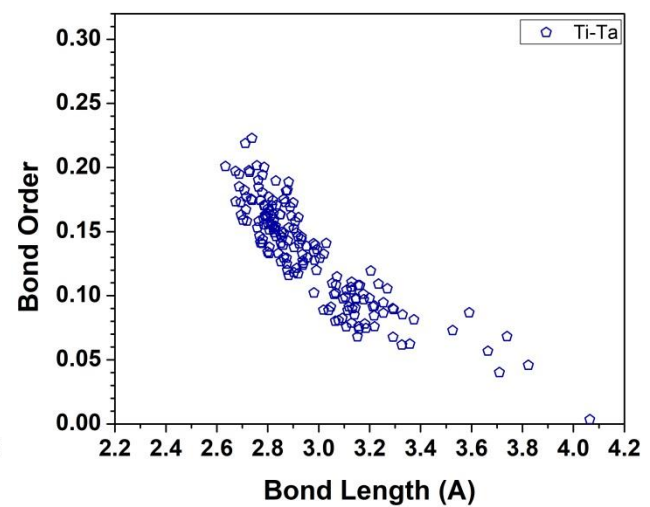
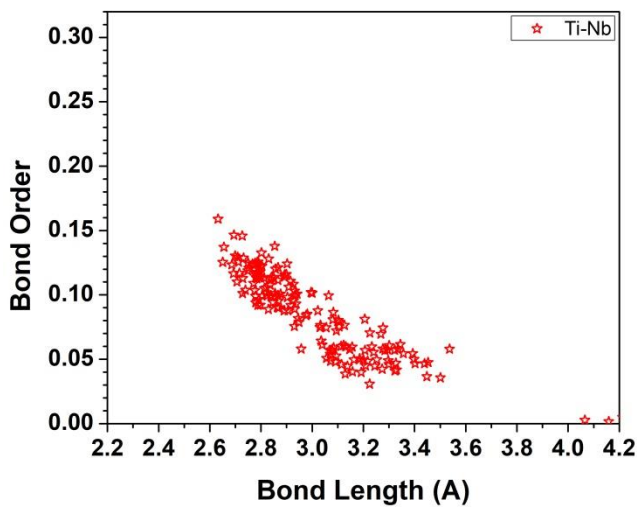
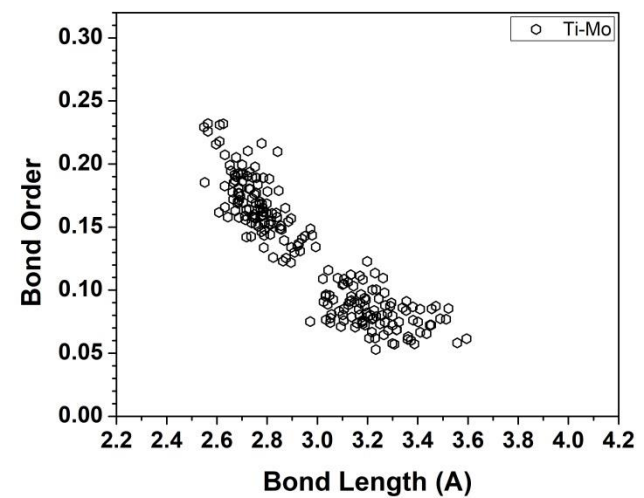
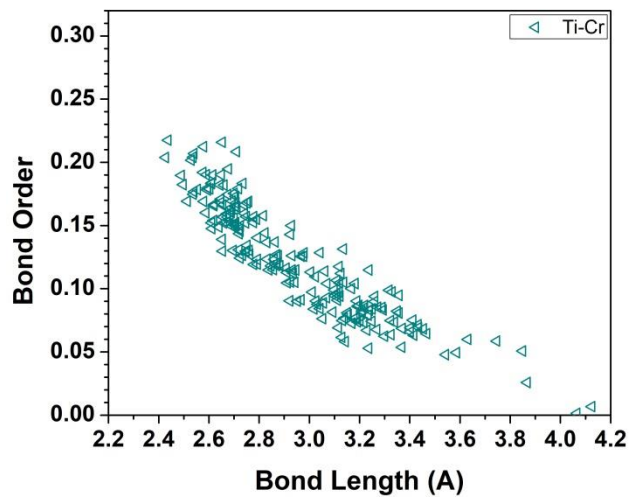
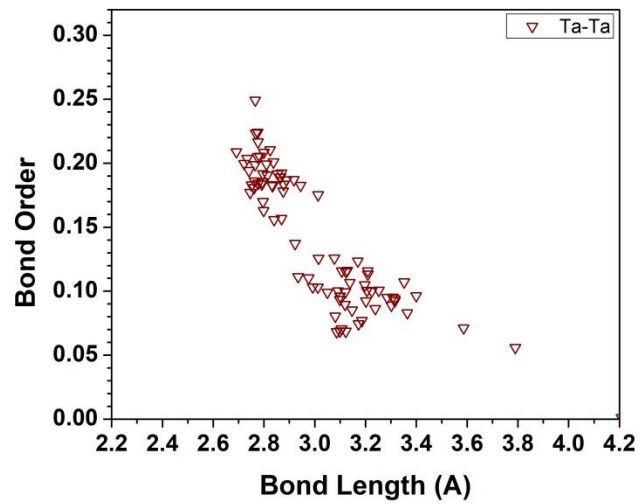
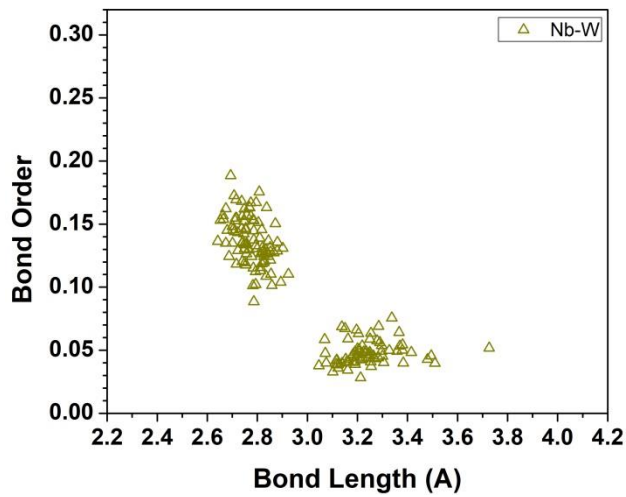


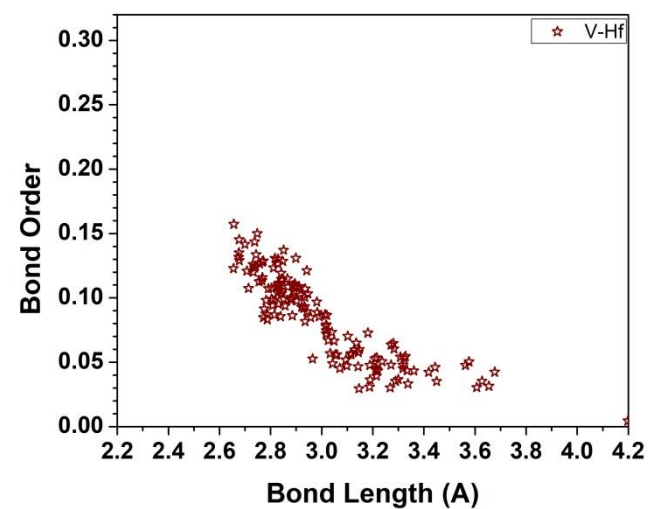
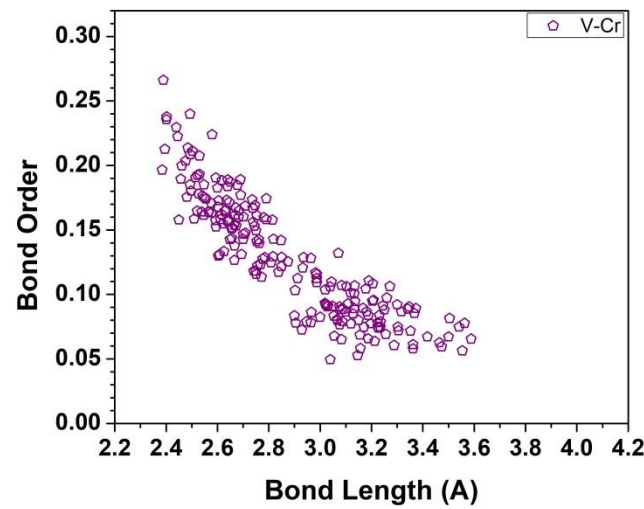
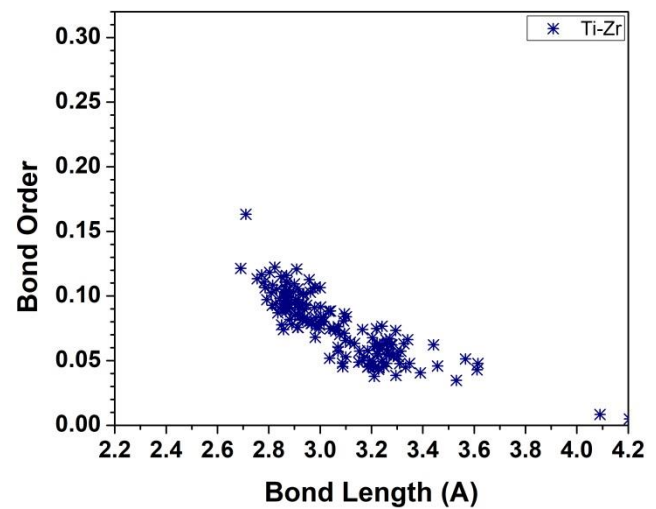
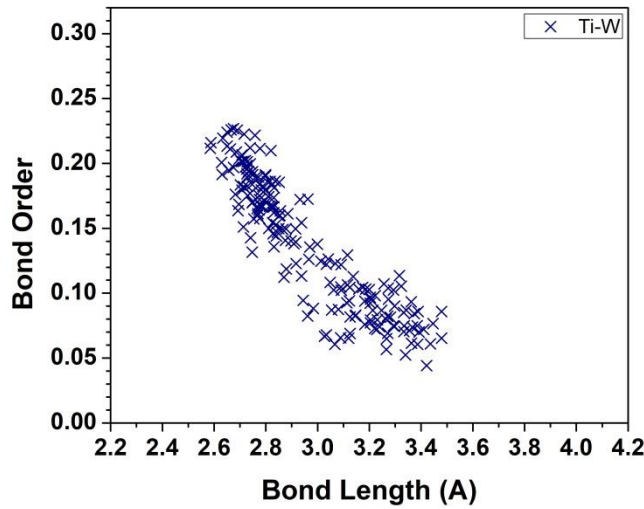
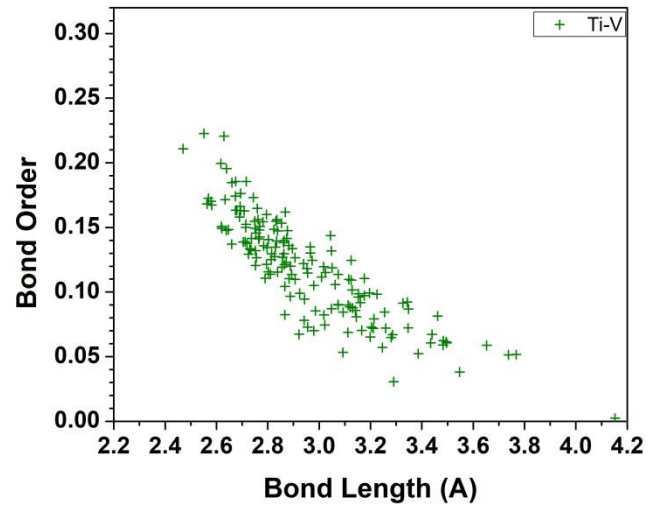
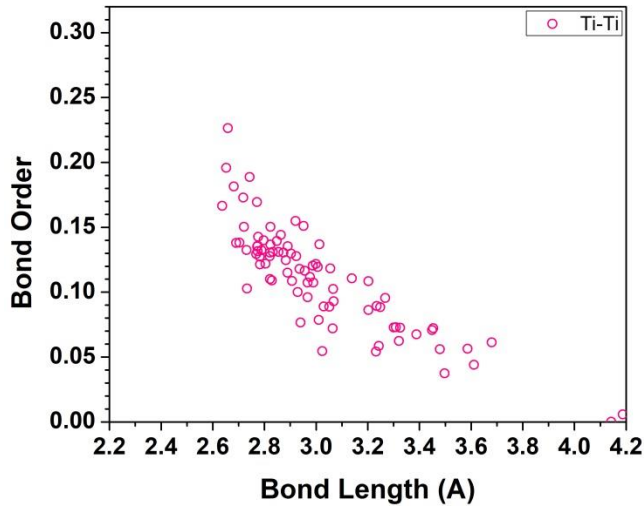
m3

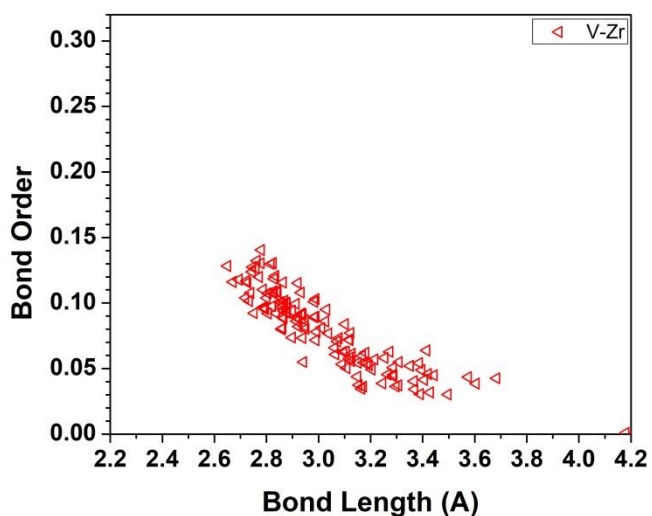
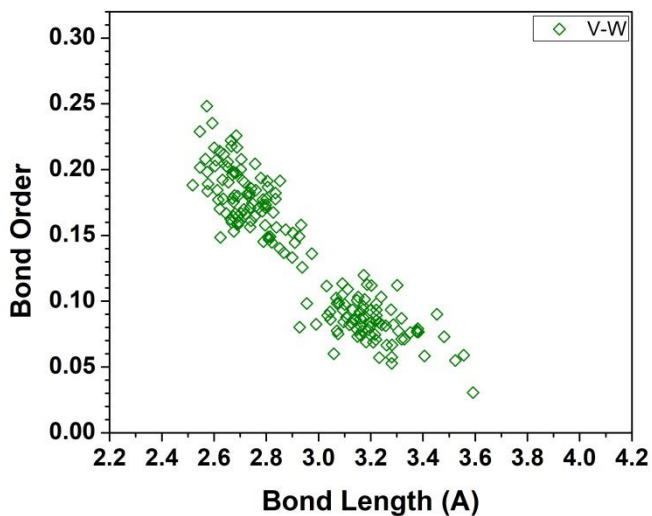
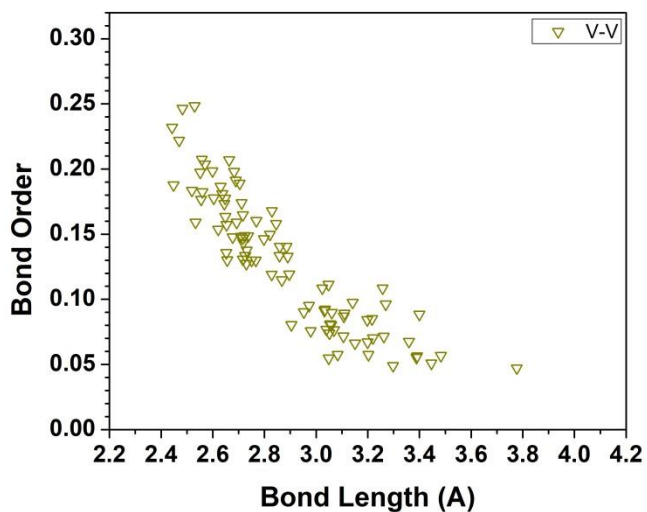
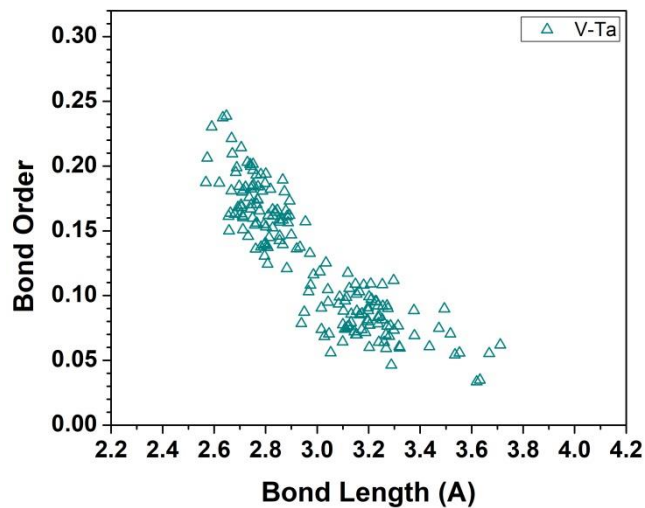
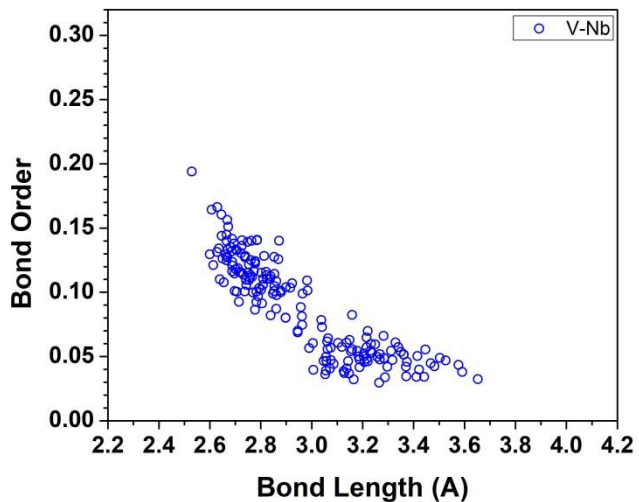
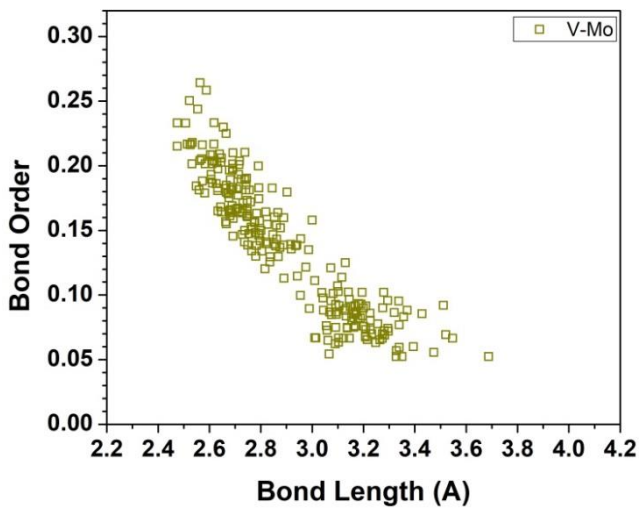


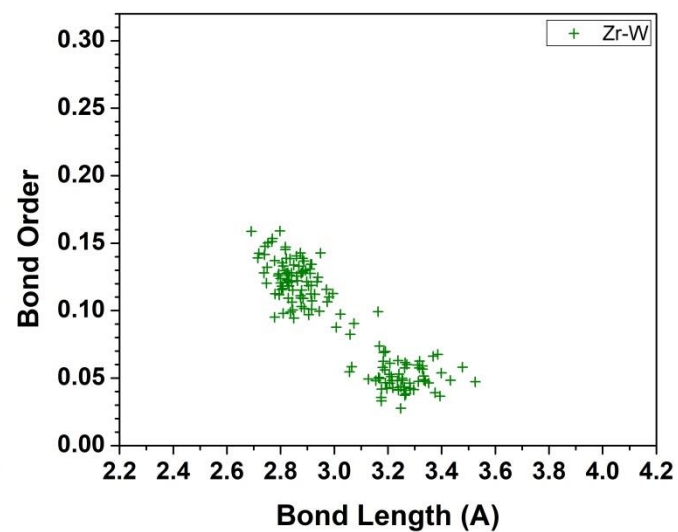
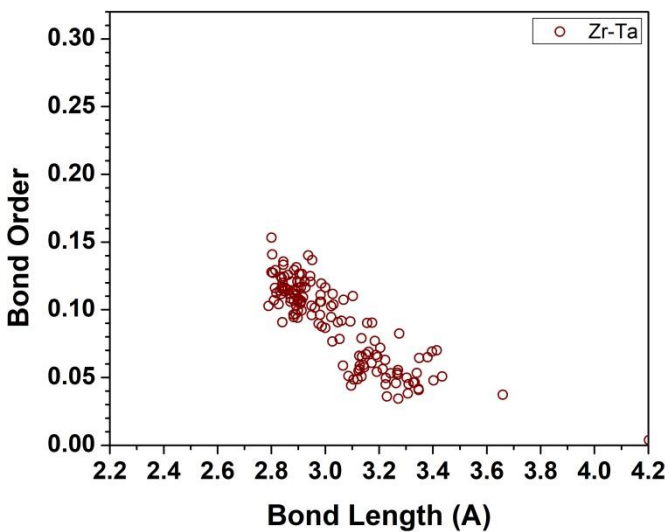
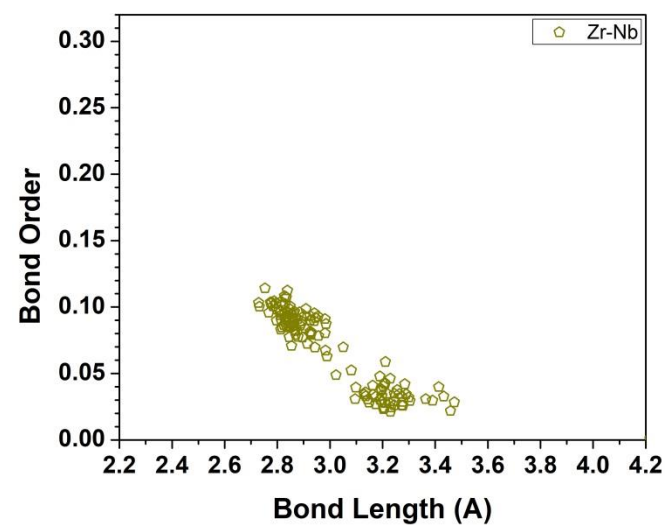
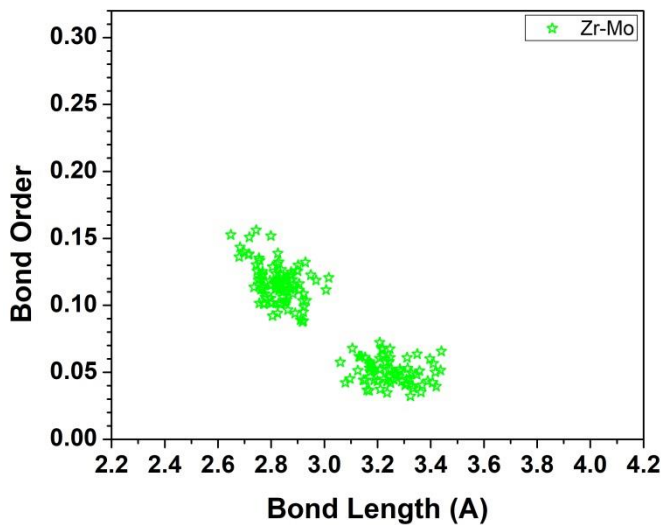
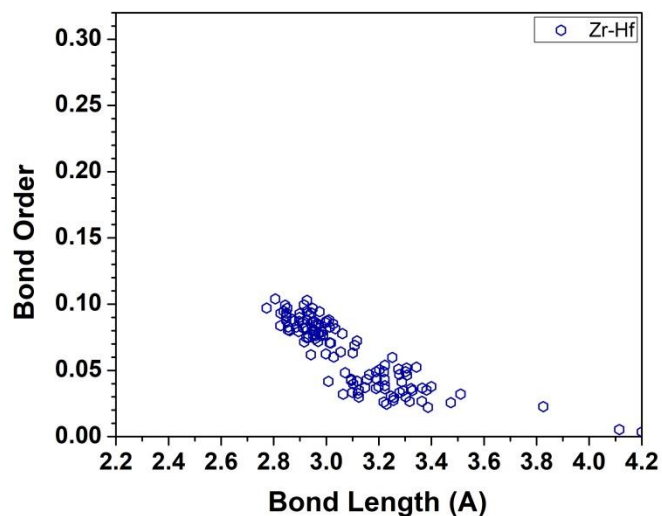
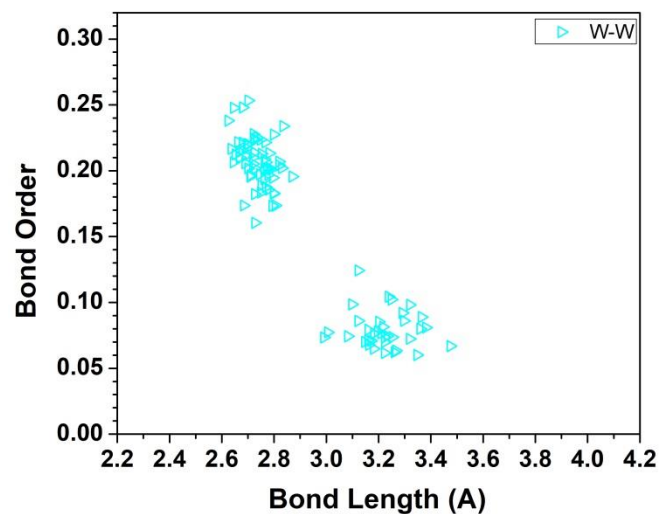


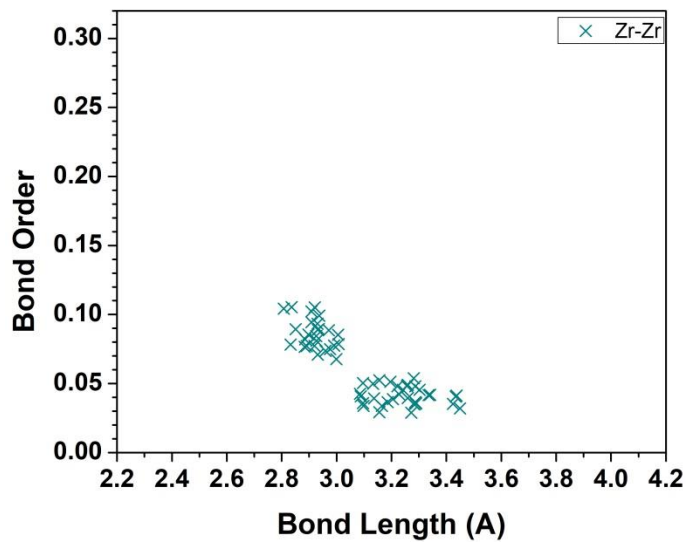




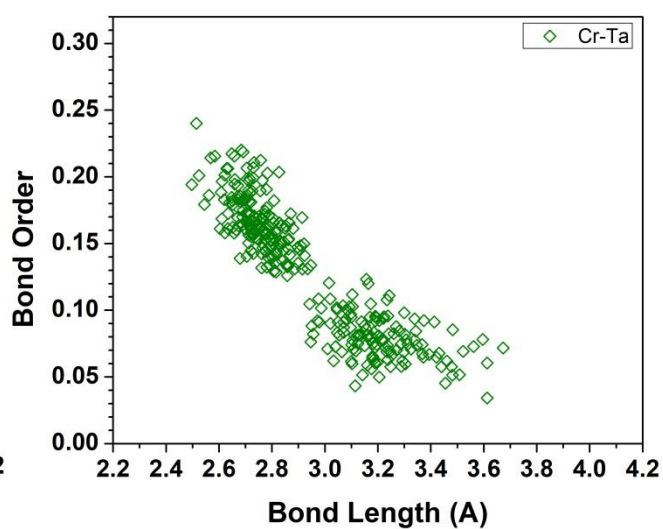
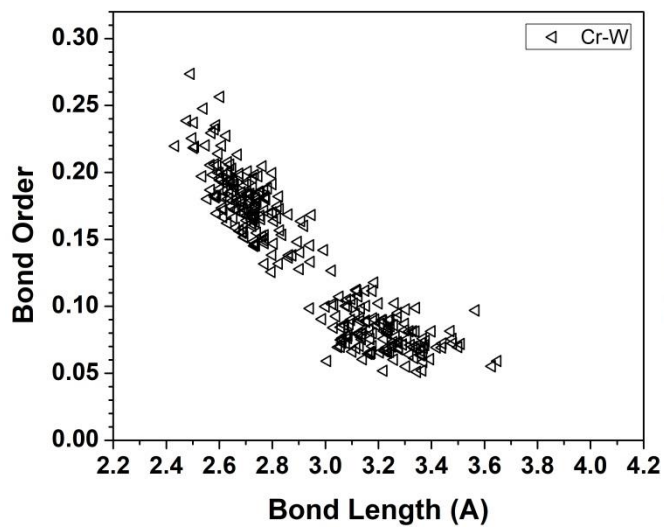
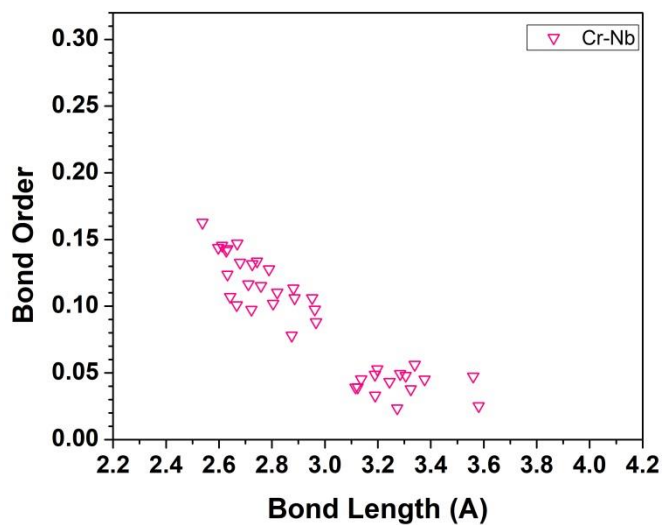
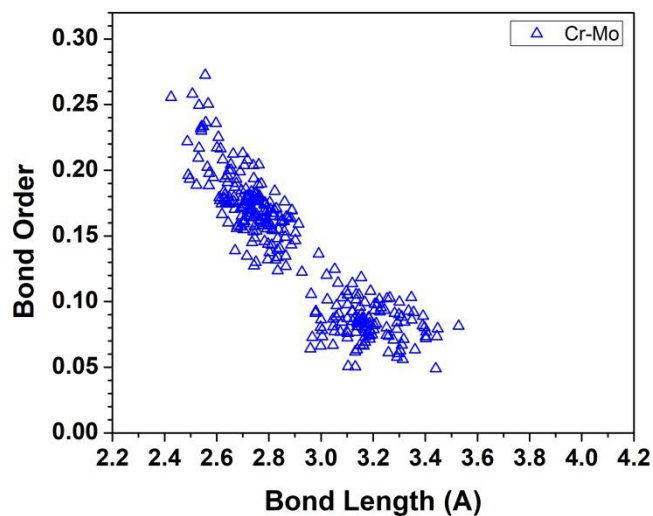
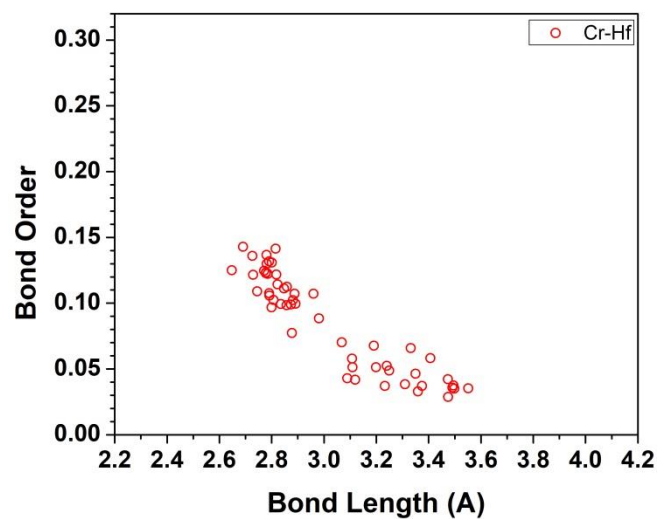
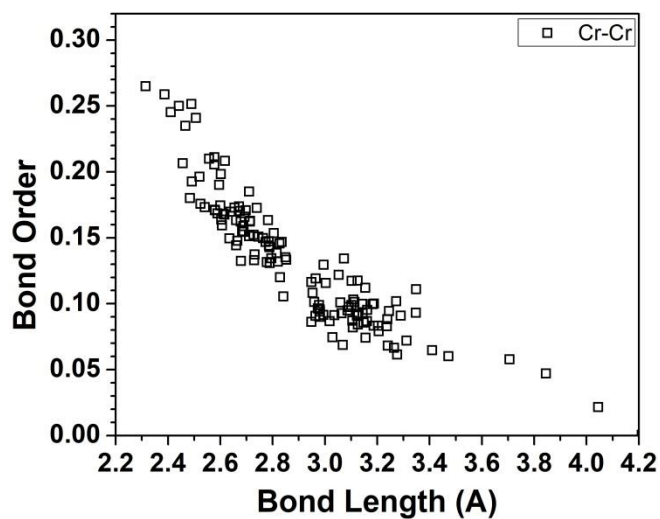


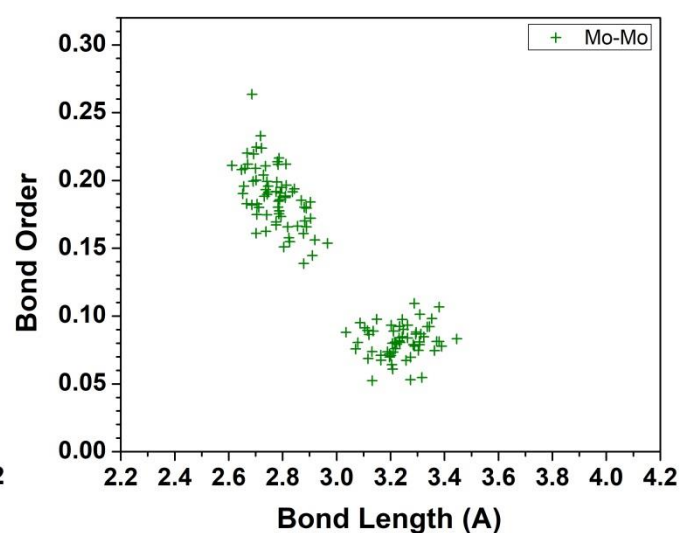
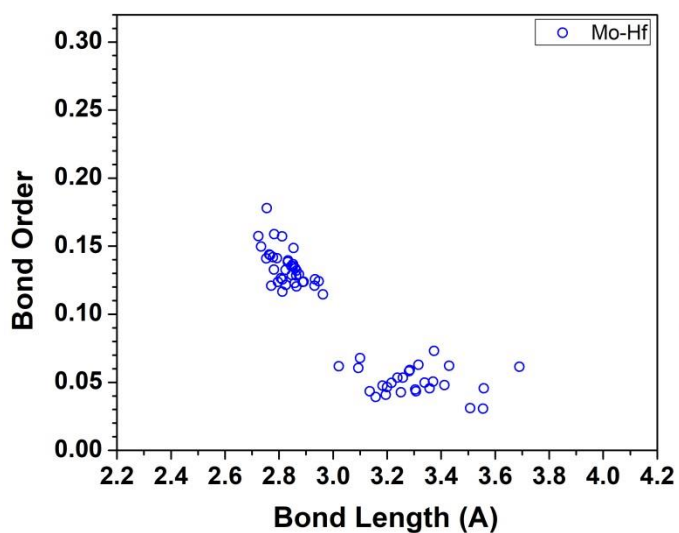
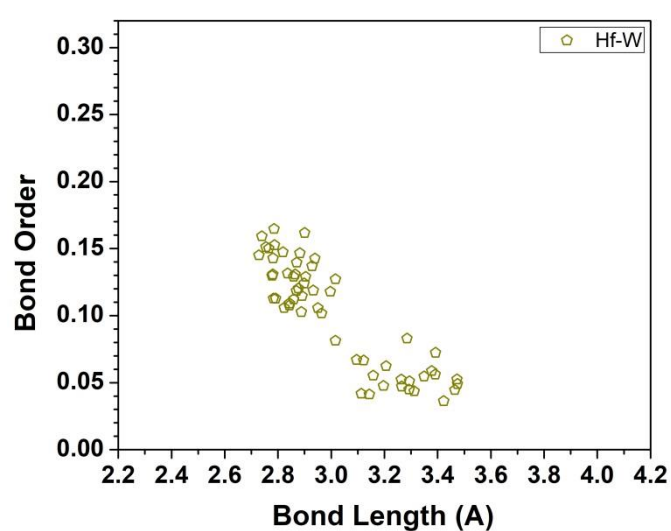
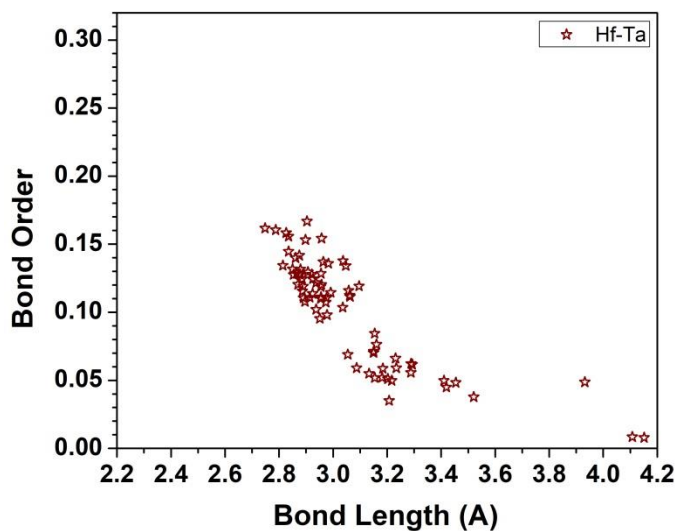
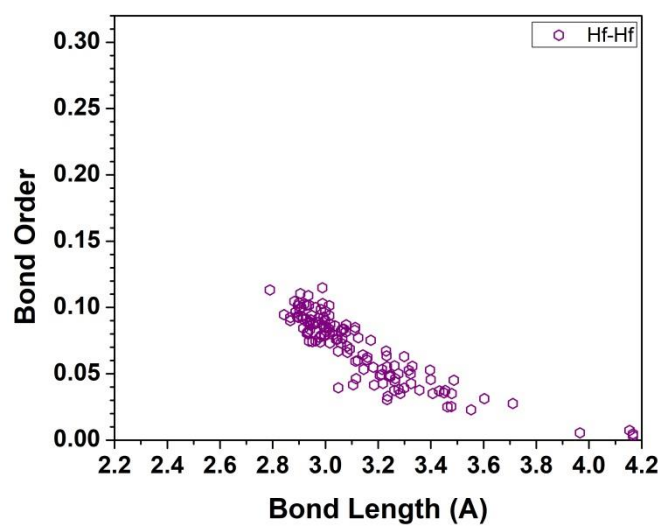
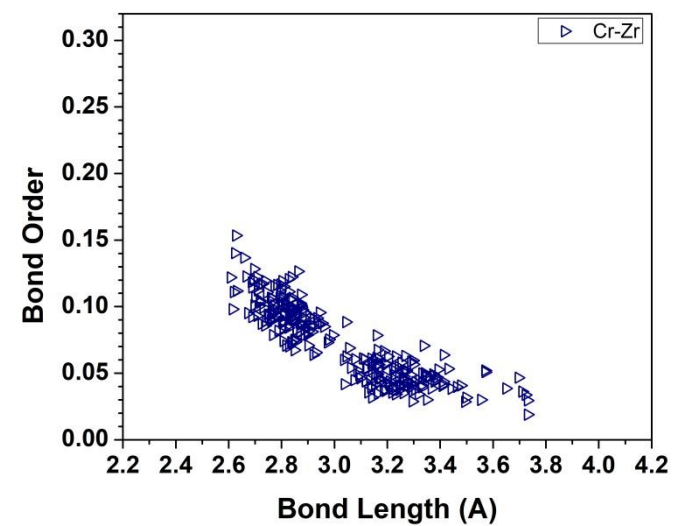


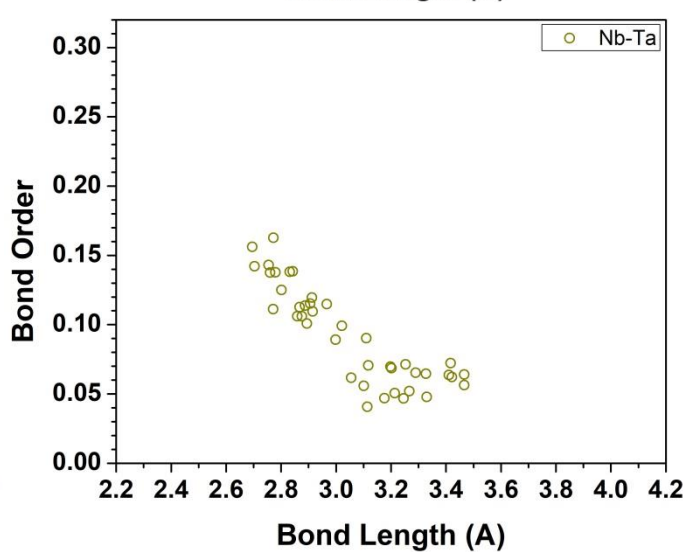
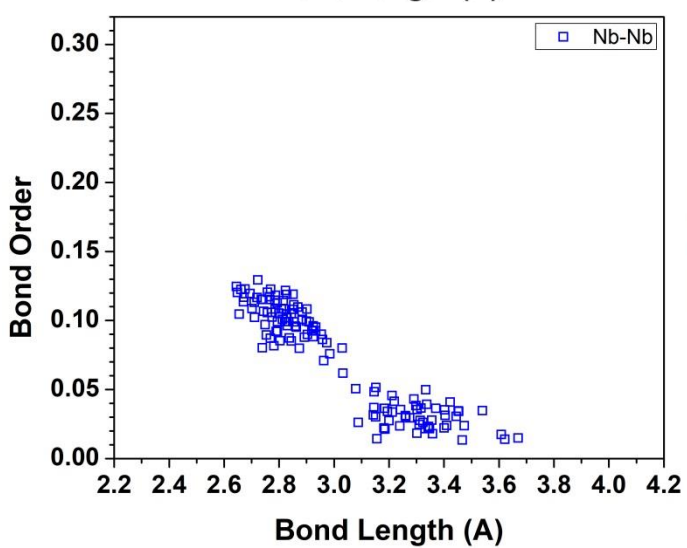
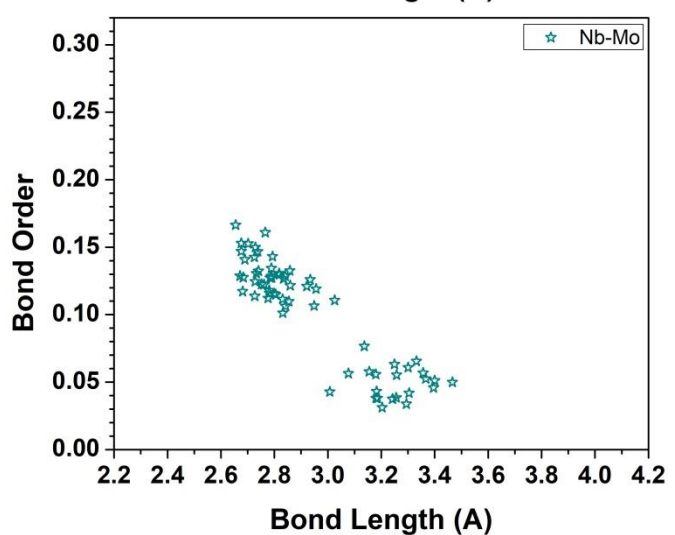
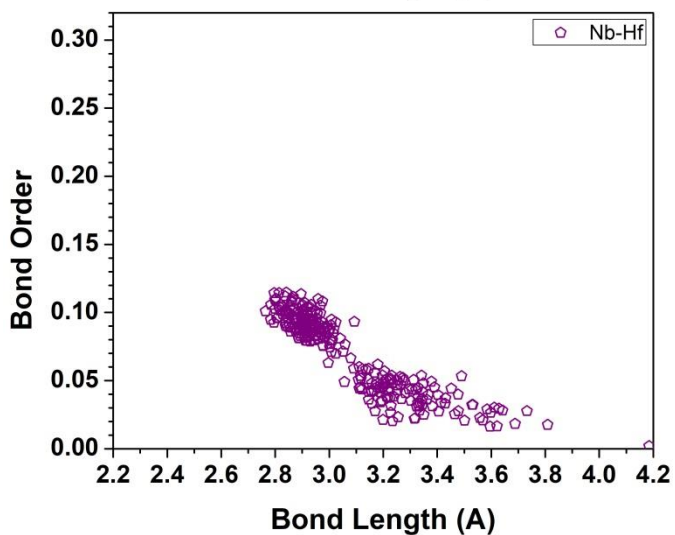
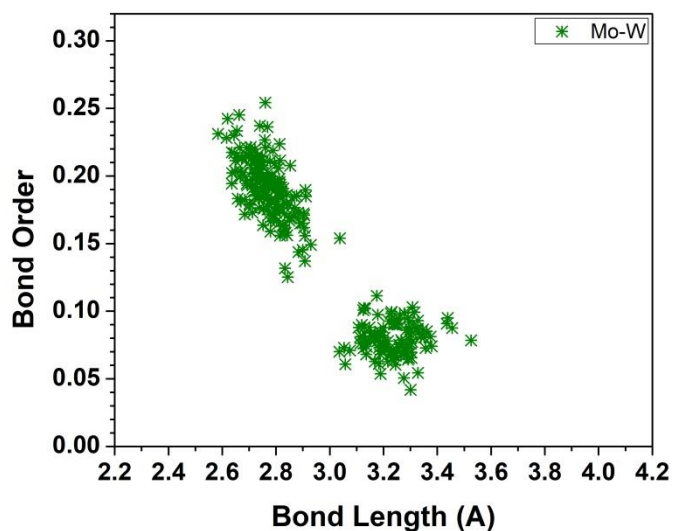
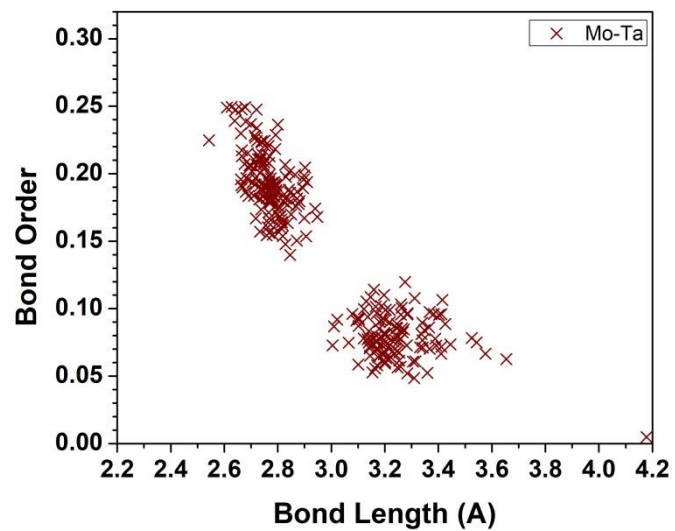


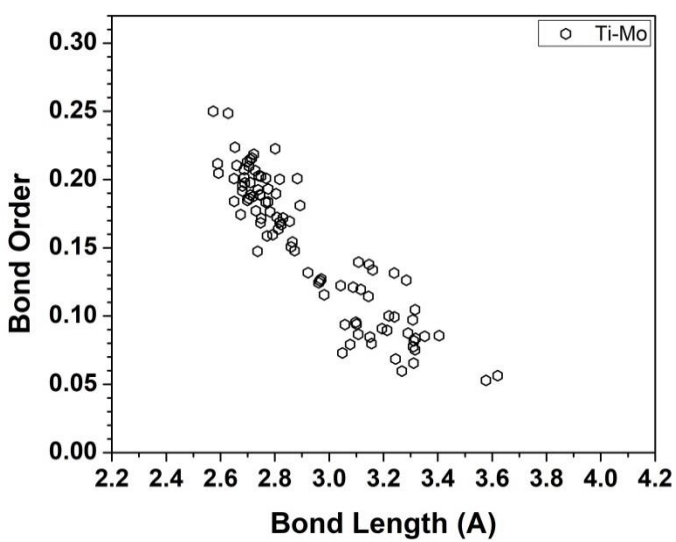
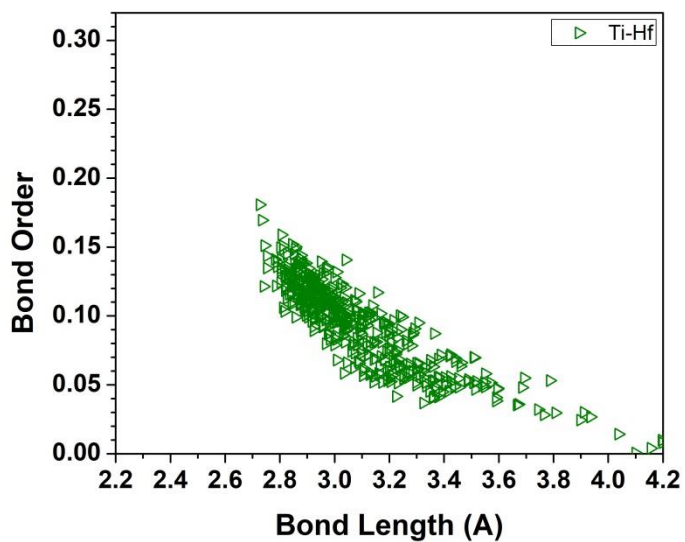
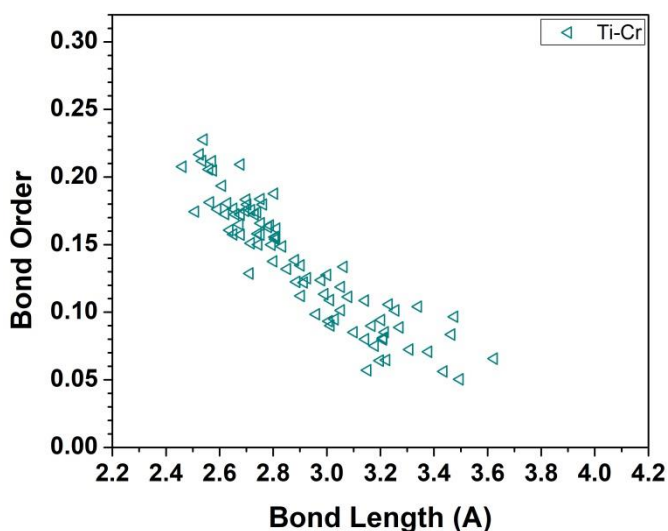
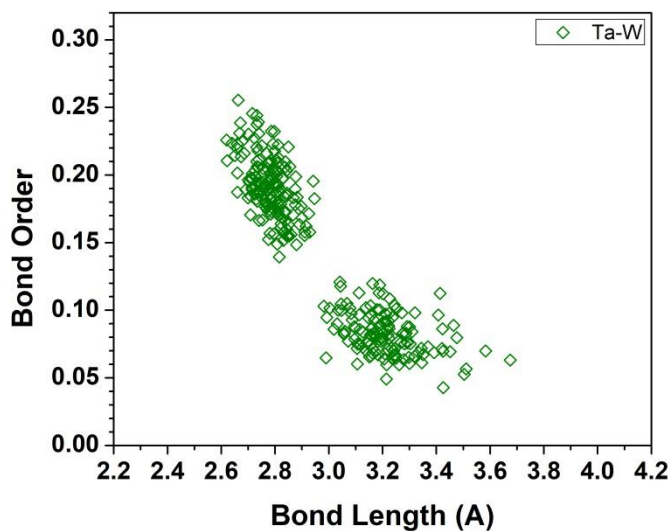
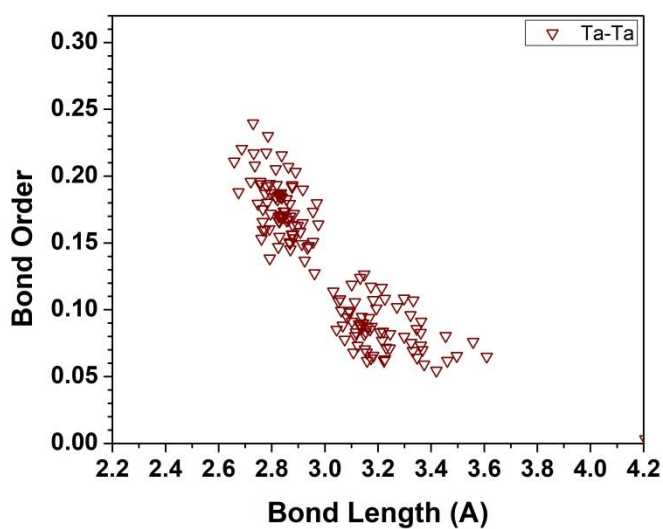
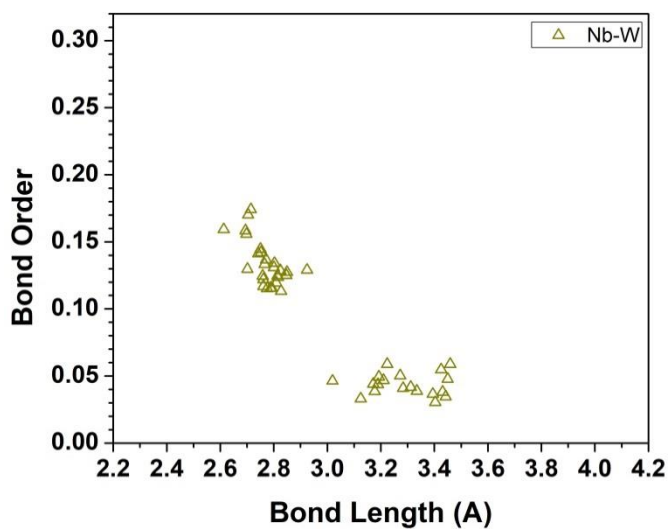


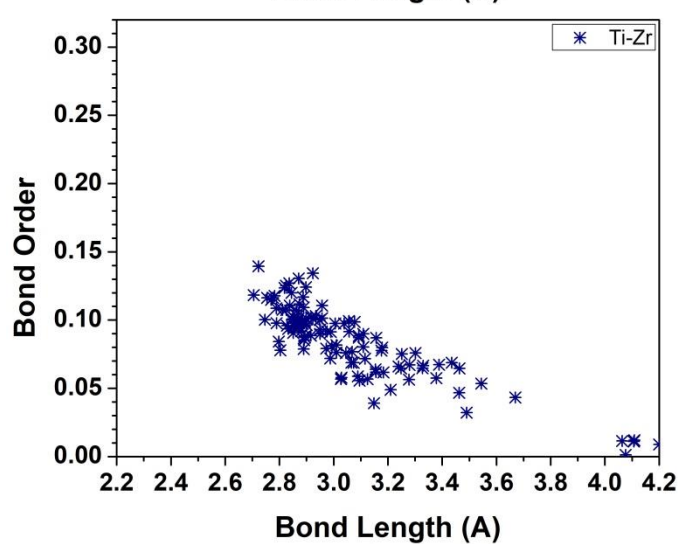
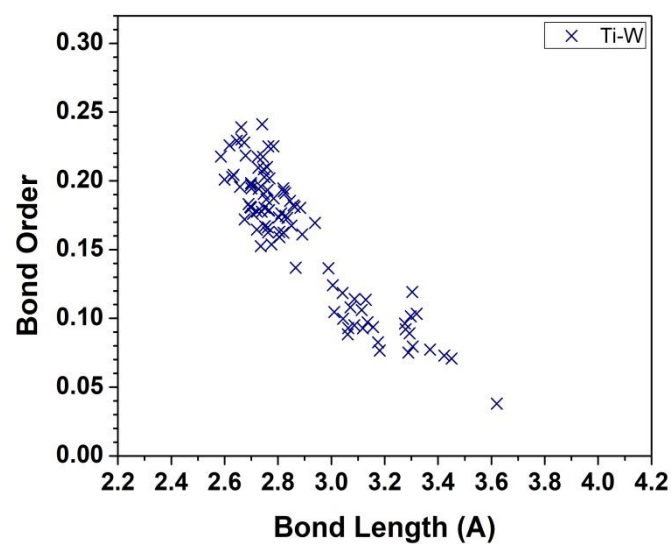
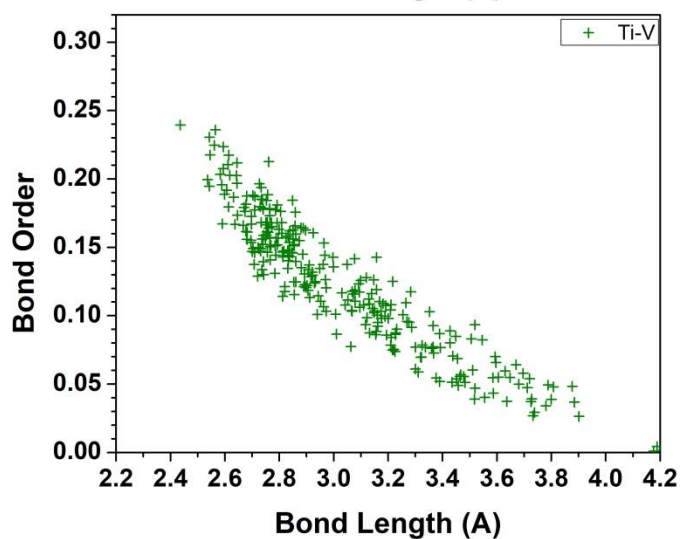
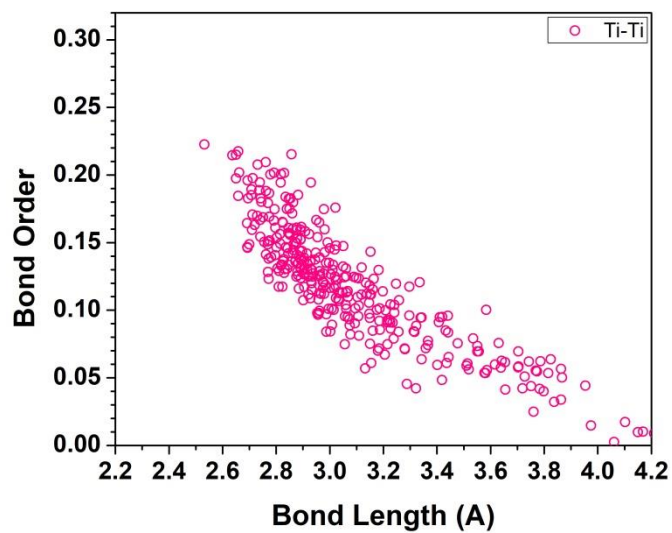
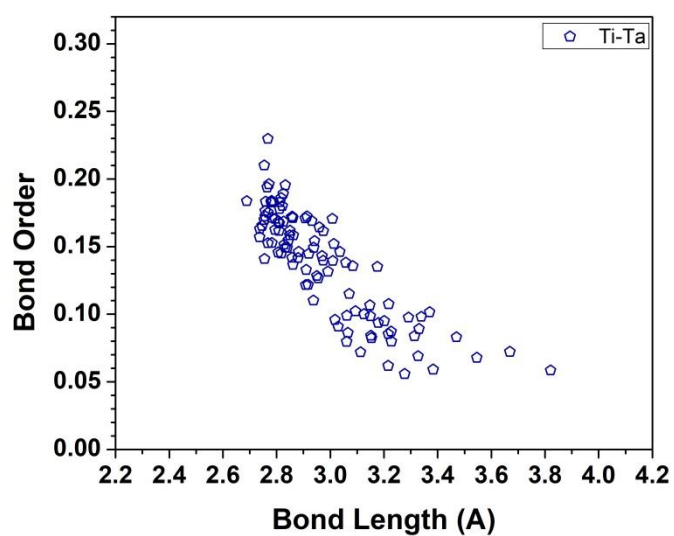
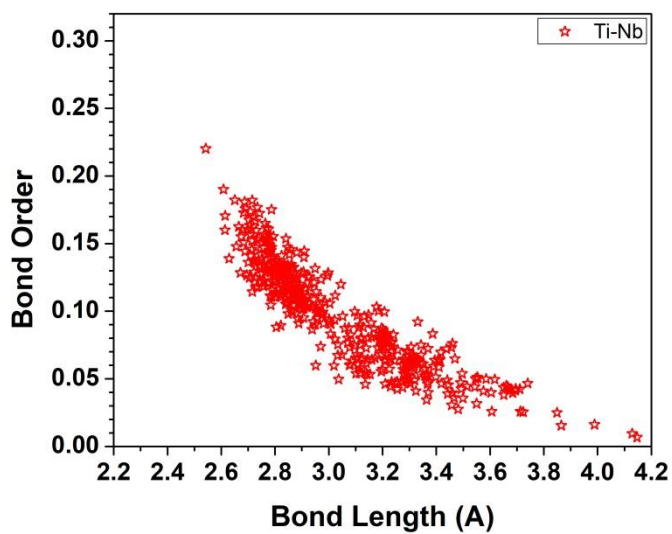
m4

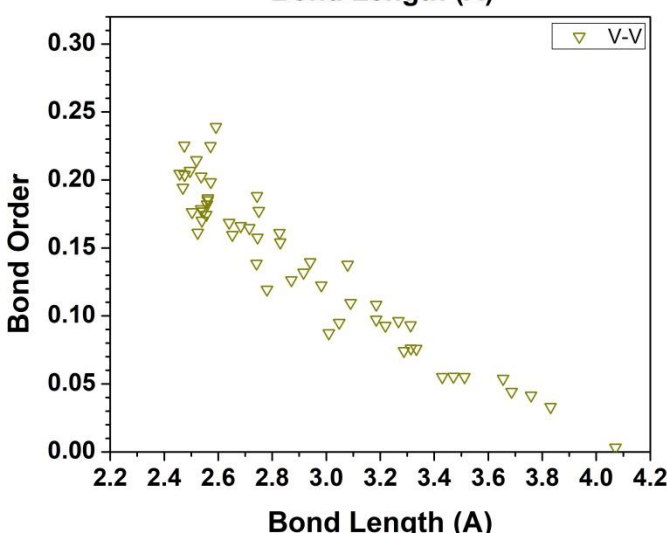
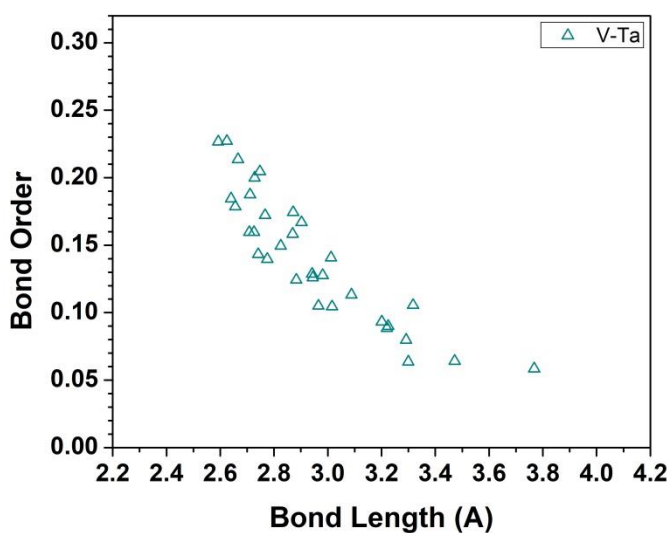
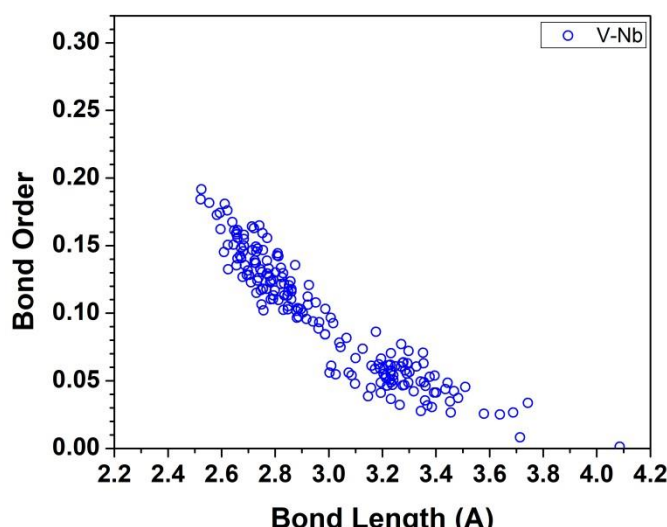
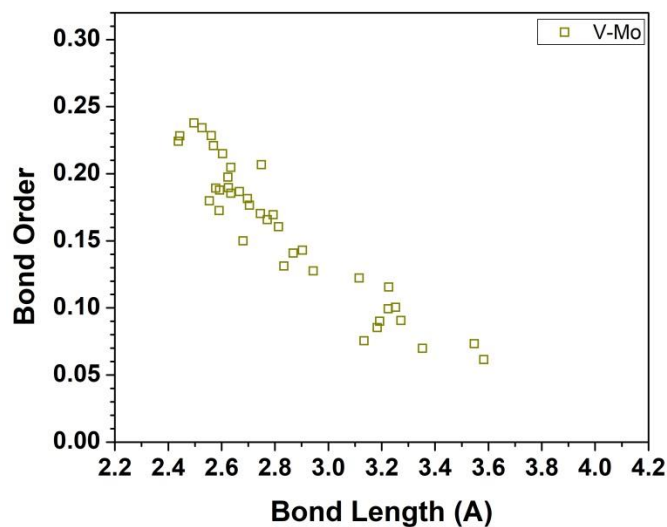
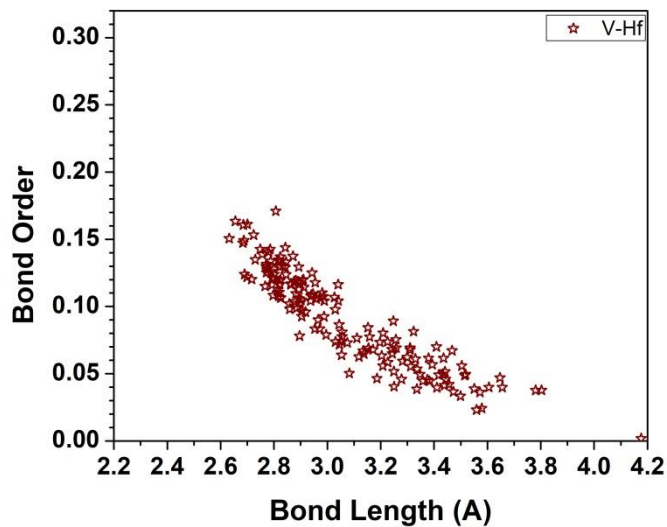
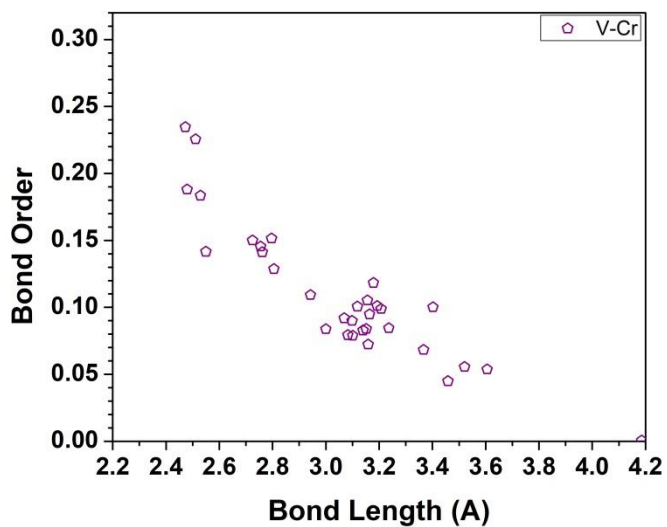


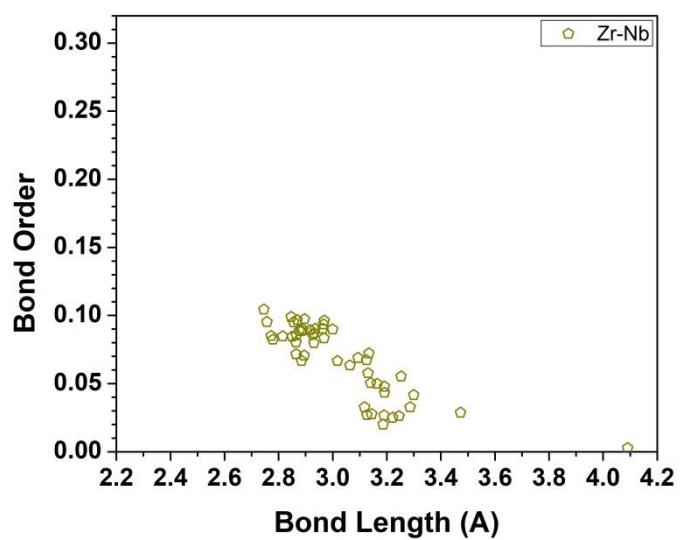
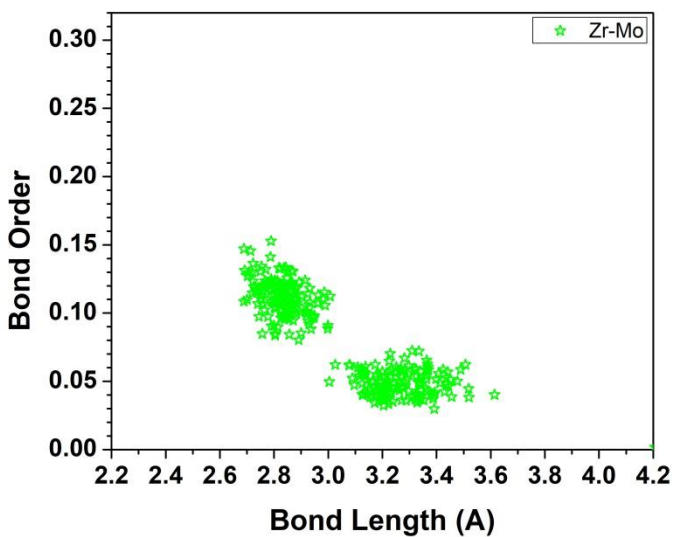
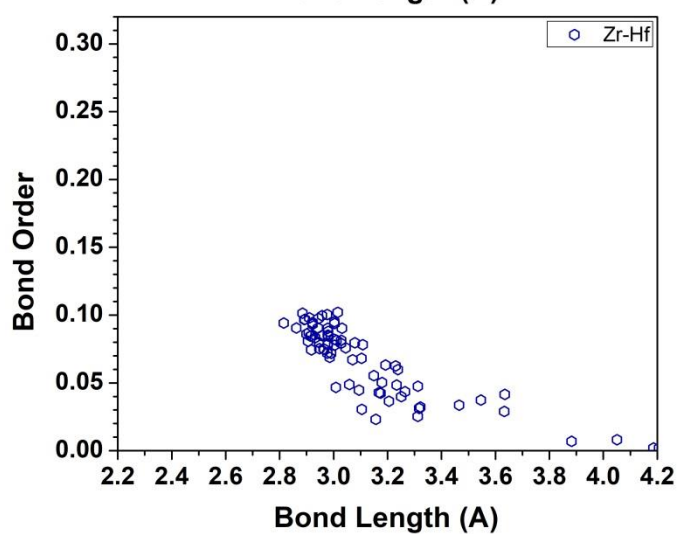
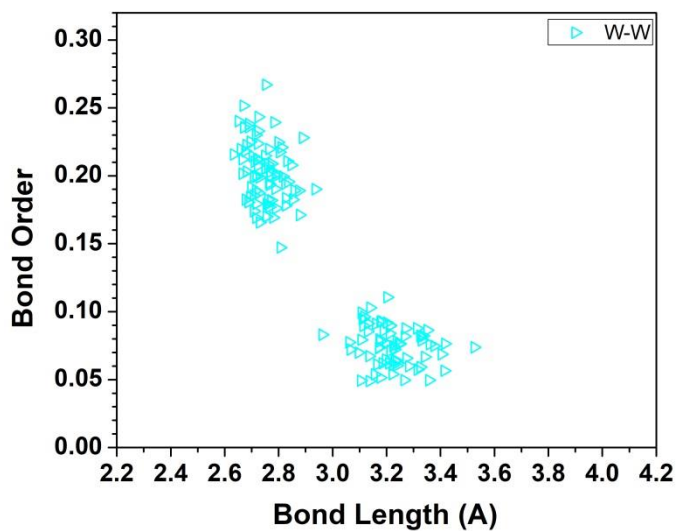
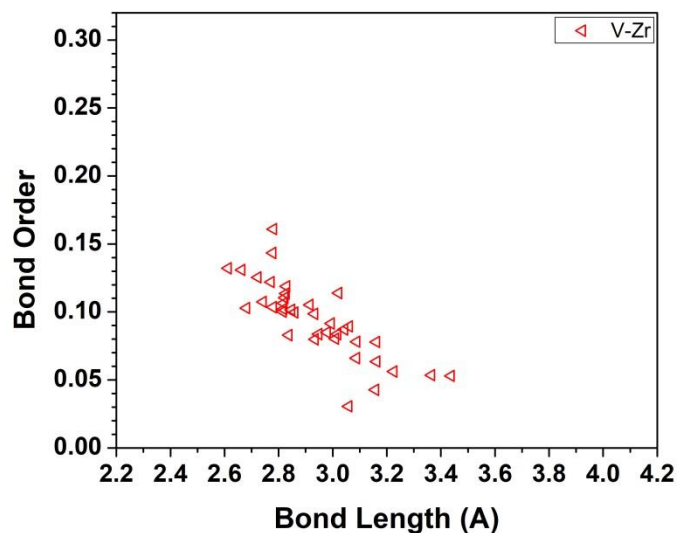
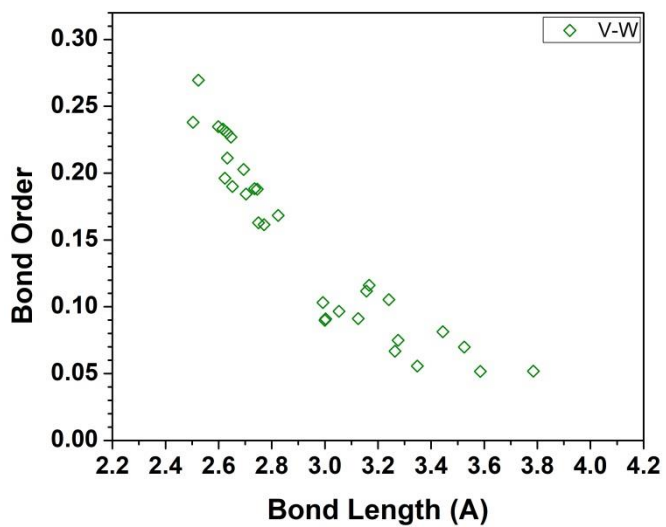


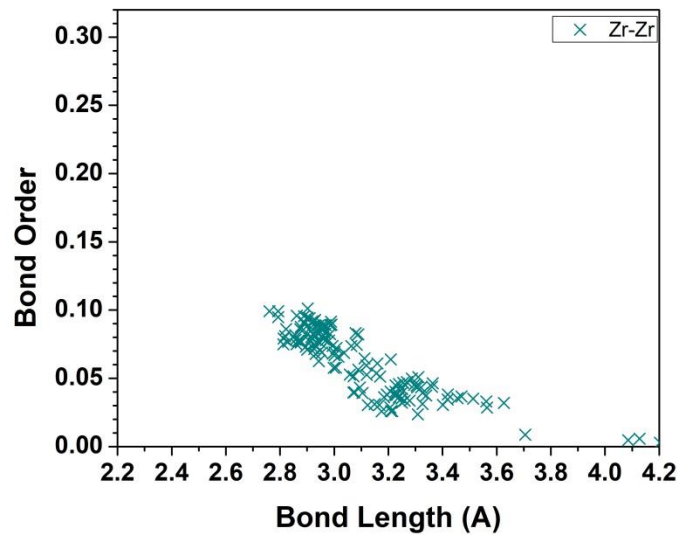
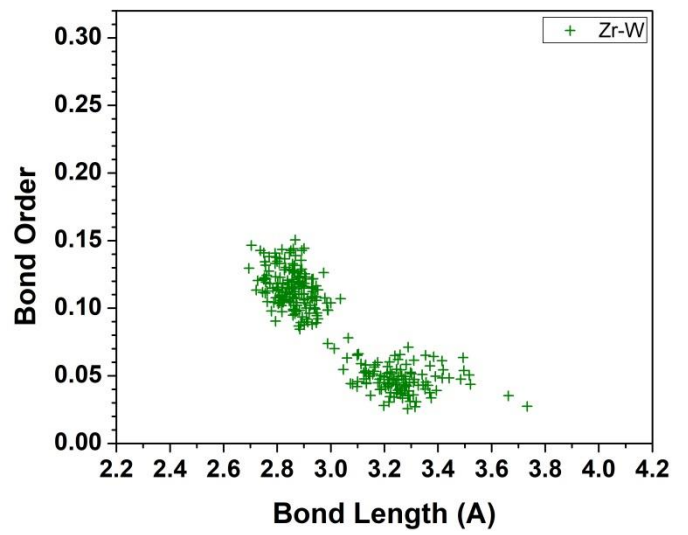
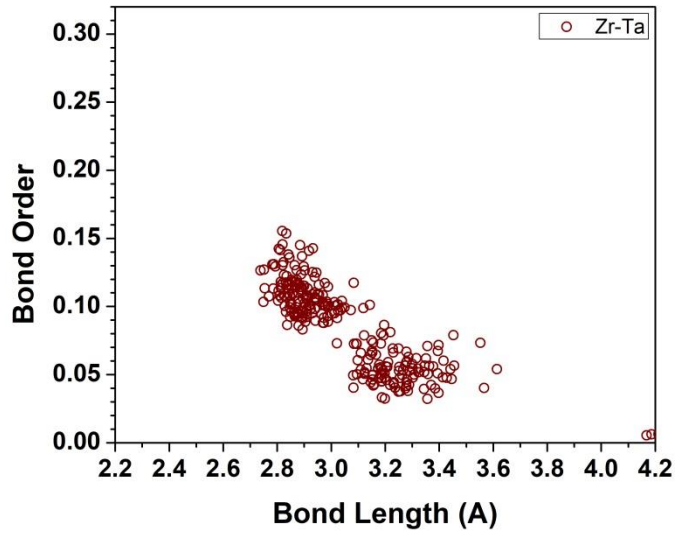




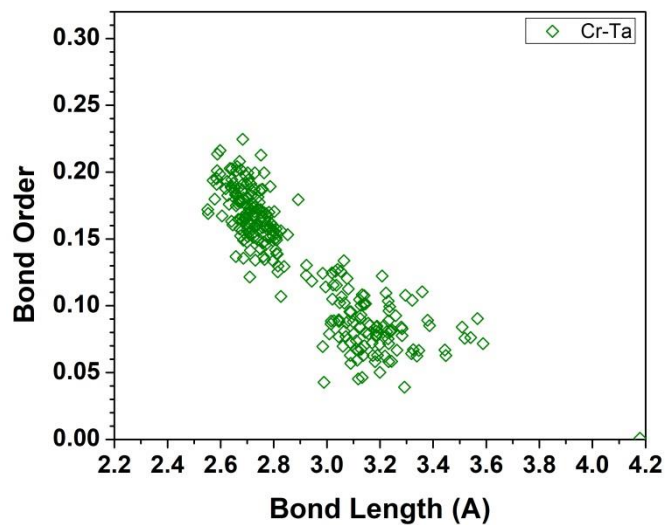
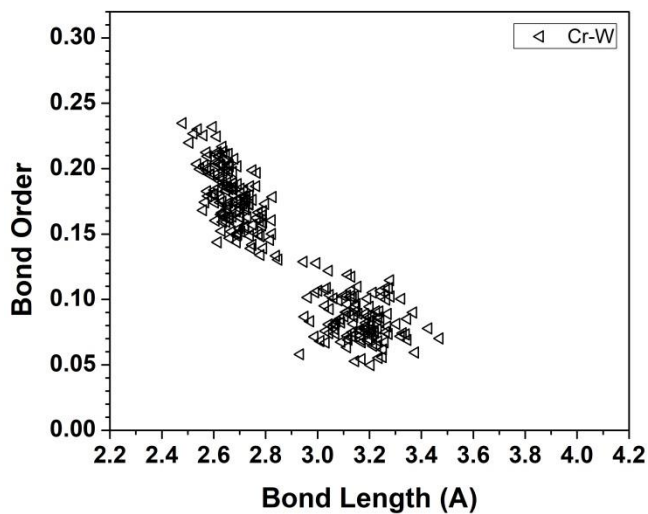
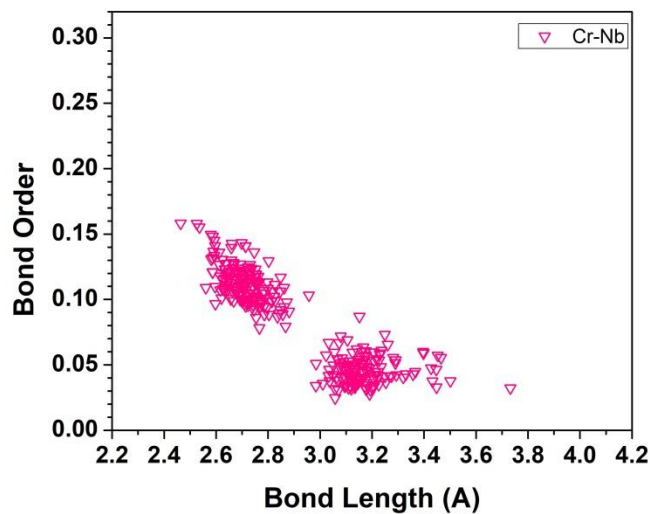
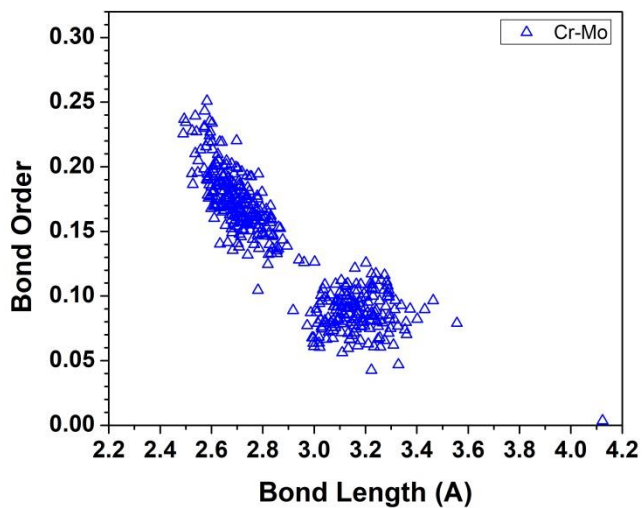
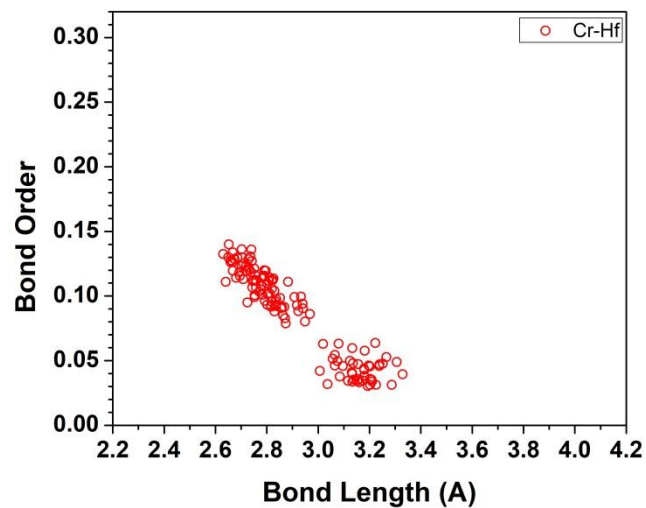
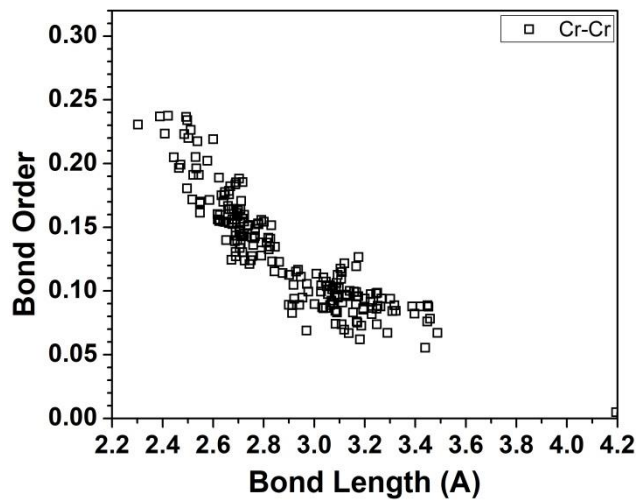


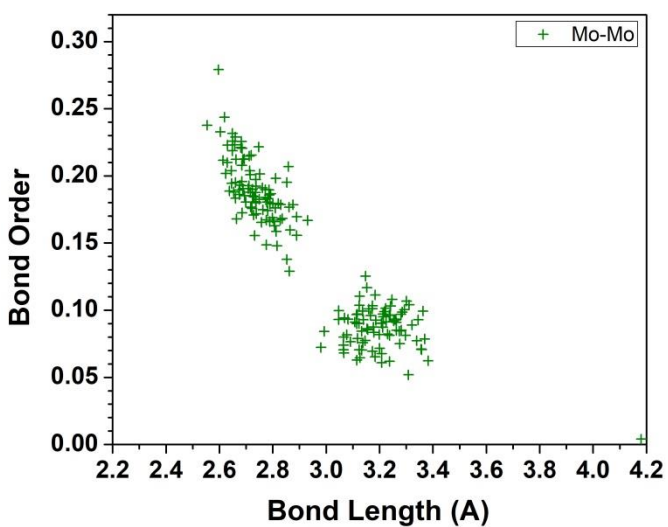
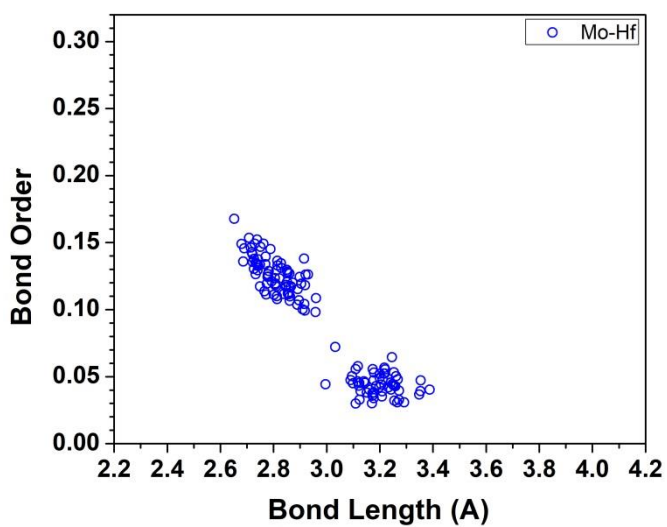
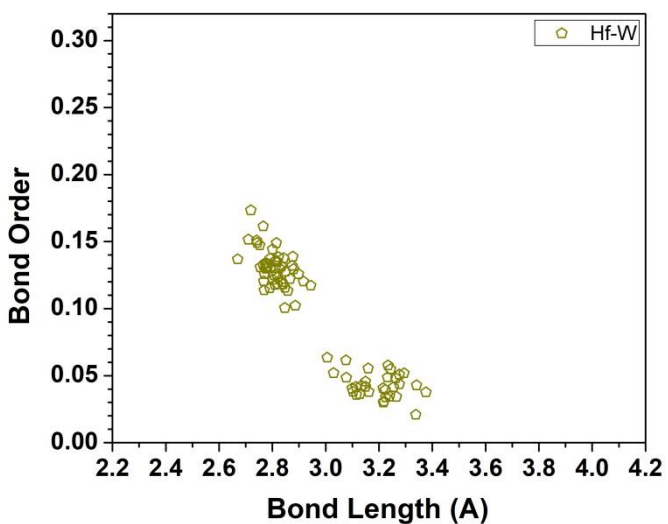
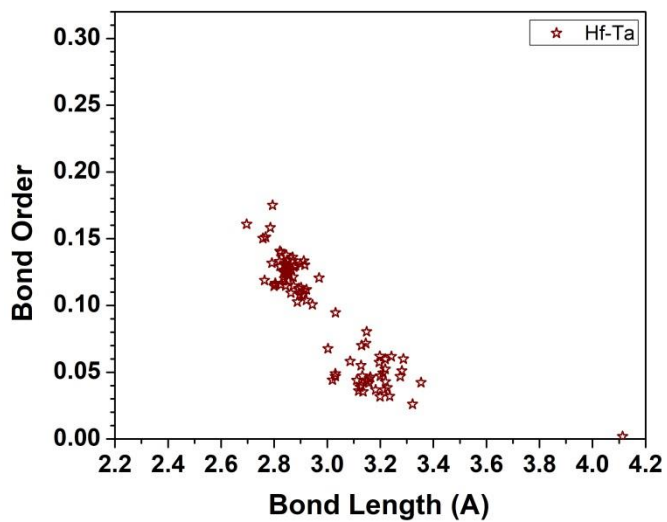
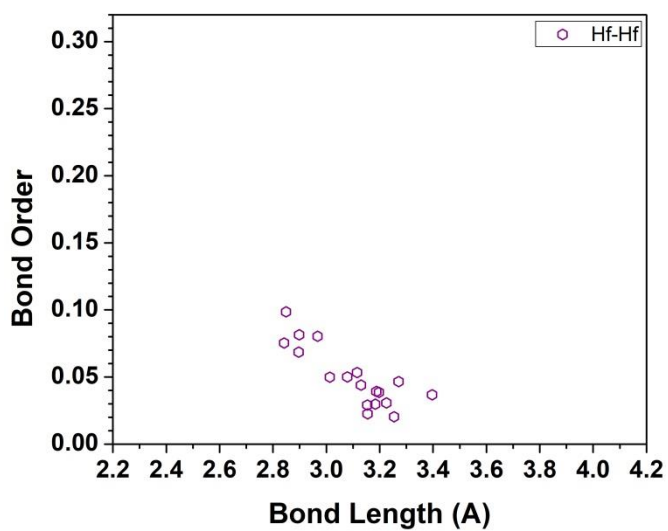
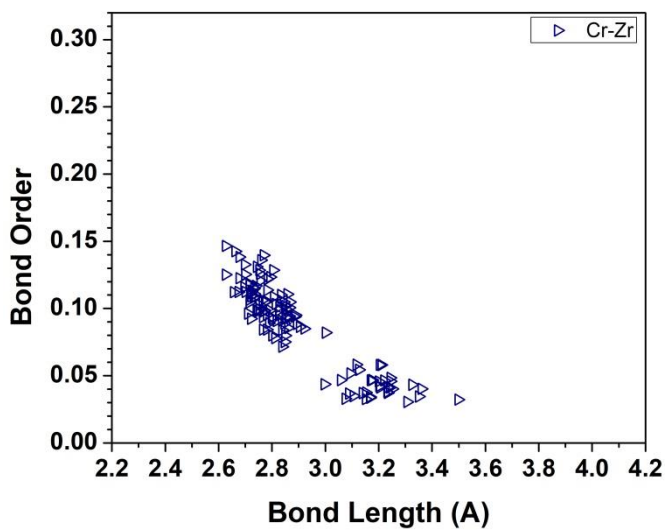


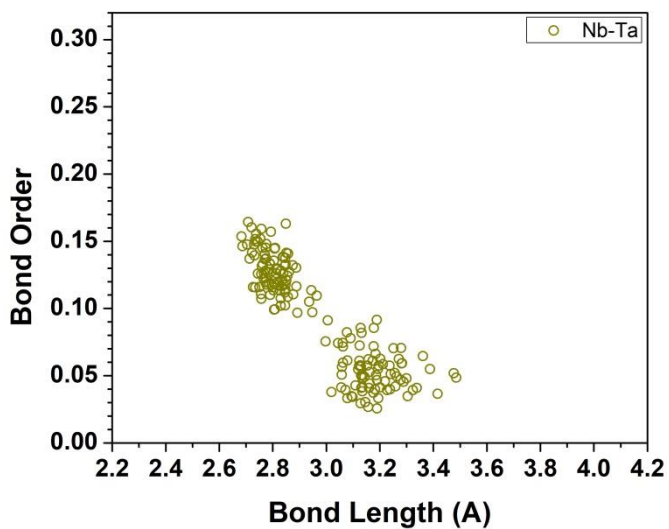
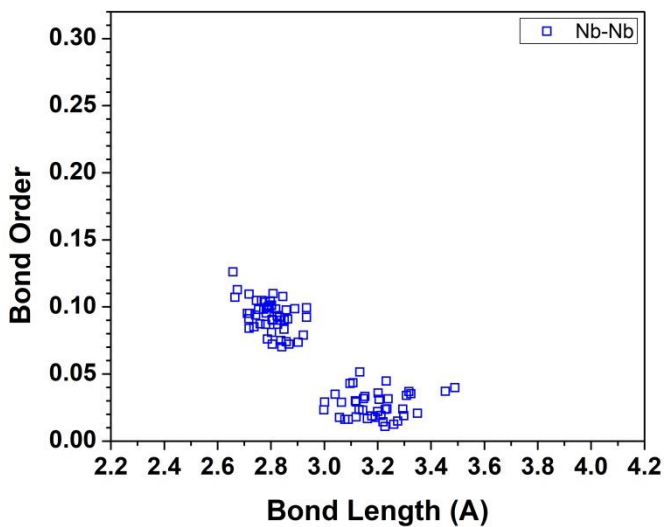
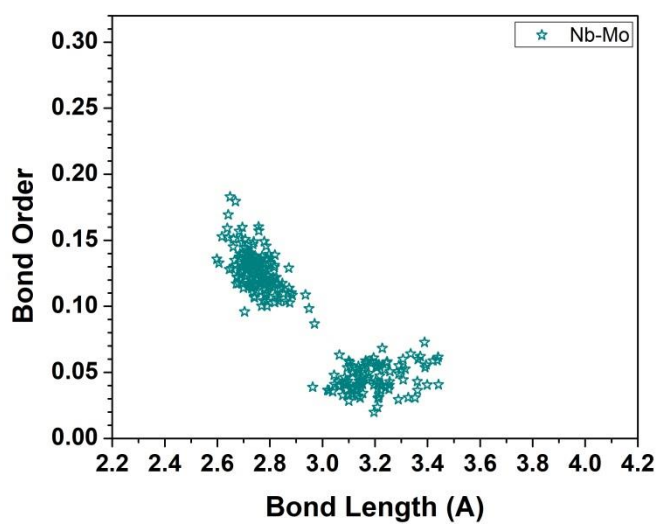
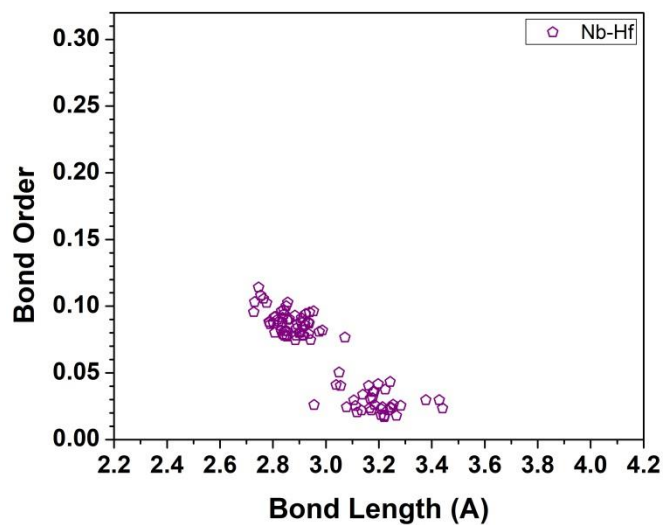
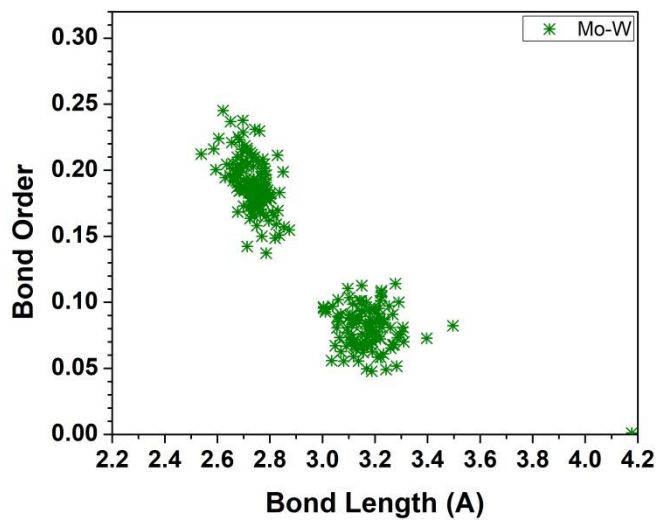
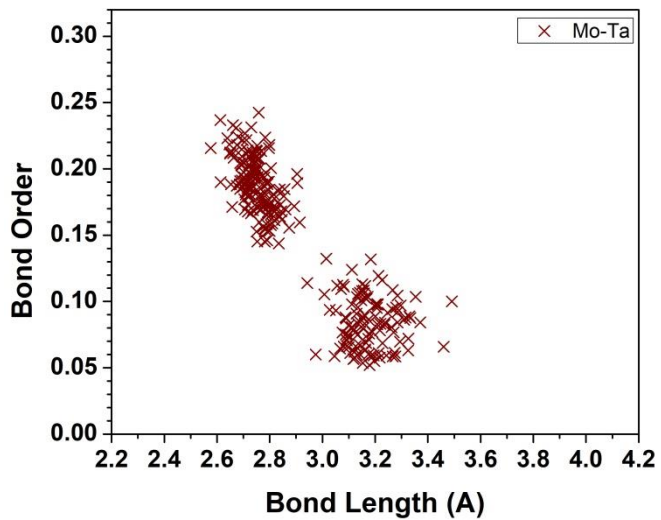


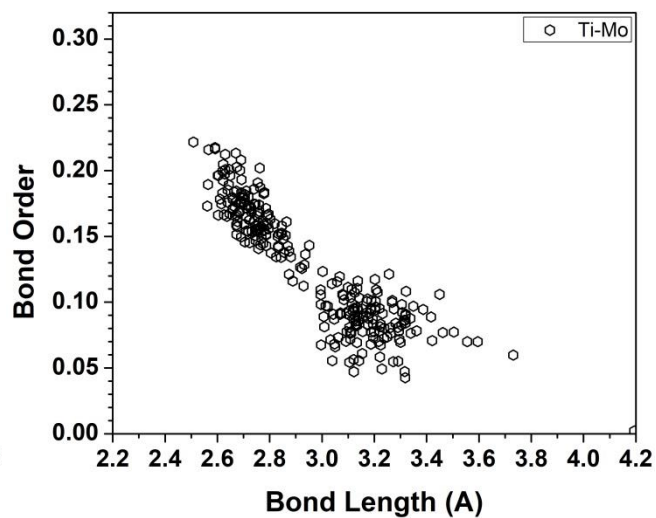
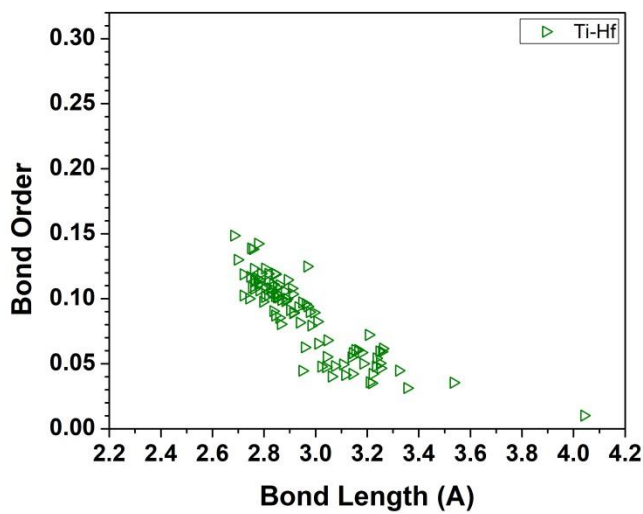
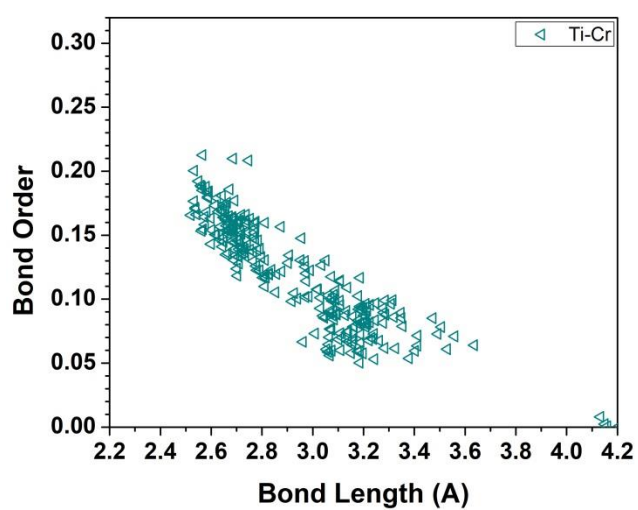
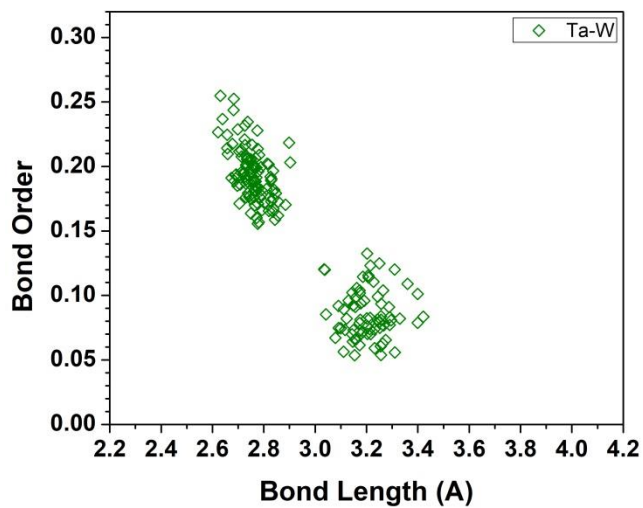
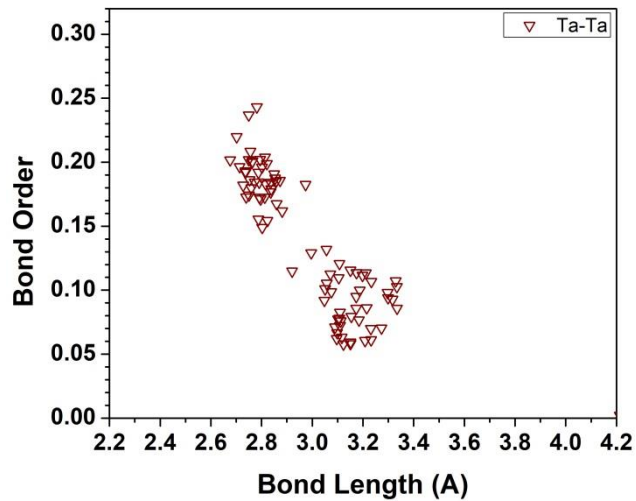
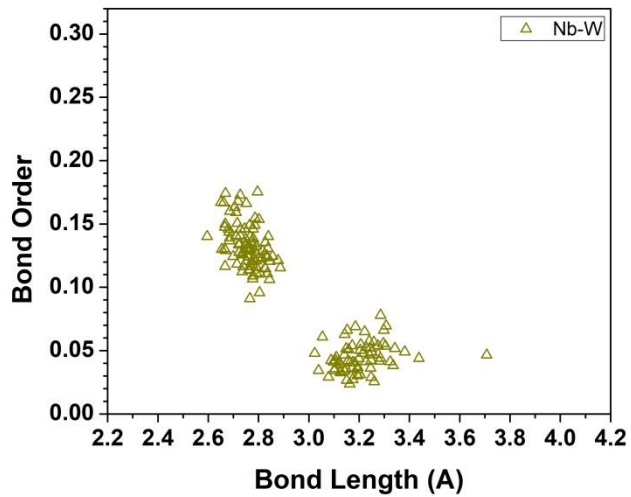


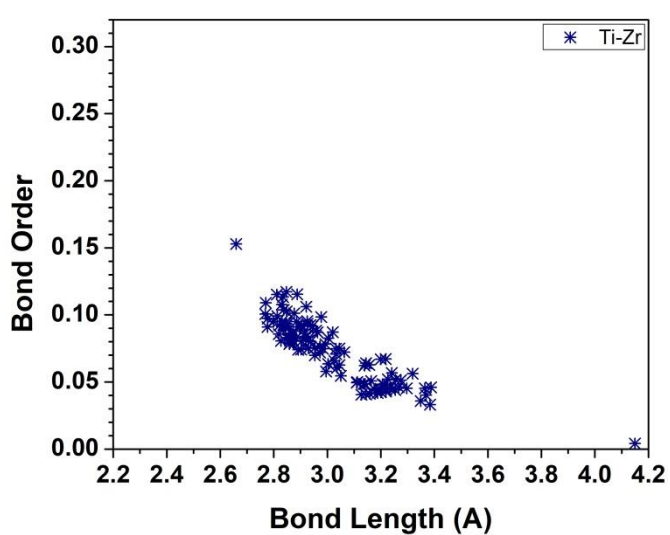
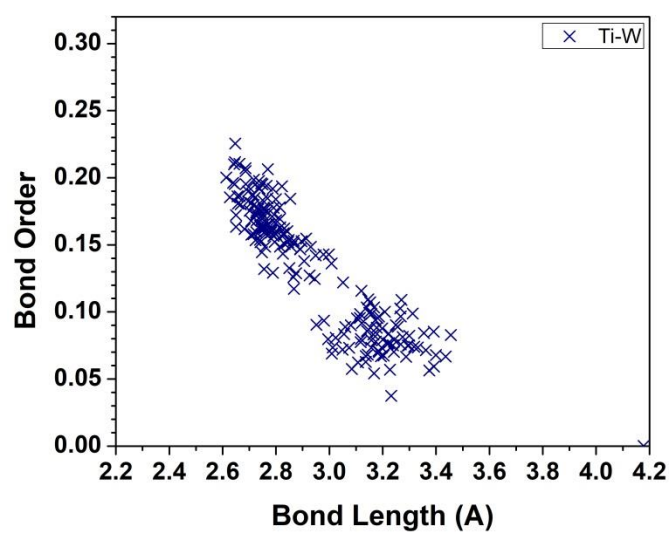
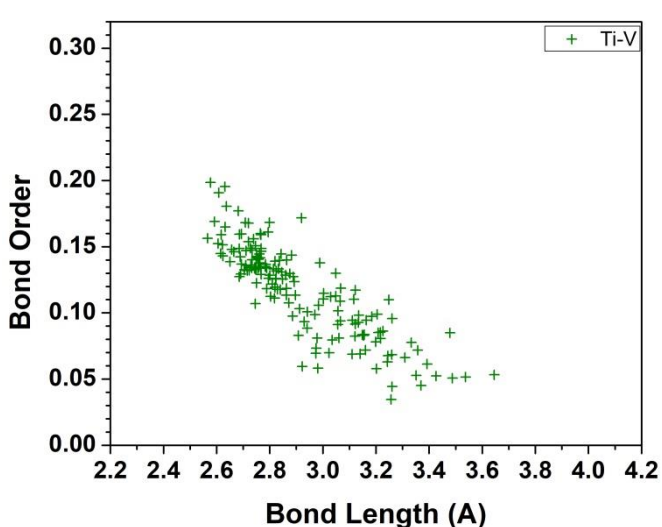
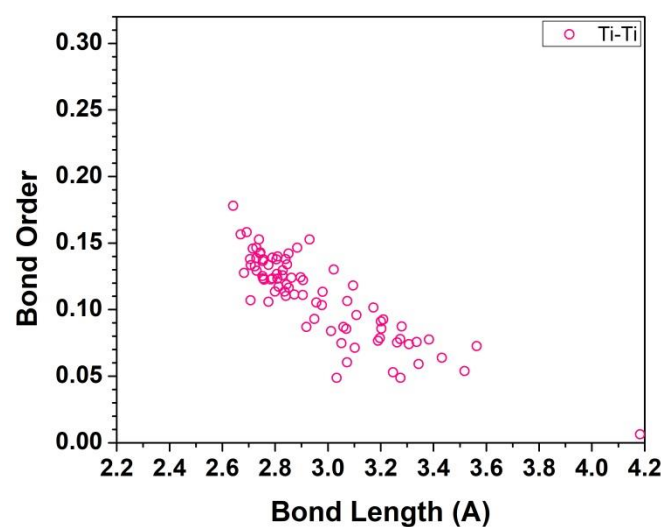
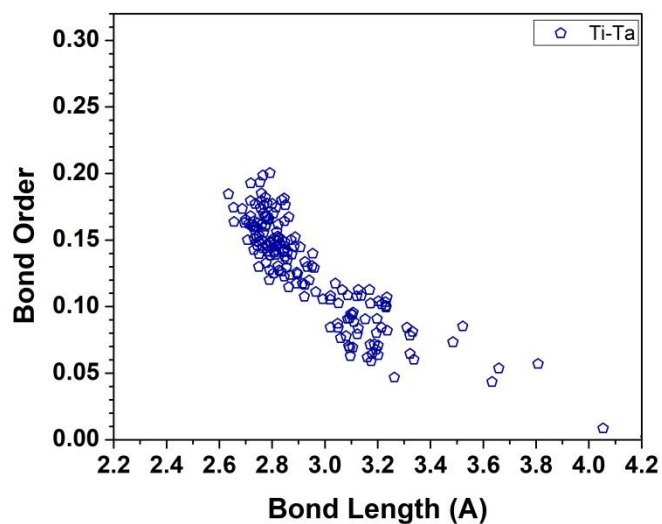
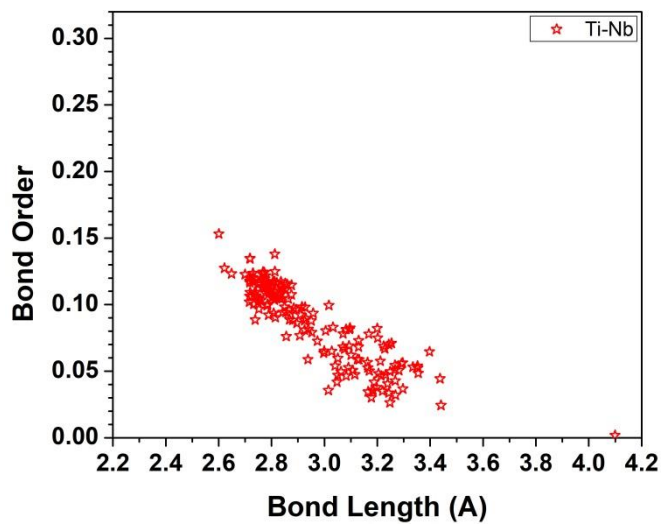
m5

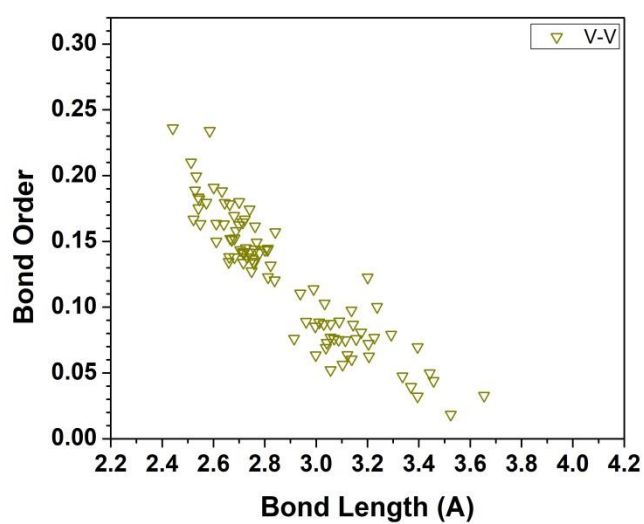
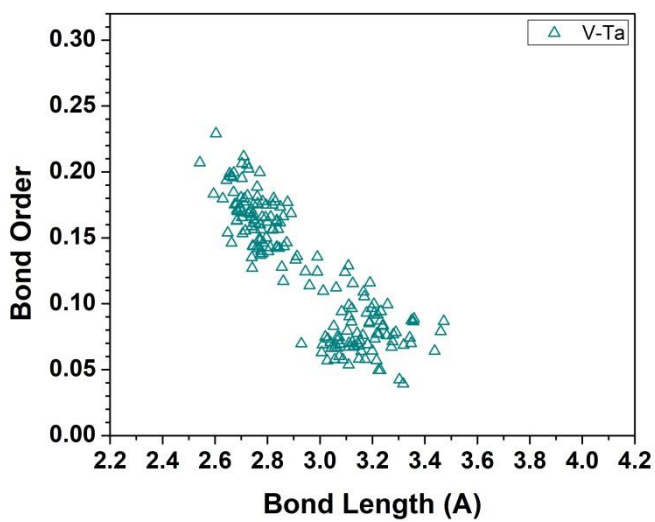
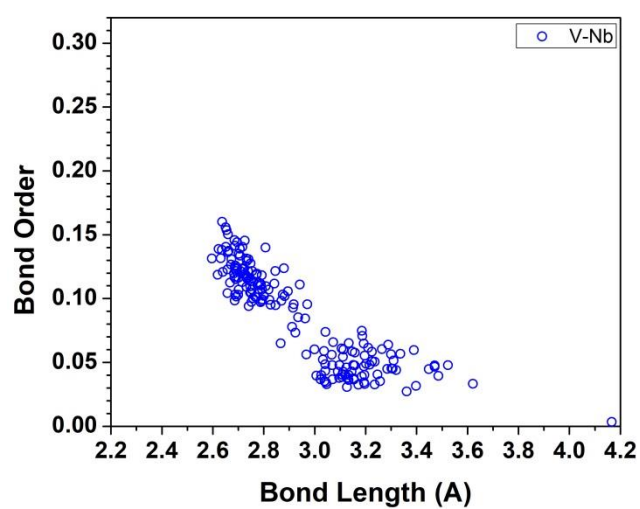
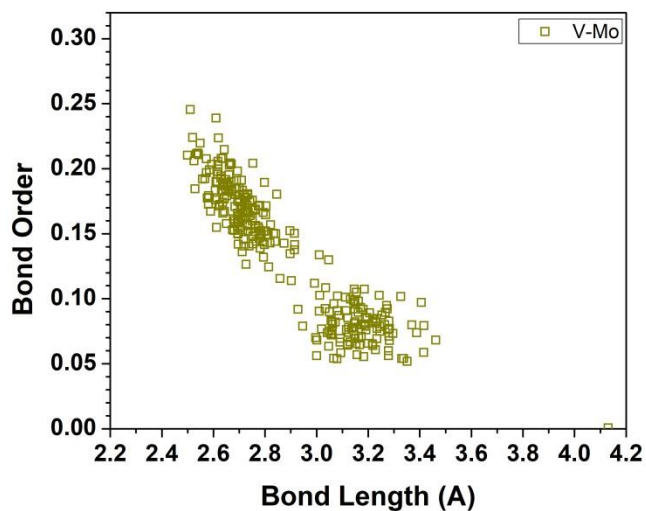
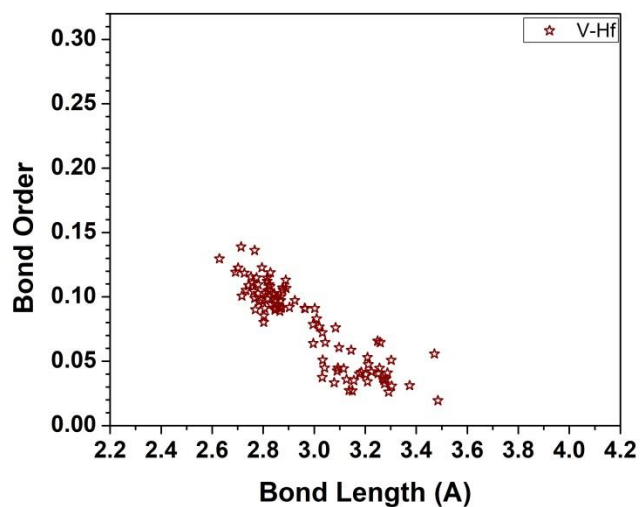
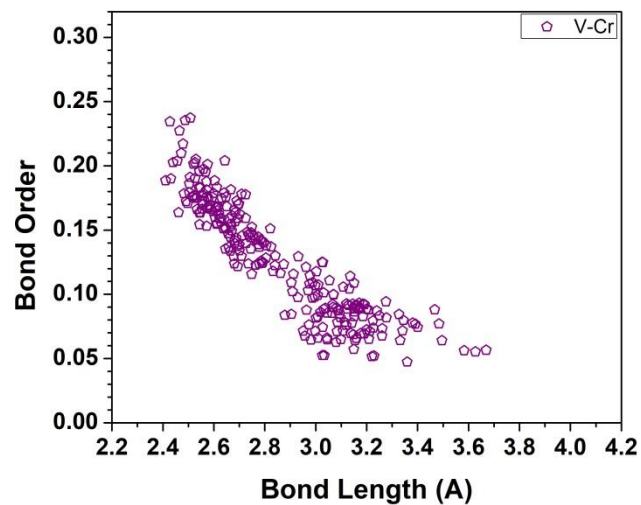


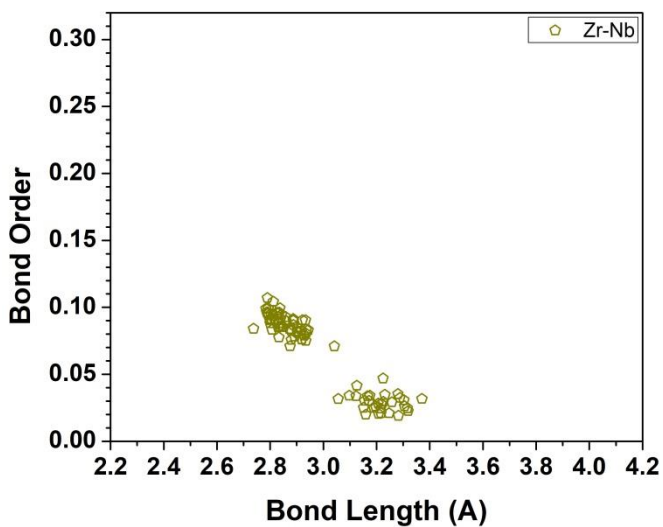
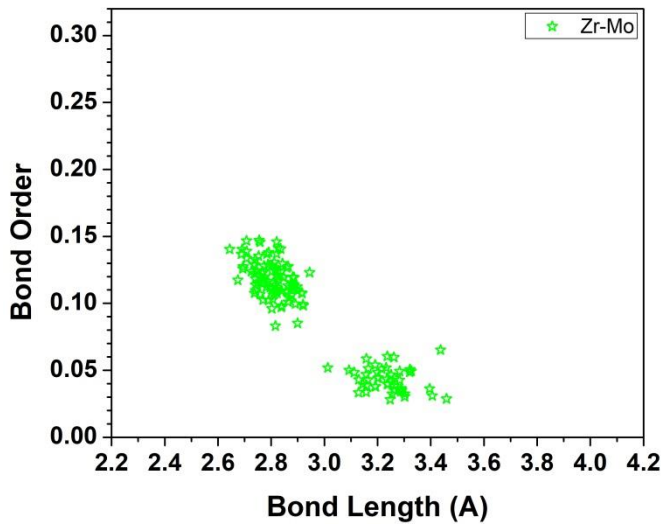
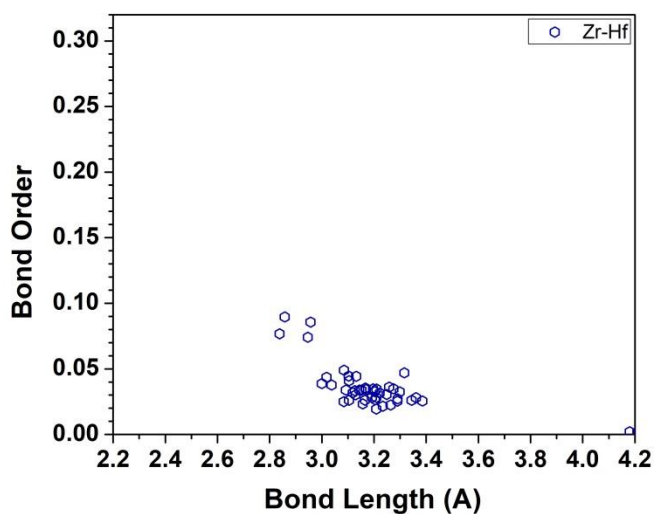
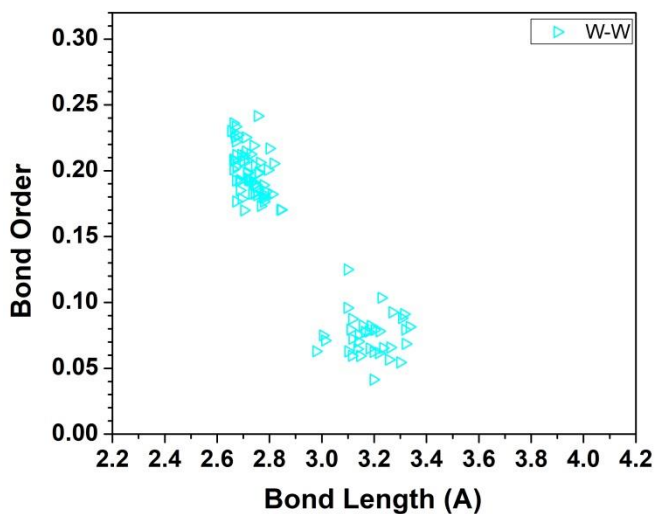
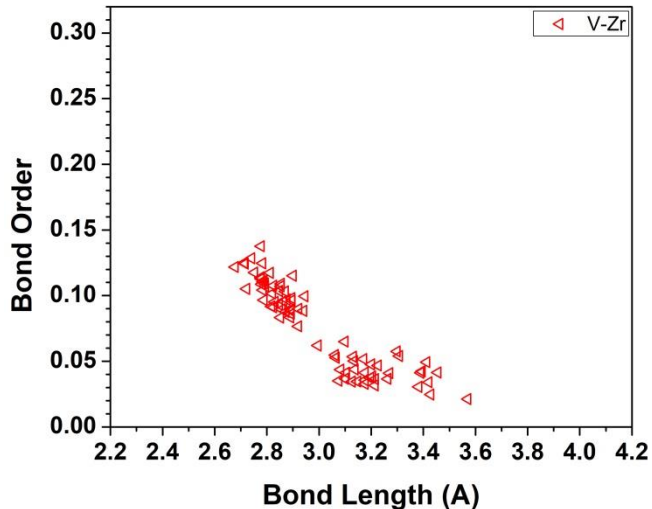
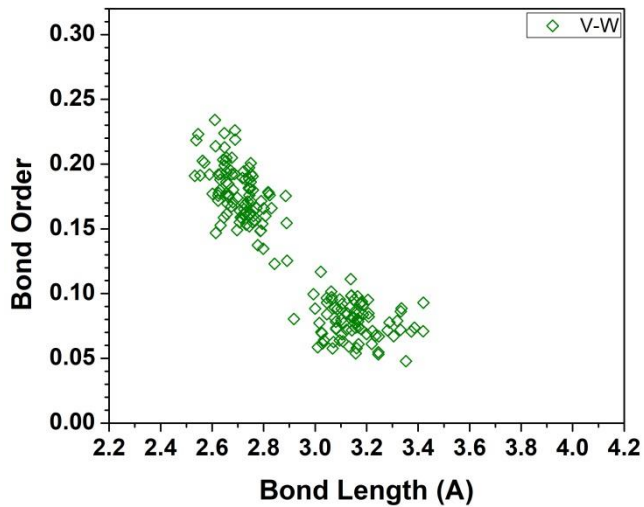


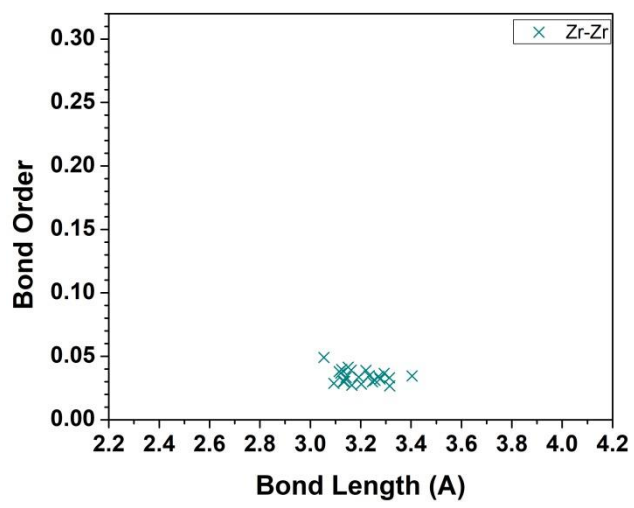
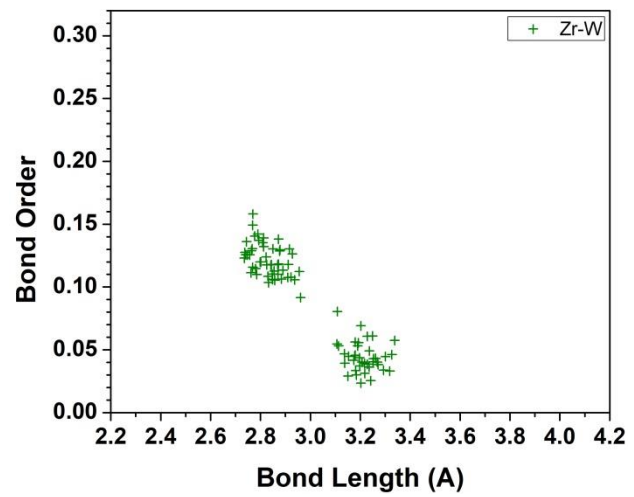
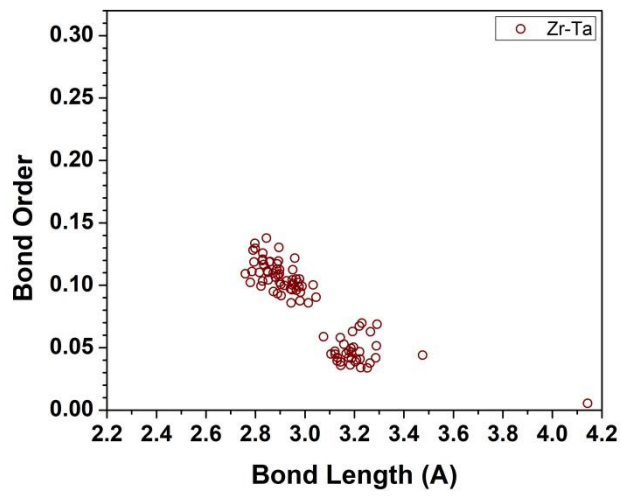




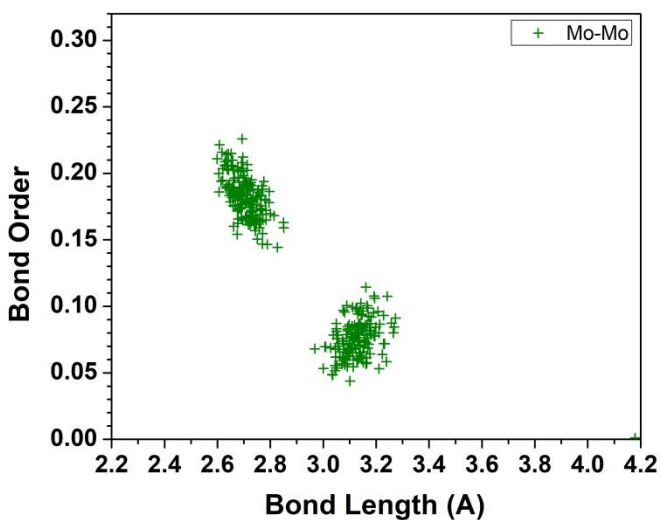
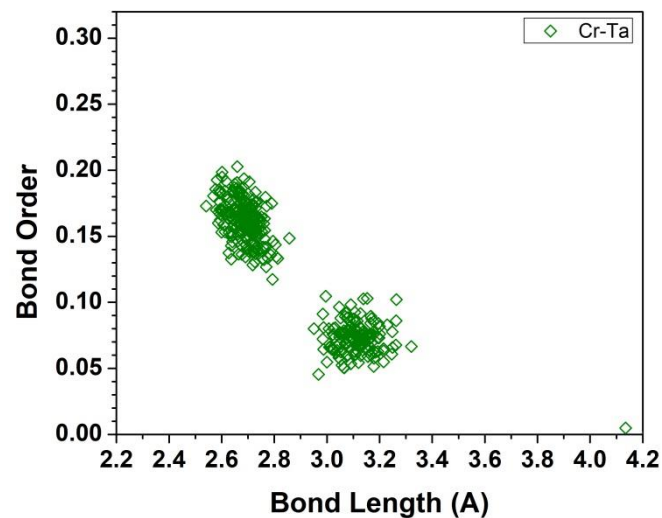
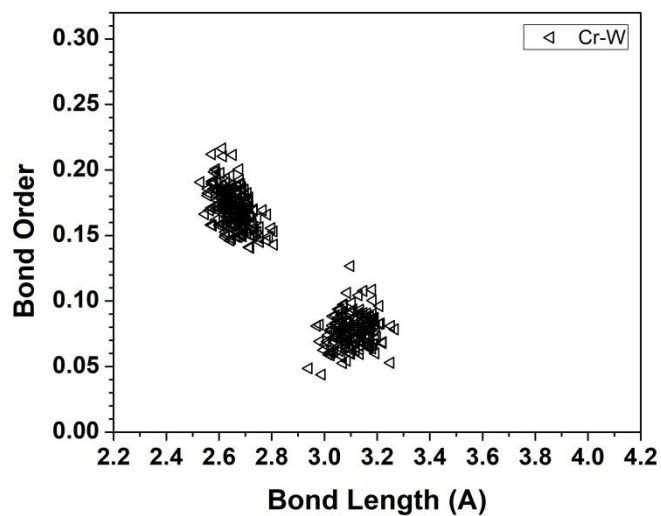
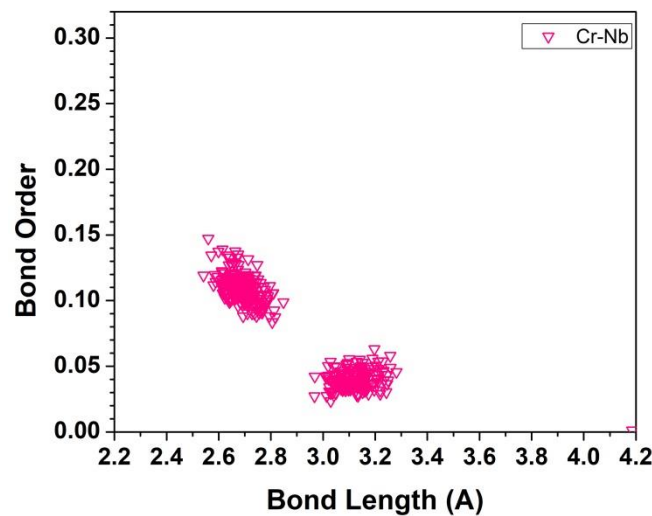
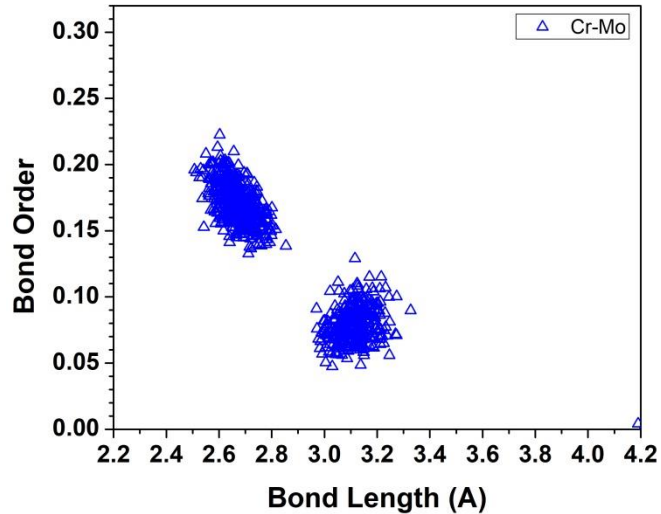
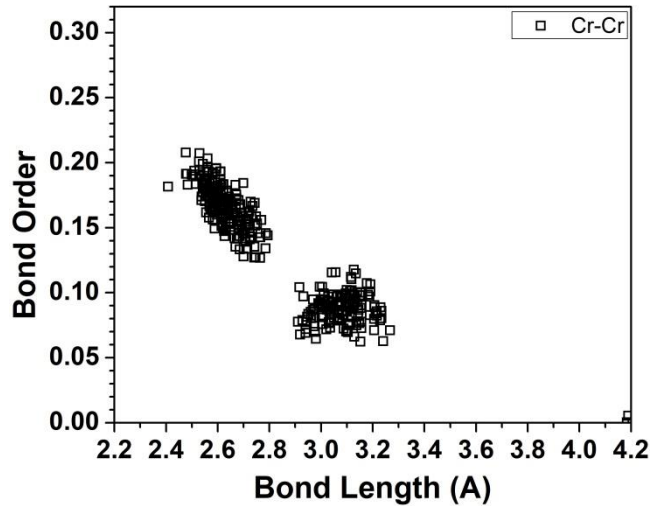


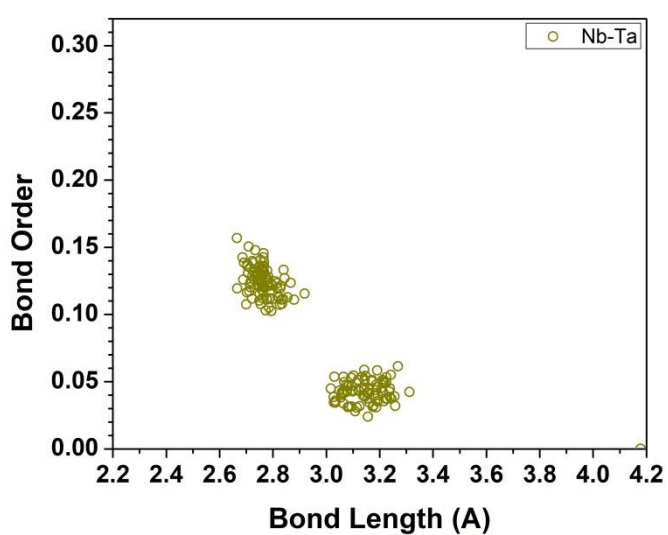
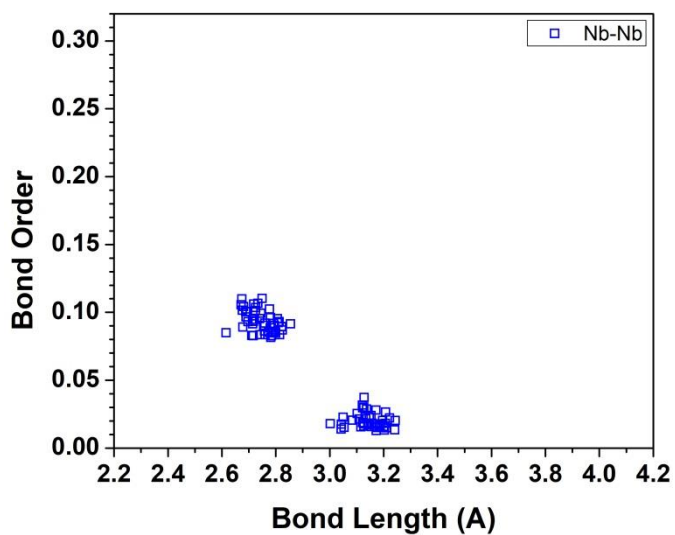
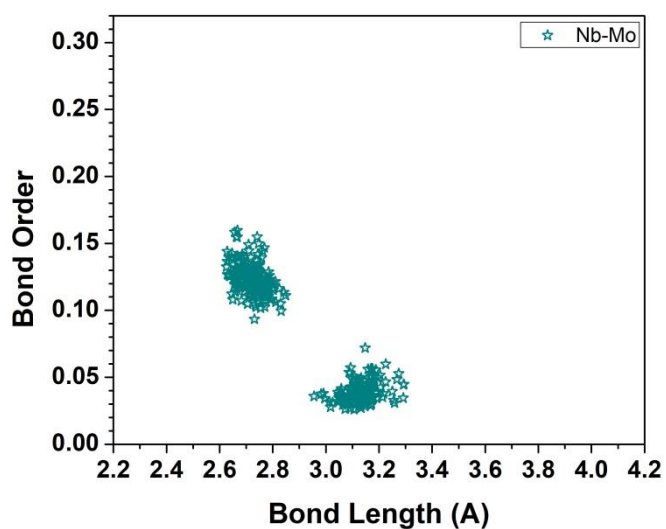
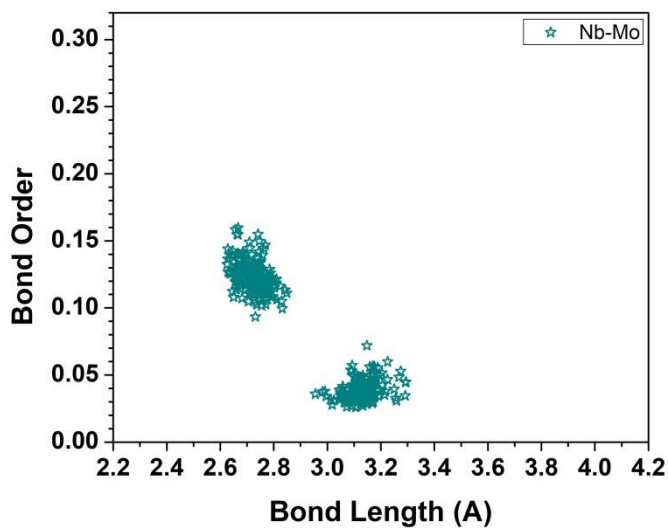
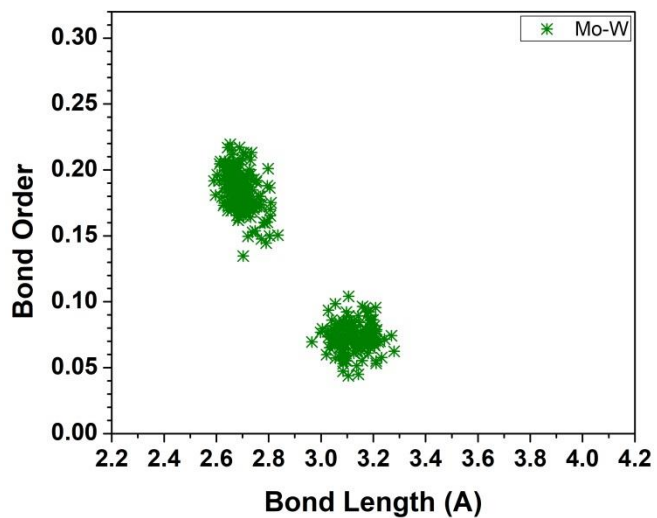
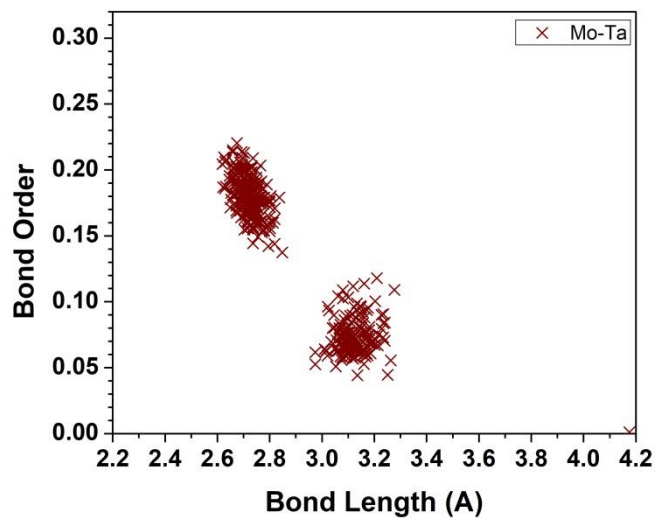


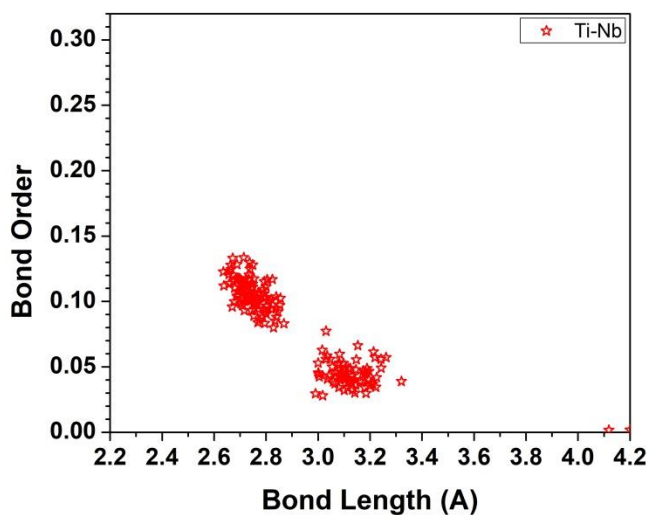
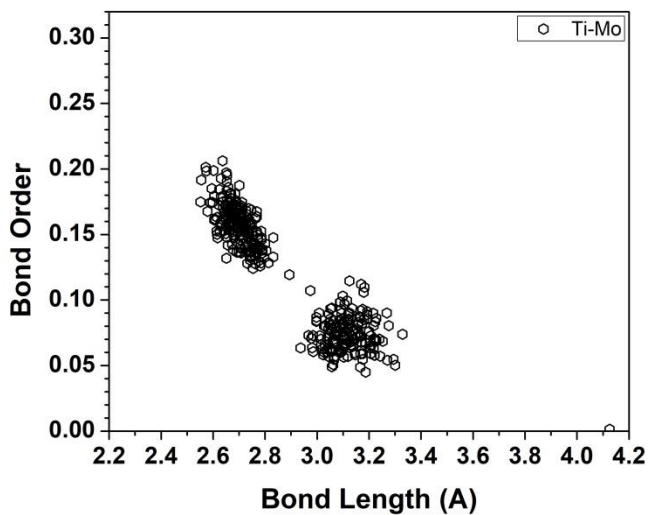
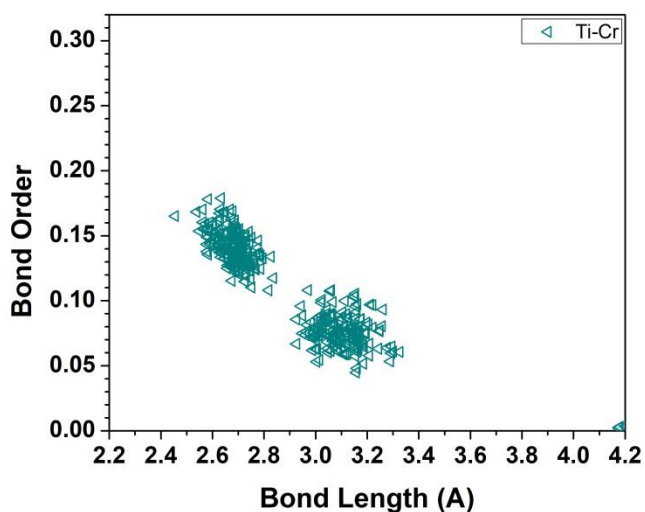
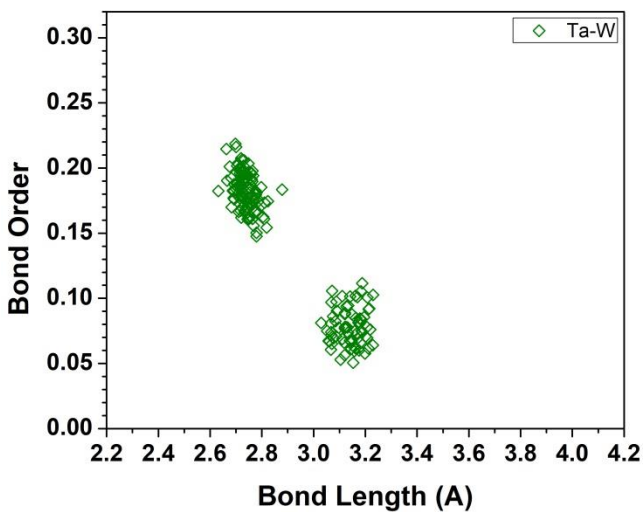
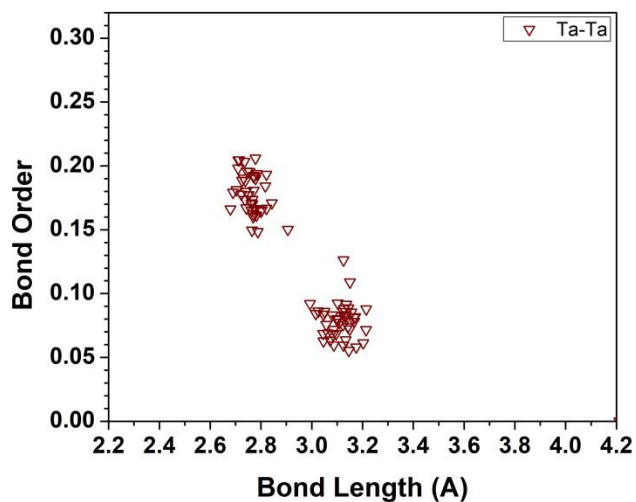
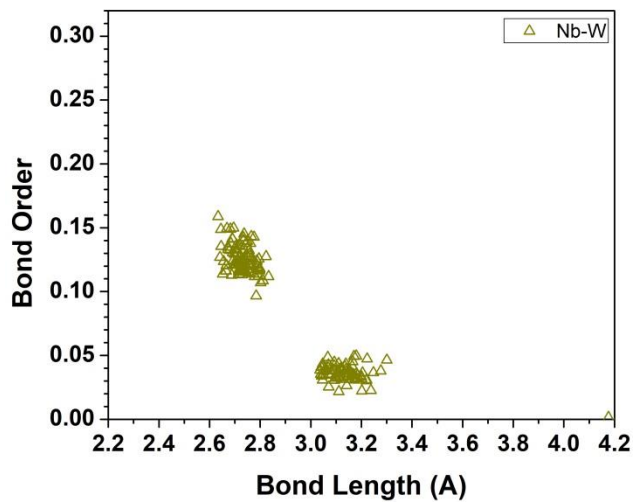


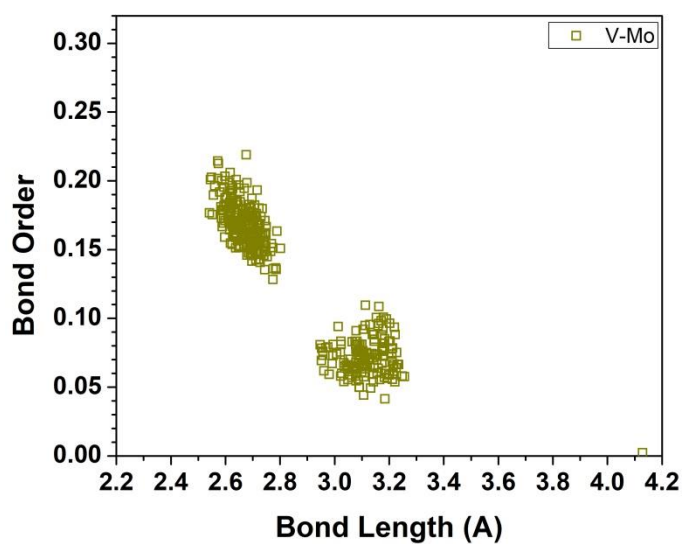
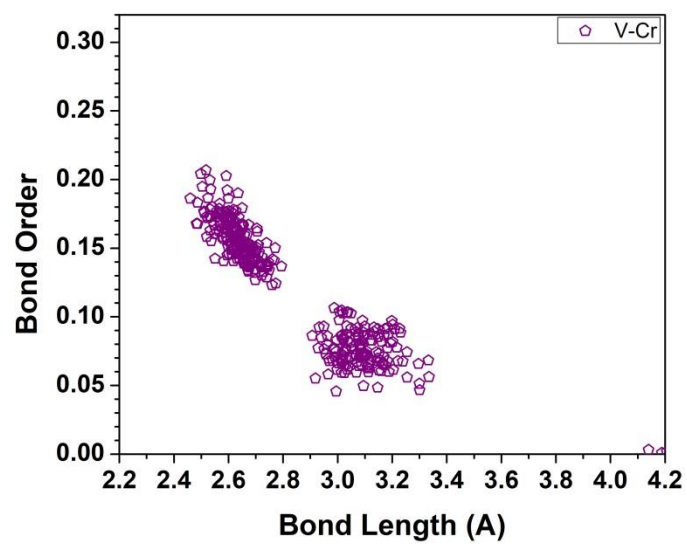
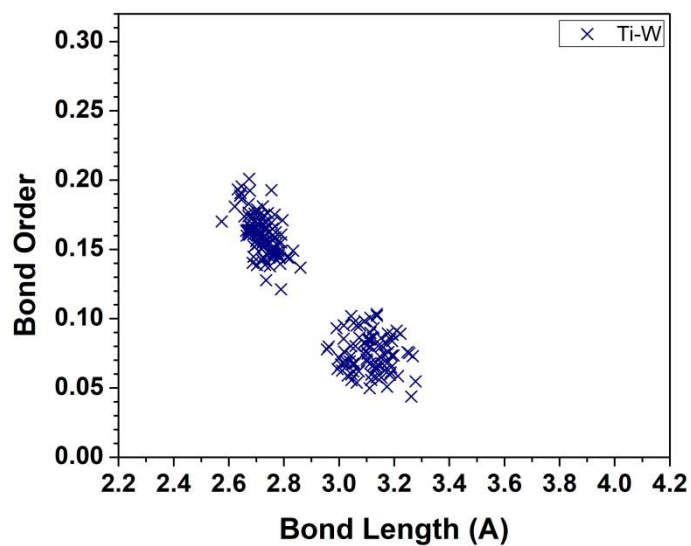
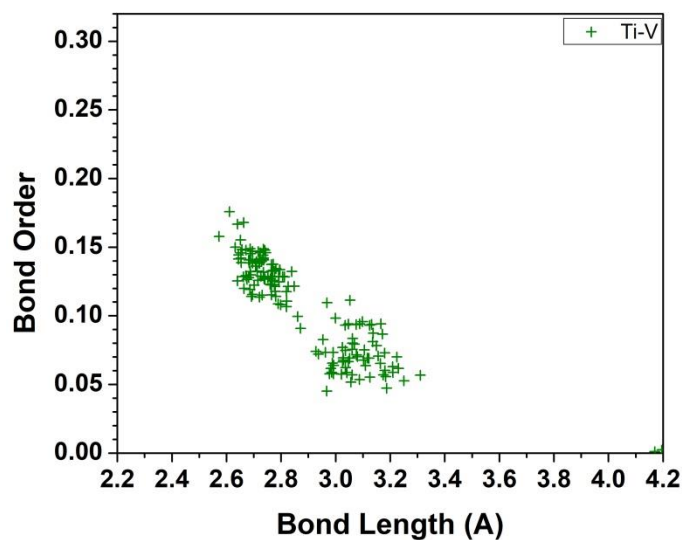
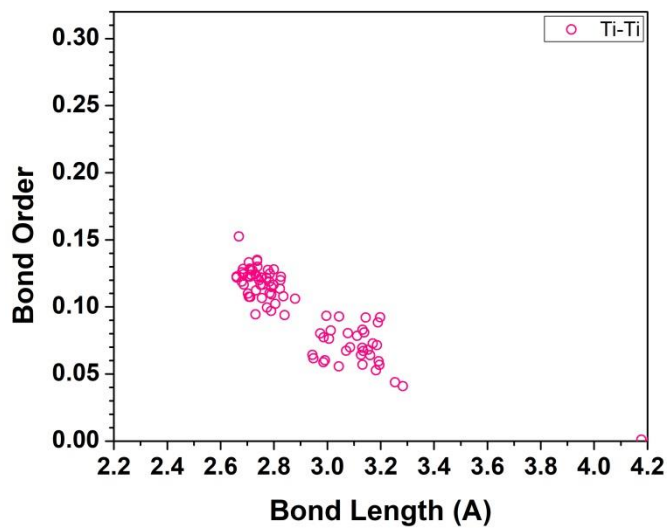
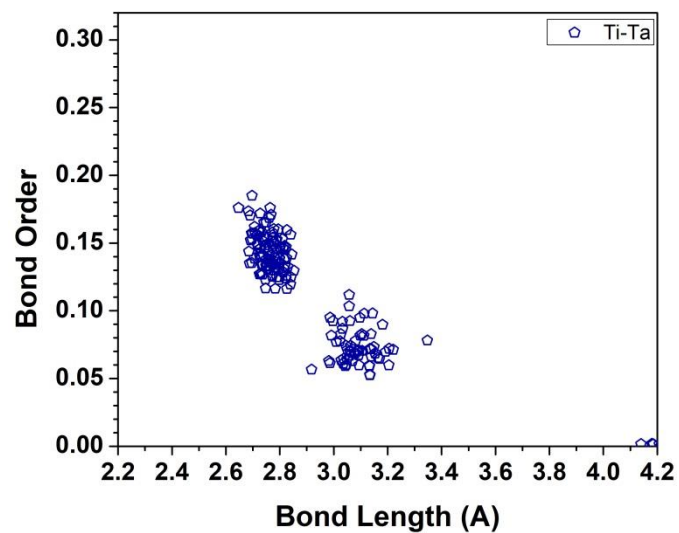


m6









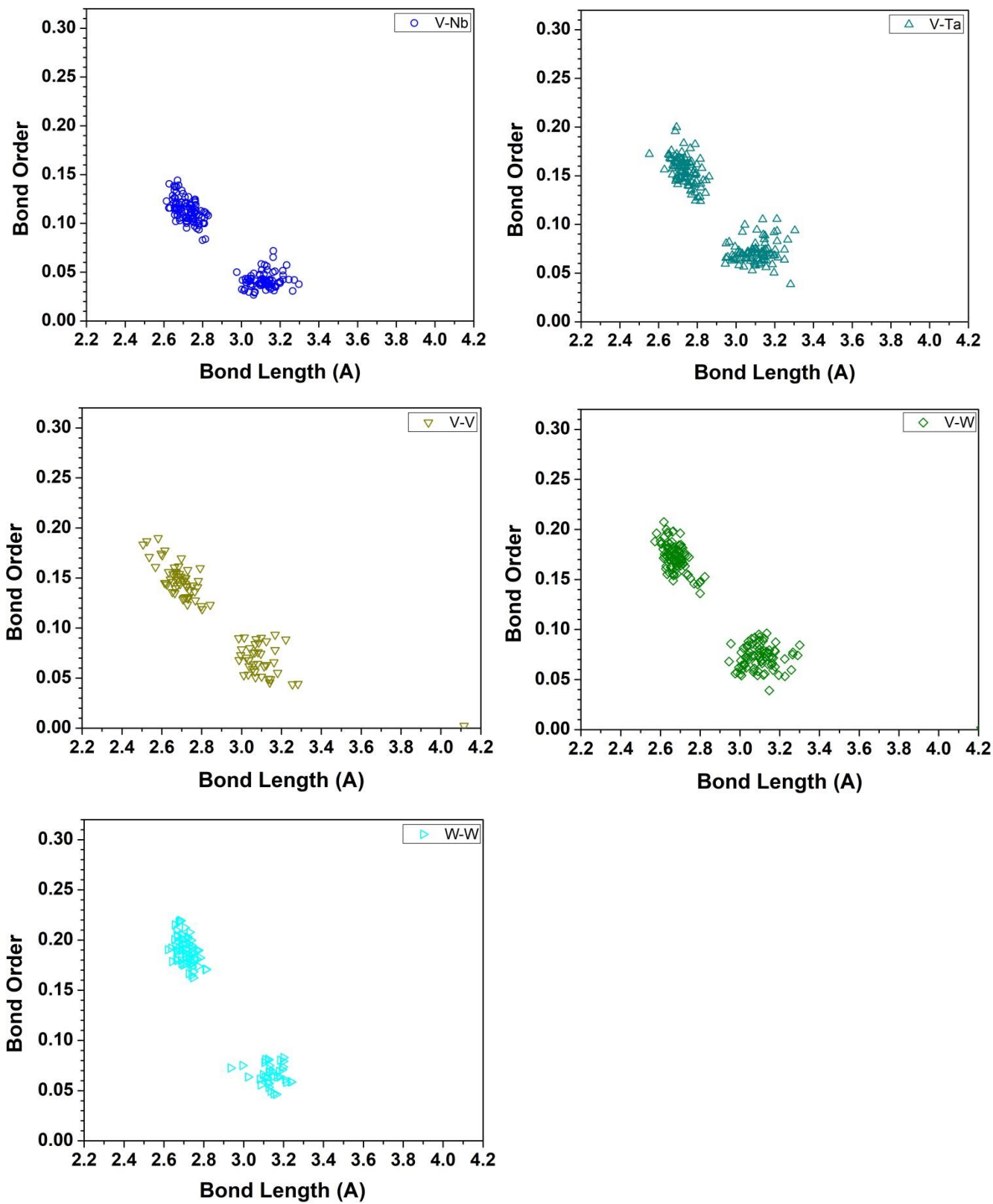
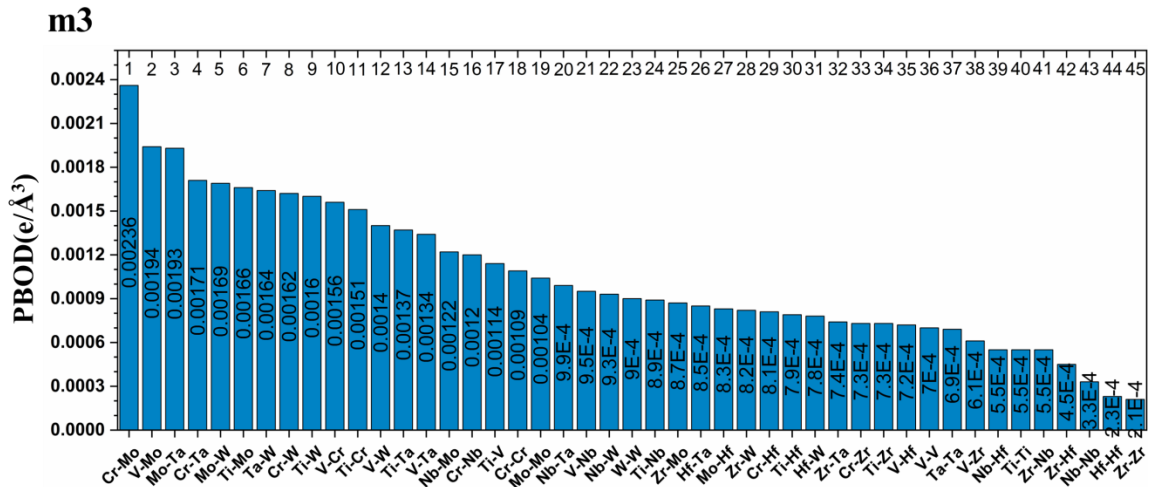
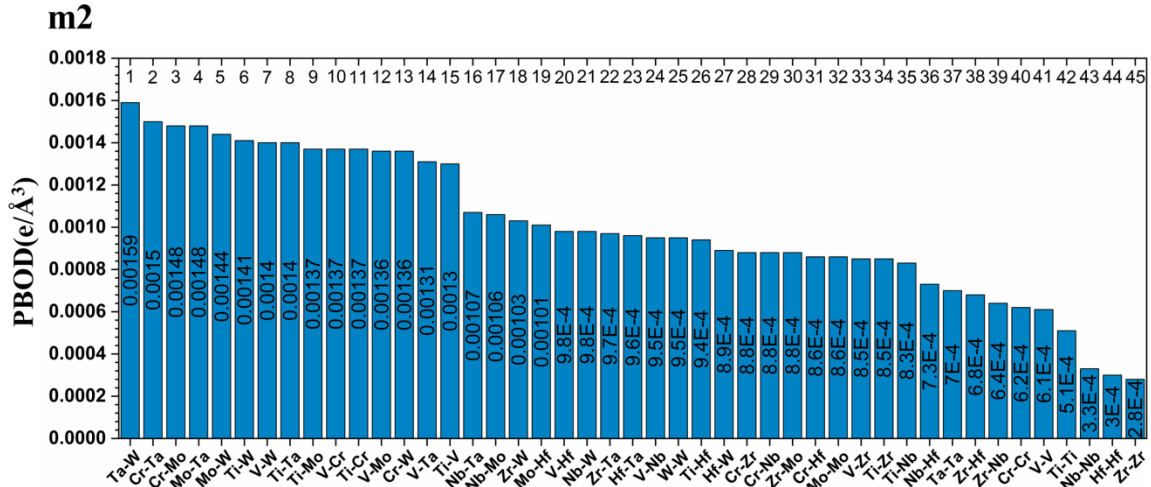
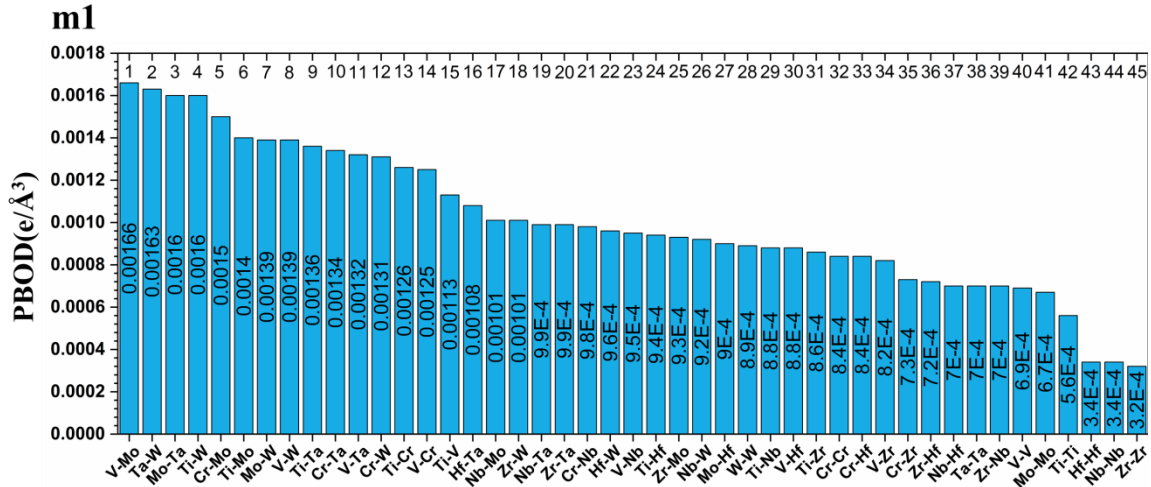


Figure S6. Bond order (BO) versus bond length (BL) distribution in the six RHEAs models.



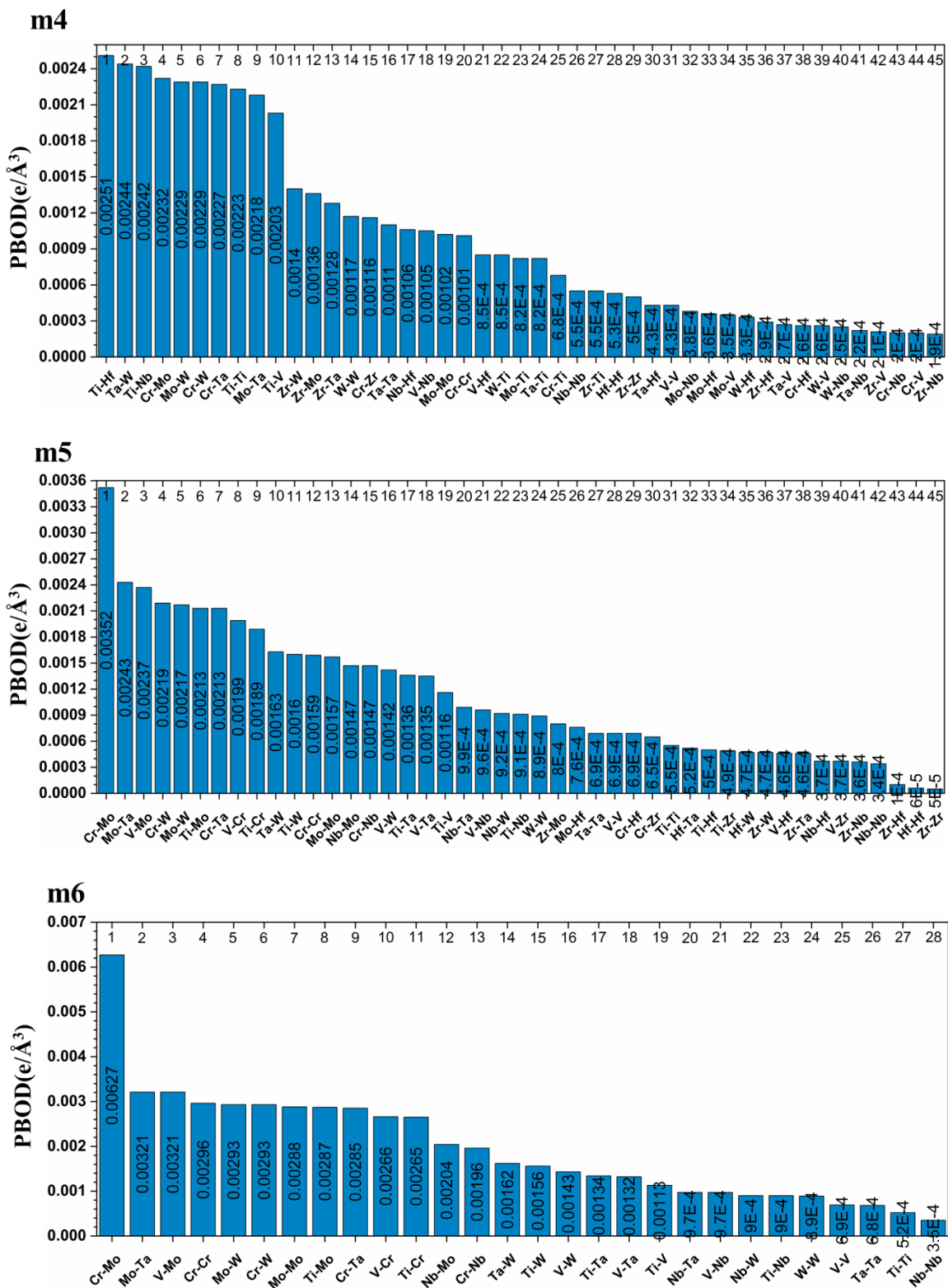


Figure S7. Distribution of the partial bond order density (PBOD) in the six RHEAs models as is displayed in bar charts.

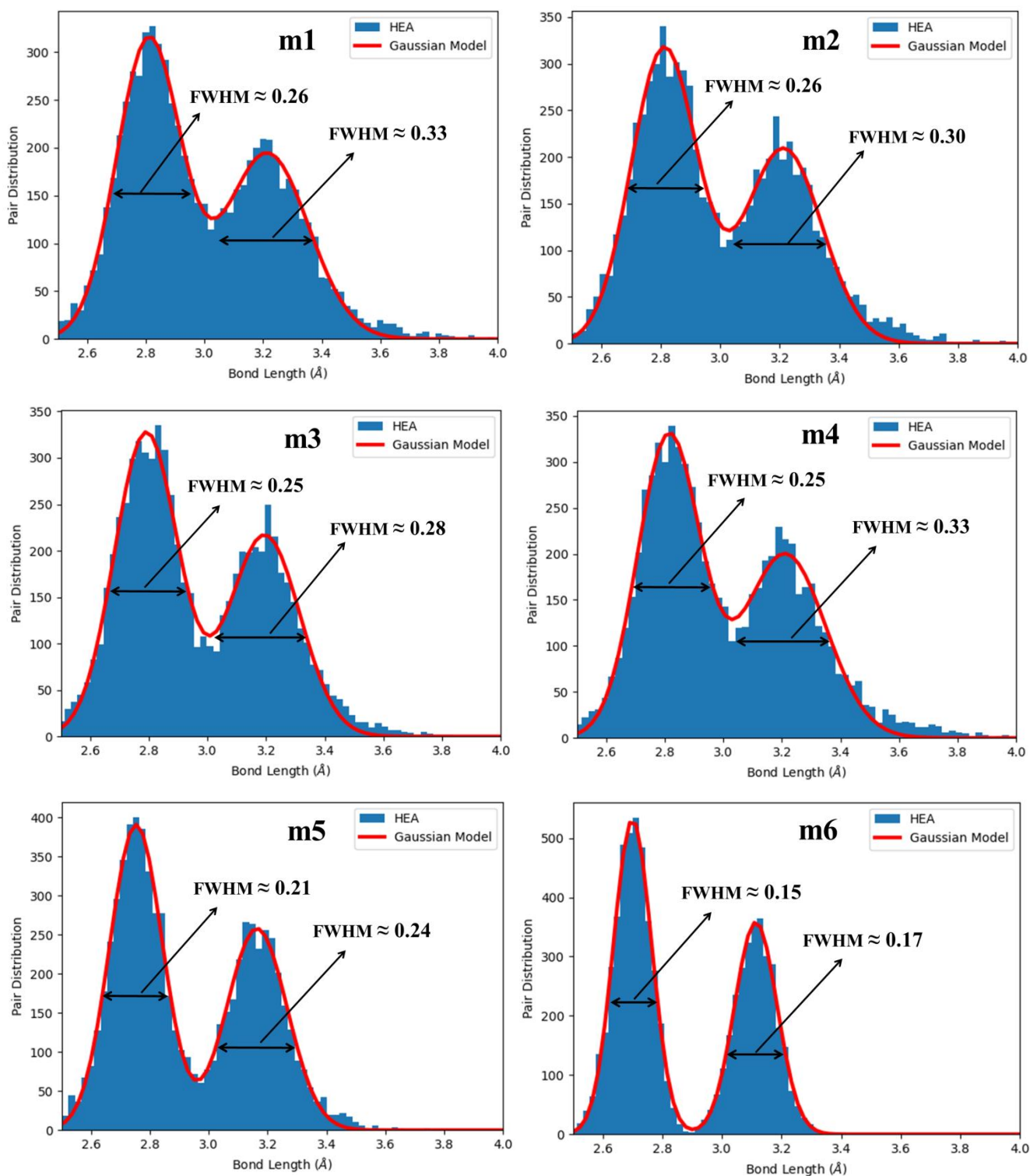


Figure S8. Lattice distortion (LD) in the six RHEAs models. FWHM of the Gaussian curve fitted to the histogram distribution of the bimodal peaks. The two peaks denote the NN and SNN.

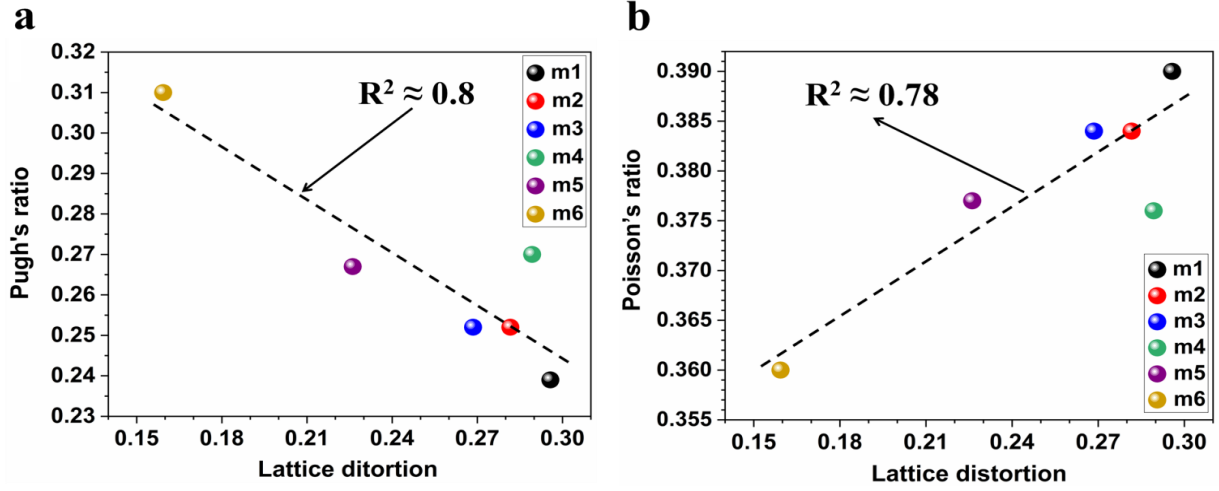


Figure S9. **a.** Lattice distortion (LD) versus Pugh's ratio and **b.** Lattice distortion (LD) versus Poisson's ratio of six BCC RHEAs. The dashed line denotes linear fit.

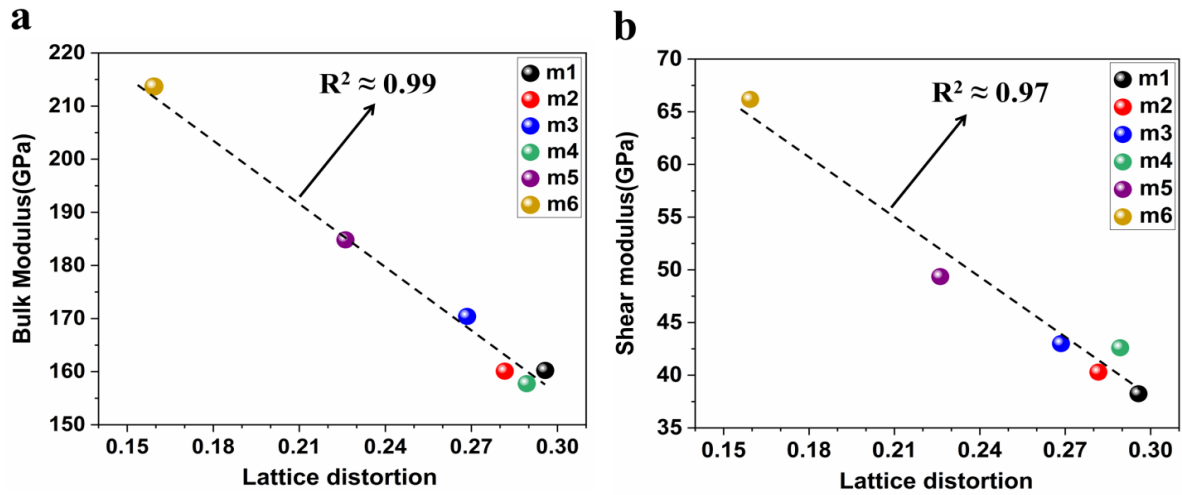


Figure S10. **a.** Lattice distortion (LD) versus bulk modulus and **b.** Lattice distortion (LD) versus shear modulus of six BCC RHEAs. The dashed line denote linear fit.

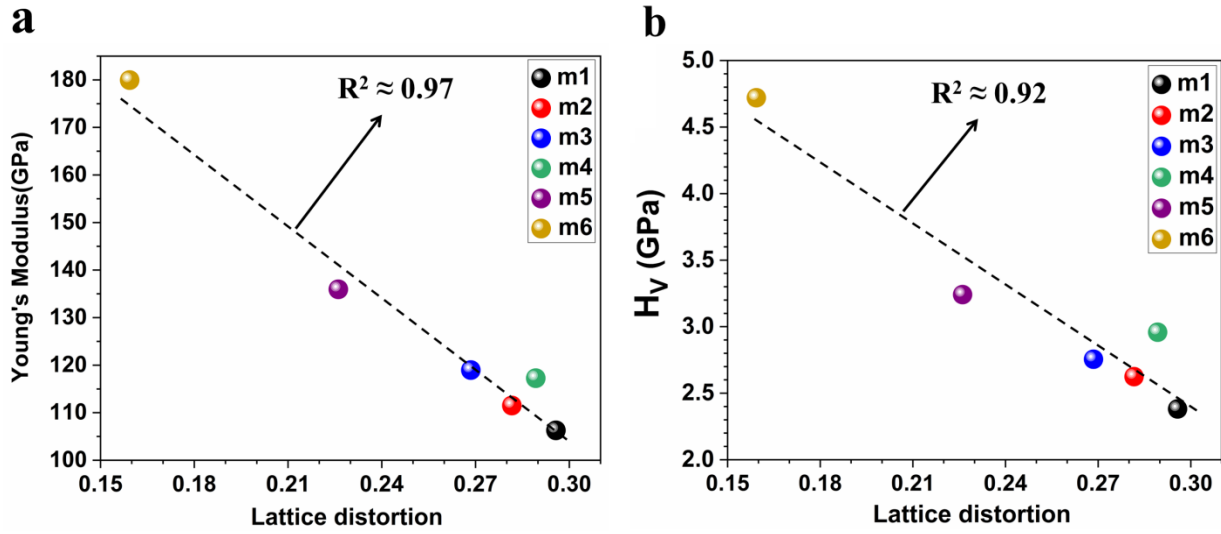


Figure S11. **a.** Lattice distortion (LD) versus Young's modulus and **b.** Lattice distortion (LD) versus Vicker's hardness (H_V) of six BCC RHEAs. The dashed line denote linear fit.

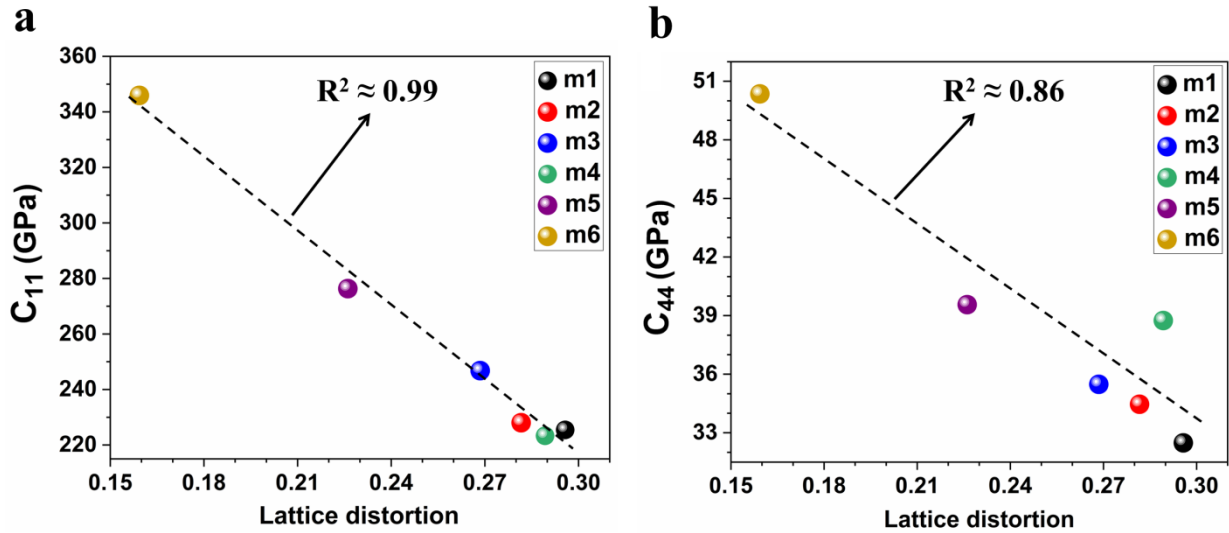


Figure S12. **a.** Lattice distortion (LD) versus elastic constant (C_{11}) and **b.** Lattice distortion (LD) versus elastic constant (C_{44}) of six BCC RHEAs. The dashed line denote linear fit.

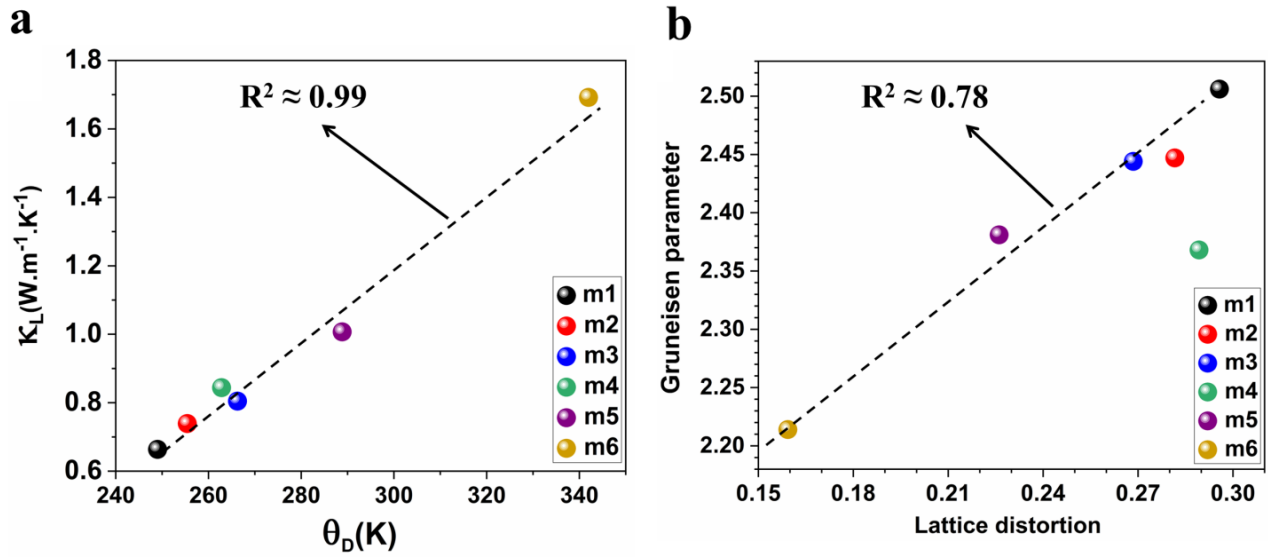


Figure S13. **a.** lattice thermal conductivity (κ_L) versus Debye temperature (θ_D), and **b.** Lattice distortion (LD) versus Gruneisen parameter of 6 BCC RHEAs. The dashed line denote linear fit.

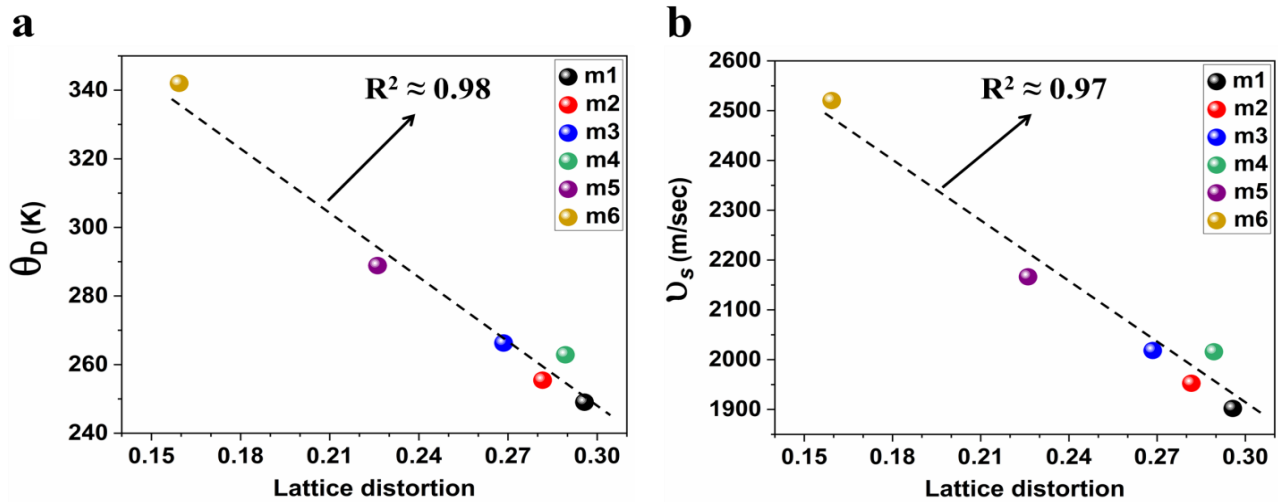


Figure S14. **a.** Lattice distortion (LD) versus Debye temperature (θ_D), and **b.** lattice distortion (LD) versus transverse velocity (v_s) of 6 BCC RHEAs. The dashed line denotes linear fit.

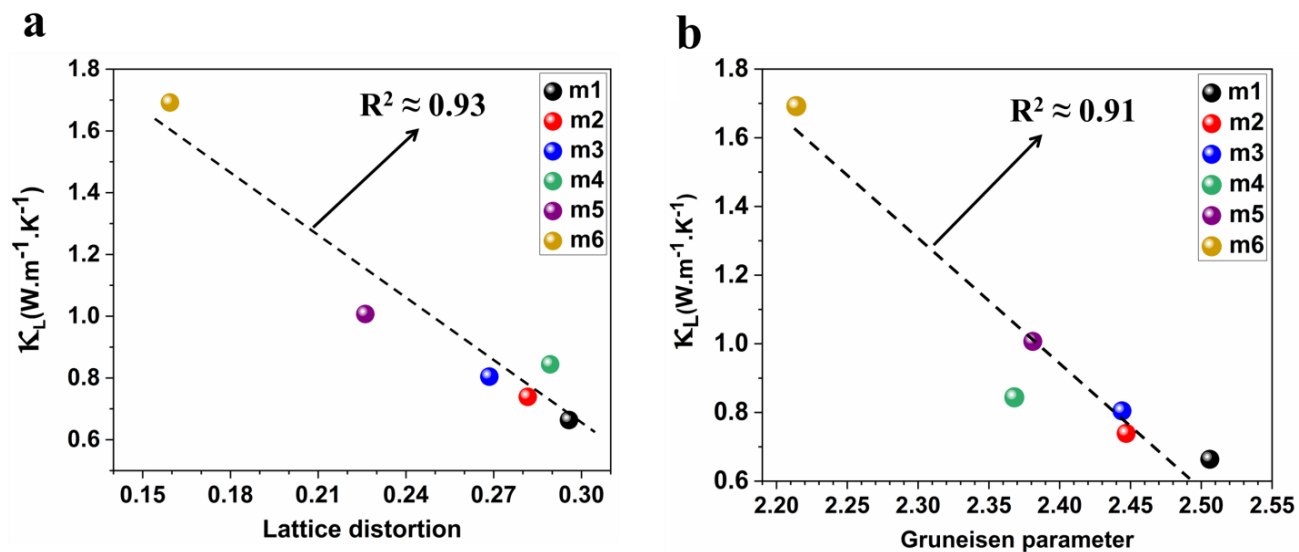


Figure S15. a. Lattice distortion (LD) versus lattice thermal conductivity (κ_L), and b. Gruneisen parameter versus lattice thermal conductivity (κ_L) of 6 BCC RHEAs. The dashed line denote linear fit.

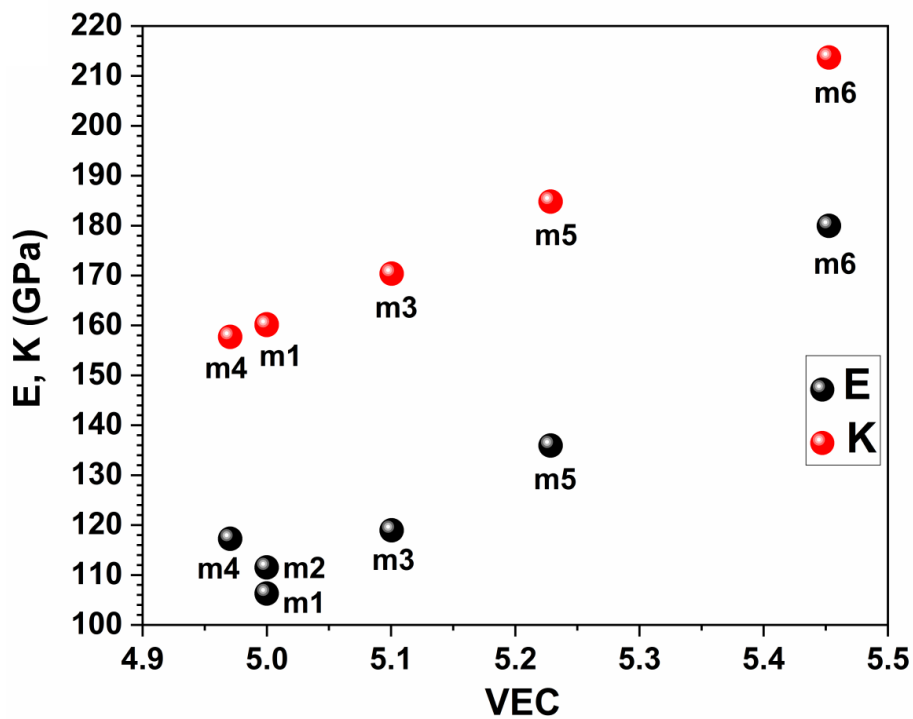


Figure S16. a. Young's modulus (E) and Bulk modulus (K) versus the valence electron concentration (VEC) of 6 BCC RHEAs.

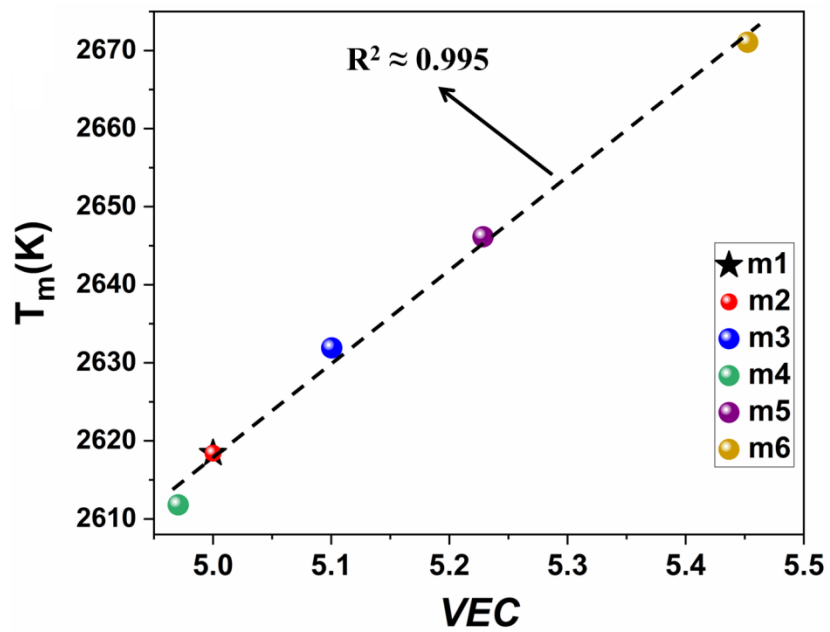


Figure S17. The valence electron concentration (*VEC*) versus the melting point (T_m) for the 6 BCC RHEAs. The dashed line denote linear fit.

Supplementary Tables

Table S1. The atomic fraction (c_i) of Ti, V, Cr, Zr, Nb, Mo, Hf, Ta, and W elements in the six RHEAs models.

Model	Atomic fraction								
	Ti	V	Cr	Zr	Nb	Mo	Hf	Ta	W
m1	0.11111	0.11111	0.11111	0.11111	0.11111	0.11111	0.11111	0.11111	0.11111
m2	0.11111	0.11111	0.11111	0.11111	0.11111	0.11111	0.11111	0.11111	0.11111
m3	0.11111	0.11111	0.135	0.088	0.11111	0.135	0.088	0.111	0.111
m4	0.1604	0.064	0.115	0.115	0.097	0.115	0.102	0.116	0.116
m5	0.1111	0.1111	0.167	0.056	0.11111	0.167	0.056	0.111	0.111
m6	0.11111	0.11111	0.223	0.0	0.11111	0.223	0.0	0.111	0.111

Table S2. Crystal structure (HCP stands for hexagonal close packed), atomic radius⁷⁵, elemental valence electron concentration (VEC)^{76,77}, elemental Pauling electronegativity ($\chi_{Pauling}$)^{76,77}, elemental Allen electronegativity (χ_{Allen})⁷⁶, and elemental melting point (T_m)⁷⁷ of Ti, V, Cr, Zr, Nb, Mo, Hf, Ta, and W elements.

Element	Elemental structure	Elemental radius (nm)	Elemental VEC	Elemental $\chi_{Pauling}$	Elemental χ_{Allen}	Elemental T_m (K)
Ti	HCP or BCC	0.1462	4	1.54	1.38	1941
V	BCC	0.1316	5	1.63	1.53	2183
Cr	BCC	0.1249	6	1.66	1.65	2180
Zr	HCP or BCC	0.1603	4	1.33	1.32	2125
Nb	BCC	0.1429	5	1.6	1.41	2750
Mo	BCC	0.1363	6	2.16	1.47	2896
Hf	HCP	0.1578	4	1.3	1.16	2506
Ta	BCC	0.1430	5	1.5	1.34	3290
W	BCC	0.1367	6	2.36	1.47	3695

Table S3. The parameter Ω , Gibbs free energy (ΔG_{mix}), combination parameter (Λ), Pauling electronegativity ($\Delta\chi_{Pauling}$), and Allen electronegativity ($\Delta\chi_{Allen}$) of various TiVCrZrNbMoHfTaW system.

Model	Ω	ΔG_{mix} (kJ/mol.) at 300 K	Λ (J.K ⁻¹ mol. ⁻¹)	$\Delta\chi_{Pauling}$	$\Delta\chi_{Allen}$ %
m1	9.9851	-10.27013	0.3131	0.3368	9.2908
m2	9.9851	-10.27013	0.3131	0.3368	9.2908
m3	9.4638	-10.52081	0.3655	0.3349	9.2505
m4	9.4442	-10.42422	0.3227	0.3416	9.0476
m5	9.0787	-10.52893	0.3303	0.3283	9.1897
m6	8.7423	-9.513834	0.3098	0.3053	9.1287

Python code

This python was used to generate random solid solutions:

<https://github.com/Asif-Iqbal-Bhatti/High-Entropy-Alloys>.

```
.....  
#!/usr/bin/env python3  
  
#####  
# USAGE :: python3 sys.argv[0] bcc/fcc c/d  
  
#####  
import numpy as np  
import sys, random  
from numpy import linalg as LA  
#-----INPUT PARAMETERS-----#  
  
lattice_parameter = 3.405  
supercellx = 8  
supercelly = 8  
supercellz = 8  
#-----#  
  
def HEAs_supercell():  
    cartesian_units=[]  
    count=0  
    lattice_vector = np.array([[1,0,0],  
                                [0,1,0],  
                                [0,0,1]])*lattice_parameter  
  
    lattice_bcc = np.array([[0,0,0],  
                            [0.5,0.5,0.5]])*lattice_parameter  
  
    lattice_fcc = np.array([[0,0,0],  
                            [0.5,0.0,0.5],  
                            [0.5,0.5,0.0]])*lattice_parameter  
    fcc = lattice_fcc;  
    if (sys.argv[1]!='fcc'): b = lattice_parameter*np.sqrt(2)/2.0; print("Burgers vector::", b)  
    bcc = lattice_bcc  
    if (sys.argv[1]!='bcc'): b = lattice_parameter*np.sqrt(3)/2.0; print("Burgers vector::", b)  
  
    for i in range(supercellx):  
        for j in range(supercelly):  
            for k in range(supercellz):  
                atom_position = np.array([i,j,k])
```

```

        cartesian_basis = np.inner(lattice_vector.T, atom_position)
        if (sys.argv[1] == 'bcc'):
            for atom in lattice_bcc:
                cartesian_units.append(cartesian_basis + atom)
                count+=1
        elif (sys.argv[1] == 'fcc'):
            for atom in lattice_fcc:
                cartesian_units.append(cartesian_basis + atom)
                count+=1

    with open("POSCAR","w") as POSCAR:
        POSCAR.write(f'#{sys.argv[1]}\n')
        POSCAR.write('{:6.6f}\n'.format(1.0))
        POSCAR.write(" {::12.9f} {::12.9f}
{:12.9f}\n".format(lattice_vector[0][0]*supercellx,lattice_vector[0][1]*supercellx,lattice_vector[0][2]*supercellx ))
        POSCAR.write(" {::12.9f} {::12.9f}
{:12.9f}\n".format(lattice_vector[1][0]*supercelly,lattice_vector[1][1]*supercelly,lattice_vector[1][2]*supercelly ))
        POSCAR.write(" {::12.9f} {::12.9f}
{:12.9f}\n".format(lattice_vector[2][0]*supercellz,lattice_vector[2][1]*supercellz,lattice_vector[2][2]*supercellz ))
        print("{:12.9f} {::12.9f}
{:12.9f}".format(lattice_vector[0][0]*supercellx,lattice_vector[0][1]*supercellx,lattice_vector[0][2]*supercellx ))
        print("{:12.9f} {::12.9f}
{:12.9f}".format(lattice_vector[1][0]*supercelly,lattice_vector[1][1]*supercelly,lattice_vector[1][2]*supercelly ))
        print("{:12.9f} {::12.9f}
{:12.9f}".format(lattice_vector[2][0]*supercellz,lattice_vector[2][1]*supercellz,lattice_vector[2][2]*supercellz ))
        POSCAR.write('Ta\n')
        POSCAR.write(f'{count}\n')
    #----- In Cartesian UNITS -----#
    if sys.argv[2] in ["c", "C"]:
        POSCAR.write("Cartesian\n")
        for cartesian_unit in cartesian_units:
            #print("{:12.9f} {::12.9f} {::12.9f}".format(cartesian_units[i][0], cartesian_units[i][1],
cartesian_units[i][2]))

            POSCAR.write(
                "{:12.9f} {::12.9f} {::12.9f}\n".format(
                    cartesian_unit[0], cartesian_unit[1], cartesian_unit[2]
                )
            )

    #----- In fractional/Direct UNITS -----#
    u = np.cross(lattice_vector[1]*supercelly, lattice_vector[2]*supercellz)
    v = np.cross(lattice_vector[0]*supercellx, lattice_vector[2]*supercellz)
    w = np.cross(lattice_vector[0]*supercellx, lattice_vector[1]*supercelly)
    V = np.array([ lattice_vector[0]*supercelly,lattice_vector[1]*supercelly,lattice_vector[2]*supercellz ] )
    print ("Volume of the cell: ", LA.det(V) )
    Vx = np.inner(lattice_vector[0]*supercellx,u)
    Vy = np.inner(lattice_vector[1]*supercelly,v)
    Vz = np.inner(lattice_vector[2]*supercellz,w)

    if sys.argv[2] in ["d", "D"]:
        POSCAR.write("Direct\n")
        for cartesian_unit_ in cartesian_units:
            POSCAR.write(
                "{:12.9f} {::12.9f} {::12.9f}\n".format(
                    np.dot(cartesian_unit_, u) / Vx,
                    np.dot(cartesian_unit_, v) / Vy,
                    np.dot(cartesian_unit_, w) / Vz,
                )
            )

```

```

)

#----- Randomly distribute atoms for HEA -----#
with open("newPOSCAR","w") as fdata:
    for _ in range(int(1e3)):
        randomArrx = random.sample(range(count), count)
        if (count%4 == 0):
            fdata.write(f'#{sys.argv[1]}\n')
            fdata.write('{:6.6f}\n'.format(1.0))
            fdata.write("{:12.9f} {:12.9f}
{:12.9f}\n".format(lattice_vector[0][0]*supercellx,lattice_vector[0][1]*supercellx,lattice_vector[0][2]*supercellx ))
            fdata.write("{:12.9f} {:12.9f}
{:12.9f}\n".format(lattice_vector[1][0]*supercelly,lattice_vector[1][1]*supercelly,lattice_vector[1][2]*supercelly ))
            fdata.write("{:12.9f} {:12.9f}
{:12.9f}\n".format(lattice_vector[2][0]*supercellz,lattice_vector[2][1]*supercellz,lattice_vector[2][2]*supercellz ))
            fdata.write('V Nb Ta Ti \n')
            fdata.write('{0} {0} {0} \n'.format((int(count/4))) )

#----- In Cartesian UNITS -----#
if sys.argv[2] in ["c", "C"]:
    fdata.write("Cartesian\n")
    print(
        f'# of atoms per element -> {count / 5}. File generated in Cartesian
coordinates'
    )

    for i in range(len(cartesian_units) ):
        #print("{:12.9f} {:12.9f}
{:12.9f}".format(cartesian_units[randomArrx[i]][0],cartesian_units[randomArrx[i]][1],cartesian_units[randomArrx[i]][2] ) )
        fdata.write("{:12.9f} {:12.9f}
{:12.9f}\n".format(cartesian_units[randomArrx[i]][0],cartesian_units[randomArrx[i]][1],cartesian_units[randomArrx[i]][2] ) )

#----- In fractional/reduced UNITS -----#
if sys.argv[2] in ["d", "D"]:
    fdata.write("Direct\n")
    print(
        f'# of atoms per element -> {count / 5}. File generated in Direct coordinates'
    )

    for i in range(len(cartesian_units) ):
        fdata.write("{:12.9f} {:12.9f}
{:12.9f}\n".format(np.dot(cartesian_units[randomArrx[i]],u)/Vx, np.dot(cartesian_units[randomArrx[i]],v)/Vy,
np.dot(cartesian_units[randomArrx[i]],w)/Vz )
    else:
        print(
            f'{count / 5} is not an integer number for equal composition -> HEAs not generated'
        )

def help():
    print('A simple script to generate FCC or BCC supercell for HEAs.')
    print('To execute just run python3 sys.argv[0] <bcc/fcc> <c/d>.')
    print('THIS script is valid for equimolar composition !!!')
    print('HEAs consists of five or more elements. The elements has already been typed into the')
    print('script just change according to your need also lattice vectors should be')
    print('equal and atomic composition should corresponds to integer multiple of atoms.')

```

```

if __name__ == '__main__':
    if len(sys.argv) < 3 or len(sys.argv) > 3:
        help()
    else:
        HEAs_supercell()

```

References

1. Yao, H., Ouyang, L. & Ching, W. Ab Initio Calculation of Elastic Constants of Ceramic Crystals. **3204**, 3194–3204 (2007).
2. Yang, A., Bao, L., Peng, M. & Duan, Y. Explorations of elastic anisotropies and thermal properties of the hexagonal TMSi₂ (TM = Cr, Mo, W) silicides from first-principles calculations. *Mater. Today Commun.* **27**, 102474 (2021).
3. Wang, A. J. *et al.* Structural and elastic properties of cubic and hexagonal TiN and AlN from first-principles calculations. *Comput. Mater. Sci.* **48**, 705–709 (2010).
4. Reuss, A. Berechnung der Fließgrenze von Mischkristallen auf Grund der Plastizitätsbedingung für Einkristalle. *ZAMM - J. Appl. Math. Mech. / Zeitschrift für Angew. Math. und Mech.* **9**, 49–58 (1929).
5. Hill, R. The elastic behaviour of a crystalline aggregate. *Proc. Phys. Soc. Sect. A* **65**, 349–354 (1952).
6. Sun, Z., Music, D., Ahuja, R. & Schneider, J. M. Theoretical investigation of the bonding and elastic properties of nanolayered ternary nitrides. *Phys. Rev. B - Condens. Matter Mater. Phys.* **71**, 3–5 (2005).
7. Tian, Y., Xu, B. & Zhao, Z. Microscopic theory of hardness and design of novel superhard crystals. *Int. J. Refract. Met. Hard Mater.* **33**, 93–106 (2012).
8. Jiang, S. *et al.* Elastic and thermodynamic properties of high entropy carbide (HfTaZrTi)C and (HfTaZrNb)C from ab initio investigation. *Ceram. Int.* **46**, 15104–15112 (2020).
9. Boudiaf, K. *et al.* Structural, Elastic, Electronic and Optical Properties of LaOAgS-Type Silver Fluoride Chalcogenides: First-Principles Study. *J. Electron. Mater.* **46**, 4539–4556 (2017).
10. Guo, F. *et al.* Structural, mechanical, electronic and thermodynamic properties of cubic TiC compounds under different pressures: A first-principles study. *Solid State Commun.* **311**, 113856 (2020).
11. Anderson, O. L. a Simplified Method for Calculating the. *J. Phys. Chem. Solids* **24**, 909–917 (1963).
12. Wachter, P., Filzmoser, M. & Rebizant, J. Electronic and elastic properties of the light actinide tellurides. *Phys. B Condens. Matter* **293**, 199–223 (2001).
13. Clarke, D. R. Materials selections guidelines for low thermal conductivity thermal barrier coatings. *Surf. Coatings Technol.* **163–164**, 67–74 (2003).

14. Clarke, D. R. & Levi, C. G. Materials design for the next generation thermal barrier coatings. *Annu. Rev. Mater. Res.* **33**, 383–417 (2003).
15. Cahill, D. G., Watson, S. K. & Pohl, R. O. Lower limit to the thermal conductivity of disordered crystals. *Phys. Rev. B* **46**, 6131–6140 (1992).
16. Cahill, D. G. *et al.* Nanoscale thermal transport. *J. Appl. Phys.* **93**, 793–818 (2003).
17. Morelli, D. T. & Slack, G. A. High lattice thermal conductivity solids. *High Therm. Conduct. Mater.* 37–68 (2006) doi:10.1007/0-387-25100-6_2.
18. Morelli, D. T. & Heremans, J. P. Thermal conductivity of germanium, silicon, and carbon nitrides. *Appl. Phys. Lett.* **81**, 5126–5128 (2002).
19. Arab, F., Sahraoui, F. A., Haddadi, K., Bouhemadou, A. & Louail, L. Phase stability, mechanical and thermodynamic properties of orthorhombic and trigonal MgSiN₂: An ab initio study. *Phase Transitions* **89**, 480–513 (2016).
20. JULIAN, C. L. Theory of Heat Conduction in Rare-Gas Crystals. *Phys. Rev.* **137**, (1965).
21. Qin, G. *et al.* High-throughput computational evaluation of lattice thermal conductivity using an optimized Slack model. *Mater. Adv.* **3**, 6826–6830 (2022).
22. Toberer, E. S., Zevalkink, A. & Snyder, G. J. Phonon engineering through crystal chemistry. *J. Mater. Chem.* **21**, 15843–15852 (2011).
23. Fine, M. E., Brown, L. D. & Marcus, H. L. Elastic constants versus melting temperature in metals. *Scr. Metall.* **18**, 951–956 (1984).
24. K. Benkaddour, A. Chahed, A. Amar, H. Rozale, A. Lakdja, O. Benhelal, A. S. First-principles study of structural, elastic, thermodynamic, electronic and magnetic properties for the quaternary Heusler alloys CoRuFeZ (Z = Si, Ge, Sn). *J. Alloys Compd.* (2016).
25. Liu, S. *et al.* Journal of the European Ceramic Society Phase stability , mechanical properties and melting points of high-entropy quaternary metal carbides from first-principles. *J. Eur. Ceram. Soc.* (2021) doi:10.1016/j.jeurceramsoc.2021.05.022.
26. Naher, M. I., Afzal, M. A. & Naqib, S. H. A comprehensive DFT based insights into the physical properties of tetragonal superconducting Mo₅PB₂. *Results Phys.* **28**, 104612 (2021).